MANY-BODY CONTRIBUTIONS TO SPIN RELAXATION IN SEMICONDUCTORS

A Dissertation presented to

the Faculty of the Department

of Physics and Astronomy

In Partial Fulfillment

of the Requirements for the Degree

Doctor of Philosophy

---

by

MATTHEW D. MOWER

Dr. Giovanni Vignale, Primary Advisor

DEC 2013

The undersigned, appointed by the Dean of the Graduate School, have examined the dissertation entitled:

MANY-BODY CONTRIBUTIONS TO SPIN
RELAXATION IN SEMICONDUCTORS

presented by Matthew D. Mower,

a candidate for the degree of Doctor of Philosophy and hereby certify that, in their opinion, it is worthy of acceptance.

Dr. Giovanni Vignale

Dr. H. R. Chandrasekhar

Dr. Sashi Satpathy

Dr. Carsten Ullrich

Dr. Carlos Wexler

Dr. Gregory Triplett

ACKNOWLEDGEMENTS

I would like to acknowledge my advisor, Dr. Giovanni Vignale, for his uncanny ability to see the physical picture long before results are available. His guidance, based on tremendous depth of understanding and breadth of experience, has been instrumental to my competence as a researcher today. Furthermore, I am extremely appreciative of the connections I have made with other researchers due to his large network of coauthors. As I exit graduate studies, I have a small network of my own, containing names I would otherwise be intimated to approach alone.

I'm quite proud to be a graduate of the University of Missouri. The education I received in the Department of Physics and Astronomy at the University of Missouri has prepared me well for work in academia. My doctoral committee has been a great resource when my primary advisor has been out of town. The graduate student governments, both campus-wide and within the physics department, have taught me a number of lessons about politics in academia. This has been the experience any new graduate student should hope to have.

A special thank you is in order to Drs. Meera and H.R. Chandrasekhar for helping me establish residence in Columbia, MO at a time when all of my belongings fit tidily in the back of my pickup truck. The amazing Indian cuisine is well remembered.

Finally, I'd like to give a shout-out to the sweatervesters, the Pandacondas, and those who joined for some great evenings at 44 Stone and Sycamore. These fine people were responsible for helping me maintain some level of sanity amidst frustrating calculations.

TABLE OF CONTENTS

LIST OF FIGURES

ABSTRACT

Spintronics has the potential to play a significant role in future electronic devices. The success of the field hinges on our ability to maintain and propagate spin signals over various length scales and periods of time. Common to all devices designed to carry spin signals is a need to hold the spin orientation of constituent particles, individually or in bulk. Spin relaxation is a measure of how long particle spins remain polarized while subjected to both spin-dependent and spin-independent interactions.

An effect typically driven by the spin-orbit interaction in semiconductors, spin relaxation describes the rate at which spin polarized particles return to an equilibrium spin distribution. This is generally in competition with the goals of spintronic devices which generate out-of-equilibrium spin populations to represent signals. By studying the various mechanisms of spin relaxation in different systems, we learn which materials are appropriate for specific applications and get hints about how to minimize signal loss.

This report focuses largely on Dyakonov-Perel spin relaxation of carriers in III-V semiconductors. Of the spin relaxation mechanisms in III-V semiconductors, Dyakonov-Perel often dominates or is at least a primary contributor. We study the mechanism in detail for both non-magnetic and dilute magnetic semiconductors, deriving analytic expressions that include contributions from many-body interactions. The results shed light on the validity of commonly made approximations in calculating spin relaxation for various systems. More importantly, we show how spin relaxation can affect other physical observables, such as spin diffusion. By investigating this spin relaxation mechanism in a dilute magnetic semiconductor, we include the effects of spin-dependent interactions. These interactions result in some peculiarities of spin relaxation for carriers undergoing a ferromagnetic transition.

Chapter 1

Introduction

The field of spintronics – the study of spin dynamics, primarily in solid state systems – has the potential to play a significant role in future electronic devices. With charge based circuits reaching size, speed, and power consumption limits, spintronic devices may be able to selectively replace electronic components, allowing continuation of the technology industry's rapid rate of innovation. Though promising, these devices are still immature; the physics involved in spin interactions is relatively unexplored in comparison to charge interactions in solid state systems. Spintronics is thus a rich field for both technological advance and our basic understandings of physics in the solid state.[1–6]

An important consideration when developing electronic or spintronic devices is that of stability and coherence of signals. In electronic devices, signals usually take the form of small quantities of charge, e.g. field effect transistors switch between on and off based on whether a channel is charged or not. The charges are manipulated – propagated or caused to change energy levels – via external and internal (intrinsic) electric fields. Both a useful feature and a limiting factor of charge based electronic systems is that an electron's charge is independent of applied field: apply a positive or negative electric field to an electron, and that electron will still have a negative charge at the end of the day. Seen as a luxury, one

might consider this a form of particle-stability. Alternatively, as a hindrance, one might prefer more degrees of freedom than just with or against an applied field.

Depending on how you look at it, spintronic devices do not share this luxury or hindrance. Spins can point in any direction and are generally not locked to their "original" orientation. A number of mechanisms can affect spin: spin-orbit interactions, symmetry and selection rules,[1] exchange interactions with magnetic impurities, hyperfine interactions, spin-phonon interactions, electron-hole, and electron-electron interactions.[7, 8] While the sheer number of mechanisms available to manipulate spin is encouraging, some are rather difficult to control or eliminate. Thus, maintaining spin orientation is tricky business – a spin-up electron is not guaranteed to be spin-up at the end of the day.

Spin signals can take the form of small packets of like-spins or even be individual spins in the case of quantum dots.[9, 10] Important in all forms of spin signals is the need to maintain spin-polarization over time and space. For a large collection of spins, coherence between individual spins may also be of importance. Interactions generally cause difficulty in maintaining a particular spin orientation, leading to spin dephasing and relaxation. Spin dephasing refers to the diminishing coherence between like-spin states, whereas spin relaxation refers to the population decline of a particular spin orientation.[5, 7] Spin relaxation is the primary focus of this report.

The projects in this report present derivations and calculations of spin relaxation in various systems. In *Ambipolar spin diffusion in GaAs quantum wells*, we see how spin relaxation affects the diffusion of spin polarized carriers; *Dyakonov-Perel spin relaxation in intrinsic GaAs* presents a detailed derivation of the Dyakonov-Perel mechanism in III-V semiconductors with many-body interactions explicitly taken into account; *Spin relaxation near a ferromagnetic transition* extends these derivations to a dilute magnetic semiconductor and applies the results to a model of itinerant carriers and localized magnetic impurities.

[1] Though not really interactions, these rules do put restrictions on wavefunctions and ordering in energy levels.

As a primer to introduce some of the theory, the following sections give brief descriptions of the relevant spin relaxation mechanisms in semiconductors.

1.1 Spin relaxation in semiconductors

Several types of interactions are responsible for spin relaxation in semiconductors. These are typically of the spin-orbit variety, or are at least modeled by an effective magnetic field interacting with spin(s). Depending on the origin of the effective magnetic field, certain mechanisms for spin relaxation are more effective in some systems than others. Reviews of these mechanisms can be found in references [5–7]. The mechanisms of primary relevance to III-V and II-VI semiconductors include: the Dyakonov-Perel mechanism[11], the Elliott-Yafet mechanism[12, 13], and the Bir-Aronov-Pikus mechanism[14]. For magnetically doped semiconductors, the exchange interaction between spins and magnetic impurities (e.g. *s-d*, *s-f*, *p-d*) is also relevant.

For all of the mechanisms mentioned, spins are subjected to an effective magnetic field which can be said to have correlation time τ_c (the time during which a fluctuating magnetic field is roughly constant) and to cause a spin precession frequency ω. M.I. Dyakonov presents a simple picture of spin relaxation in this effective magnetic field:[6] A spin precesses around a (random) direction of an effective magnetic field with frequency ω. After time τ_c, the direction and magnitude of the field changes randomly and the spin precesses around a new field direction. With a number of these steps, the initial spin direction is forgotten. If the correlation time τ_c is significantly smaller than the inverse of the precession frequency ω^{-1}, a spin will experience only a small precession before being subjected to a new (random) precession axis. In this sort of random walk between different spin precession axes, the spin accumulates an angular deviation from its original orientation. The spin relaxation time may be defined as the time it takes for that angle of deviation from original orientation to reach say, $\pi/3$ or $\pi/2$. In this rather qualitative argument, the rate of spin relaxation

is of order: $\tau_s^{-1} \sim \omega^2 \tau_c$.[6] A more rigorous derivation which includes both static and time-dependent magnetic fields results in

$$\frac{1}{\tau_s} = \left(\overline{\omega_x^2} + \overline{\omega_y^2}\right) \frac{\tau_c}{1 + \omega_0^2 \tau_c^2}\,, \tag{1.1}$$

where ω_x and ω_y are the precession frequencies of the fluctuating field and ω_o is that of the static field. The over-lines represent averages.[5]

Returning to the list of spin relaxation mechanisms, our studies focus primarily on the Dyakonov-Perel mechanism and we only discuss Elliott-Yafet and Bir-Aronov-Pikus at a phenomenological level. The next section is dedicated to the derivation and finer details of Dyakonov-Perel spin relaxation as it is used in this paper. As this report is not meant to be a comprehensive review of spin relaxation mechanisms, we limit discussion of the Elliott-Yafet and Bir-Aronov-Pikus mechanism to the points below

1. **Elliott-Yafet spin relaxation:** The conduction band states of carriers in semiconductors are in general not perfect spin eigenstates. This is due to spin-orbit contributions to the crystal Hamiltonian (materials with weak spin-orbit interactions, such as graphene, are not expected to exhibit this mechanism). The conduction band states are linear combinations of spin eigenstates, for example:[12, 15, 16]

$$\psi_{\mathbf{k}n\uparrow}(\mathbf{r}) = \left[a_{\mathbf{k}n}(\mathbf{r})|\uparrow\rangle + b_{\mathbf{k}n}(\mathbf{r})|\downarrow\rangle\right] e^{i\mathbf{k}\cdot\mathbf{r}}\,, \tag{1.2}$$

$$\psi_{\mathbf{k}n\downarrow}(\mathbf{r}) = \left[a^*_{-\mathbf{k}n}(\mathbf{r})|\downarrow\rangle - b^*_{-\mathbf{k}n}(\mathbf{r})|\uparrow\rangle\right] e^{i\mathbf{k}\cdot\mathbf{r}}\,. \tag{1.3}$$

   Then, the inner product $\langle \mathbf{k}'\uparrow|\,\mathbf{k}\downarrow\rangle$ can be non-zero, where it should be clear that $|\mathbf{k}\uparrow\rangle$ corresponds to $\psi_{\mathbf{k}n\uparrow}(\mathbf{r})$ in some level n. Spin polarization is determined by the eigenstate with a dominant prefactor, thus we still refer to the overall state as spin-up or spin-down. An interesting consequence of this non-zero matrix element is that a spin-independent scattering potential, like the Coulomb potential, can actually appear

to flip a particle's spin in interaction: $\langle \mathbf{k}' \downarrow | \, V(\mathbf{k}, \mathbf{k}') \, | \mathbf{k} \uparrow \rangle \neq 0$. Multiple of these "spin-flip" interactions can then lead to the unpolarization of carriers as a whole. The rate of spin relaxation is roughly proportional to the rate of scattering.

2. **Bir-Aronov-Pikus spin relaxation:** Like Elliott-Yafet, this mechanism relies on spin flips to occur in scattering. In this case though, spin flips occur as a result of exchange or annihilation of electrons with holes. The relative spin orientations of the distinct carriers is the key ingredient. Again, the rate of spin relaxation follows the rate of scattering. As this mechanism relies on a large background of holes to provide enough opportunity for exchange and annihilation, it is usually only dominant in p-type semiconductors.

1.2 Dyakonov-Perel spin relaxation

The derivation of Dyakonov-Perel spin relaxation is well known and can be found in excellent reviews[5, 17]. In a 2011 paper, we reviewed the derivation and cast it into notation typical of modern studies in semiconductor spintronics.[18] This derivation is presented here largely intact. An important message to take-home from this section is that the Dyakonov-Perel spin relaxation time is inversely related to the scattering time.

The systems in which we study spin relaxation are III-V semiconductors (e.g. GaAs, InAs, InSb) of the zincblende structure. These semiconductors exhibit spin-split bands caused by a Dresselhaus effective magnetic field.[19] The effective field arises from spin-orbit interaction and couples to electrons via the hamiltonian term

$$H_{1\mathbf{k}} = \frac{\hbar}{2} \mathbf{\Omega}_{\mathbf{k}} \cdot \boldsymbol{\sigma} \,, \tag{1.4}$$

where $\mathbf{\Omega}_{\mathbf{k}}$ defines the precession axis and precession frequency of electron spins. $\mathbf{\Omega}_{\mathbf{k}}$ is a cubic harmonic function of the Bloch wave vector $\mathbf{k}$; its component along the $\hat{\mathbf{z}}$-axis is given

by

$$\Omega_{\mathbf{k},z} = \frac{\alpha_c \hbar^2}{\sqrt{2m_c^3 E_g}} k_z (k_x^2 - k_y^2)\,, \tag{1.5}$$

where α_c is the Dresselhaus spin-orbit coupling constant, E_g is the band gap energy, and m_c is the conduction band effective mass of an electron. The other components of $\mathbf{\Omega_k}$ are obtained by cyclic permutations of x, y, and z.

The spin Boltzmann kinetic equation describes the evolution of the spin density matrix in time:

$$\frac{\partial \rho_{\mathbf{k}}}{\partial t} - \frac{1}{i\hbar}[H_{1\mathbf{k}}, \rho_{\mathbf{k}}] + \frac{\partial \rho_{\mathbf{k}}}{\partial \hbar \mathbf{k}} \cdot \mathbf{F_k} + \frac{\partial \rho_{\mathbf{k}}}{\partial \mathbf{r}} \cdot \mathbf{v_k} = I_{\mathbf{k}}(t)\,, \tag{1.6}$$

where $\rho_{\mathbf{k}}$ is the 2×2 spin density matrix and $I_{\mathbf{k}}(t)$ is the collision integral (also a 2×2 matrix). Assuming a homogeneous distribution of electrons ($\partial \rho_{\mathbf{k}} / \partial \mathbf{r} = 0$) and absence of external fields ($\mathbf{F_k} = 0$), Eq. (1.6) reduces to

$$\frac{\partial \rho_{\mathbf{k}}}{\partial t} - \frac{1}{2i}[\mathbf{\Omega_k} \cdot \boldsymbol{\sigma}, \rho_{\mathbf{k}}] = I_{\mathbf{k}}(t)\,. \tag{1.7}$$

We prepare a spin polarized distribution which evolves according to Eq. (1.7) and eventually relaxes to an equilibrium state. In the paramagnetic phase, equilibrium corresponds to an unpolarized state; in the ferromagnetic phase, equilibrium includes some degree of polarization. To describe the process, we search for a solution which contains an equilibrium component, ρ_{0k}, describing a state of uniform spin polarization along a direction denoted by $\hat{\mathbf{s}}$, and a non-equilibrium component, $\rho_{1\mathbf{k}}$:

$$\rho_{\mathbf{k}} = \rho_{0k} + \rho_{1\mathbf{k}}\,. \tag{1.8}$$

Using this definition in Eq. (1.7), we can relate terms of varying order of spin orbit interaction (α_c):

$$\frac{\partial \rho_{0k}}{\partial t} + \frac{\partial \rho_{1\mathbf{k}}}{\partial t} - \frac{1}{2i}[\mathbf{\Omega_k} \cdot \boldsymbol{\sigma}, \rho_{0k}] - \frac{1}{2i}[\mathbf{\Omega_k} \cdot \boldsymbol{\sigma}, \rho_{1\mathbf{k}}] = I_{\mathbf{k}}(t)\,. \tag{1.9}$$

The following assumptions are made about the various terms appearing in Eq. (1.9):

$$\text{1. Order of spin-orbit interaction: } \begin{cases} \rho_{0k} & \text{zero order} \\ \rho_{1\mathbf{k}} & \text{first order} \\ \partial_t \rho_{0k} & \text{second order} \\ \partial_t \rho_{1\mathbf{k}} & \text{third order} \end{cases} \tag{1.10}$$

$$\text{2. } I_{\mathbf{k}}(t) \text{ can be cast in the form of relaxation time approximation.} \tag{1.11}$$

The first of these assumptions will be shown to be consistent with the form of the kinetic equation momentarily. The legitimacy of the second assumption will be discussed in *Chapter 3: Dyakonov-Perel spin relaxation in intrinsic GaAs*. For now, we simply write

$$I_{\mathbf{k}}(t) = -\frac{\rho_{1\mathbf{k}}}{\tau^*_{\mathbf{k}}}\,, \tag{1.12}$$

where $\tau^*_{\mathbf{k}}$ is an effective scattering time on the order of the plane wave lifetime. The precise form of $\tau^*_{\mathbf{k}}$ depends on the scattering mechanism and will be explicitly constructed in subsequent chapters for various cases of interest. Notice that ρ_{0k}, being an equilibrium distribution, does not contribute to the collision integral.

Equating terms of the same order in α_c in Eq. (1.9), the following relations emerge:

$$I_{\mathbf{k}}(t) = -\frac{\rho_{1\mathbf{k}}}{\tau^*_{\mathbf{k}}} = -\frac{1}{2i}[\mathbf{\Omega}_{\mathbf{k}} \cdot \boldsymbol{\sigma}, \rho_{0k}]\,, \tag{1.13}$$

$$\frac{\partial \rho_{0k}}{\partial t} = \frac{1}{2i}\langle [\mathbf{\Omega}_{\mathbf{k}} \cdot \boldsymbol{\sigma}, \rho_{1\mathbf{k}}] \rangle\,, \tag{1.14}$$

$$\frac{\partial \rho_{1\mathbf{k}}}{\partial t} = 0\,, \tag{1.15}$$

where $\langle \dots \rangle$ stands for an angular average. Finally, $\partial_t \rho_{1\mathbf{k}}$ has no counterpart in the kinetic equation at order α_c^2, hence it must vanish at this order.

Let us now introduce the form of the equilibrium distribution, ρ_{0k}, from which we can

use the relations above to derive $\rho_{1\mathbf{k}}$. In terms of carrier density n_k and spin density $\mathbf{s}_k$, the equilibrium density matrix is

$$\rho_{0k} = n_k \hat{1} + \mathbf{s}_k \cdot \boldsymbol{\sigma} \,, \tag{1.16}$$

where $\hat{1}$ is the 2×2 identity matrix. The carrier density is the sum of spin-up/down Fermi-Dirac distributions

$$n_k = (f_{k\uparrow} + f_{k\downarrow})/2 \tag{1.17}$$

and the spin density is the difference

$$s_k = (f_{k\uparrow} - f_{k\downarrow})/2 \,. \tag{1.18}$$

These Fermi-Dirac distributions can contain an equilibrium Zeeman energy contribution $\Delta/2$ and/or a non-equilibrium perturbation Zeeman energy ε_s:

$$f_{k\uparrow/\downarrow} = \frac{1}{\exp[\beta(\varepsilon_k \mp (\Delta/2 + \varepsilon_s) - \mu] + 1} \,, \tag{1.19}$$

where $\beta = (k_B T)^{-1}$ and μ is the chemical potential.

The non-equilibrium part of the distribution function arises from the competition between spin precession, which tilts the spins away from the $\hat{\mathbf{s}}$-axis, and collisions, which attempt to restore local equilibrium. Inserting ρ_{0k} from Eq. (1.16) into the relation for $\rho_{1\mathbf{k}}$ from Eq. (1.13), we find

$$\rho_{1\mathbf{k}} = \tau_{\mathbf{k}}^* \, (\boldsymbol{\Omega}_{\mathbf{k}} \times \mathbf{s}_k) \cdot \boldsymbol{\sigma} \,, \tag{1.20}$$

At this point, the assumption made earlier in this section concerning the orders of α_c in ρ_{0k}, $\rho_{1\mathbf{k}}$, $\partial_t \rho_{0k}$, and $\partial_t \rho_{1\mathbf{k}}$ can be verified easily.

The linearizion of $\rho_{\mathbf{k}}$ has so far only been done in terms of spin-orbit coupling. We can

go a step further by associating ρ_{0k} and $\rho_{1\mathbf{k}}$ with their ε_s-linearizions as well:

$$\rho_{0k} = n_{0k}\hat{1} + \mathbf{s}_{0k}\cdot\boldsymbol{\sigma}\,, \tag{1.21}$$

$$\rho_{1\mathbf{k}} = \tau^*_{\mathbf{k}}\,(\boldsymbol{\Omega}_{\mathbf{k}}\times\mathbf{s}_{1k})\cdot\boldsymbol{\sigma}\,, \tag{1.22}$$

where

$$n_{0k} = (1/2)\sum_\alpha f^0_{k\alpha}\,, \tag{1.23}$$

$$s_{0k} = (1/2)\sum_\alpha \alpha f^0_{k\alpha}\,, \tag{1.24}$$

$$\begin{aligned} s_{1k} &= (\varepsilon_s/2)\sum_\alpha(-\partial f_{k\alpha}/\partial\varepsilon_s)_{\varepsilon_s\to 0} \\ &= (\beta\varepsilon_s/2)\sum_\alpha f^0_{k\alpha}(1-f^0_{k\alpha})\,. \end{aligned} \tag{1.25}$$

and $f^0_{k\alpha} = f_{k\alpha}|_{\varepsilon_s\to 0}$. These are the density matrices we will use throughout this report.

Notice the equilibrium spin density can be obtained from $\mathbf{s}_{0k} = \mathrm{Tr}[\rho_{0k}\boldsymbol{\sigma}]/2$. Then, the time rate of change of $\mathbf{s}_{0k}$ is found by tracing Eq. (1.14) with $\boldsymbol{\sigma}$:

$$\frac{\partial\mathbf{s}_{0k}}{\partial t} = \langle\tau^*_{\mathbf{k}}\boldsymbol{\Omega}_{\mathbf{k}}\times(\boldsymbol{\Omega}_{\mathbf{k}}\times\mathbf{s}_{0k})\rangle\,, \tag{1.26}$$

This equation can be cast into a standard relaxation time approximation

$$\frac{\partial\mathbf{s}_{0k}}{\partial t} = -\frac{\mathbf{s}_{0k}}{\tau^{(s)}_k} \tag{1.27}$$

by defining the rate of spin relaxation as

$$\frac{1}{\tau^{(s)}_k} = \langle\tau^*_{\mathbf{k}}\left(\Omega^2_{\mathbf{k}} - (\boldsymbol{\Omega}_{\mathbf{k}}\cdot\hat{\mathbf{s}})^2\right)\rangle\,. \tag{1.28}$$

The cubic symmetry of III-V semiconductors implies that (i) the relaxation rate of

Eq. (1.28) is independent of the direction of $\hat{\mathbf{s}}$, and (ii) the effective collision time $\tau^*_{\mathbf{k}}$ depends on $\mathbf{k}$ only through its modulus k. Therefore, for cubic systems, the expression for the spin relaxation rate in Eq. (1.28) simplifies to

$$\frac{1}{\tau_k^{(s)}} = \frac{2}{3}\tau_k^* \langle \Omega_{\mathbf{k}}^2 \rangle \,. \tag{1.29}$$

The experimentally measurable quantity of interest is the expectation value of the spin density:

$$\mathbf{S} = \sum_{\mathbf{k}} \mathbf{s}_{0k} \,. \tag{1.30}$$

The equation of motion for $\mathbf{S}(t)$ is obtained by summing Eq. (1.26) over all $\mathbf{k}$ and using this result in a relaxation time approximation that defines τ_s:

$$\frac{\partial \mathbf{S}}{\partial t} = -\frac{\mathbf{S}}{\tau_s} \,. \tag{1.31}$$

Then, the physical rate of spin relaxation is calculated from

$$\frac{1}{\tau_s} = \frac{2}{3}\frac{\sum_{\mathbf{k}} \tau_k^* s_{1k} \langle \Omega_{\mathbf{k}}^2 \rangle}{\sum_{\mathbf{k}} s_{1k}} \,. \tag{1.32}$$

The spin relaxation time, as an internal material parameter independent of a particular non-equilibrium state, is only meaningful in the regime of a small perturbation in spin polarization. Inserting s_{1k} from Eq. (1.25) into Eq. (1.32) we indeed find that the polarization energy ε_s cancels and the resulting expression depends only on internal characteristics of the system. For the case of finite equilibrium spin polarization, the rate of spin relaxation is

$$\frac{1}{\tau_s} = \frac{2}{3}\frac{\sum_{\mathbf{k},\alpha} \tau_k^* f_{k\alpha}^0 (1 - f_{k\alpha}^0) \langle \Omega_{\mathbf{k}}^2 \rangle}{\sum_{\mathbf{k},\alpha} f_{k\alpha}^0 (1 - f_{k\alpha}^0)} \,. \tag{1.33}$$

In a system that is unpolarized at equilibrium, this reduces to

$$\frac{1}{\tau_s} = \frac{2}{3}\frac{\sum_{\mathbf{k}} \tau_k^* f_k^0(1-f_k^0)\langle\Omega_{\mathbf{k}}^2\rangle}{\sum_{\mathbf{k}} f_k^0(1-f_k^0)}\,, \tag{1.34}$$

where $f_k^0 = f_{k\alpha}^0|_{\Delta\to 0}$. The spin relaxation time τ_s defined by this equation is the experimentally accessible quantity which determines a universal long time tail in the spin relaxation dynamics, i.e. $\mathbf{S}(t) \sim e^{-t/\tau_s}$. Subsequent chapters will put different restrictions on (1.34) depending on whether the system is in the degenerate or non-degenerate regime.

In the degenerate limit, and assuming both $\mathbf{\Omega_k}$ and τ_k^* vary slowly across the Fermi surface, the average rate of spin relaxation reduces to Eq. (1.29) with $k \to k_F$:

$$\frac{1}{\tau_s} = \frac{2}{3}\tau_{k_F}^* \langle\Omega_{\mathbf{k}}^2\rangle|_{k\to k_F}\,. \tag{1.35}$$

Referring back to the Dresselhaus spin-orbit field in Eq. (1.5), the angular average is evaluated to be

$$\langle\Omega_{\mathbf{k}}^2\rangle = \frac{16}{35}\frac{\alpha_c^2\varepsilon_k^3}{\hbar^2 E_g}\,. \tag{1.36}$$

There are two important points to be made about the above derivation. First, the whole treatment is reliant on the spin-orbit interaction being weak, leading to a clear separation of time scales between the microscopic momentum-changing collisions (fast) and the macroscopic spin relaxation (slow). In other words, we must have $\Omega_{\mathbf{k}}\tau_k^* \ll 1$; spins relax due to a combination of $\mathbf{k}$-randomizing collisions and relatively small precessions. From here, we can see that when the scattering lifetime is of the same order of magnitude as the spin-relaxation time, our treatment is no longer justified. If spins relax just as quickly as collisions occur, it makes no sense to introduce a quasi-equilibrium distribution function. In the extreme limit of infrequent collisions, the momentum of the electron becomes a constant of motion and the spin simply precesses in the Dresselhaus field at a given $\mathbf{k}$.

The second point is that Eq. (1.28) is often estimated by replacing the effective scattering

time τ_k^* with the momentum relaxation time τ_k. This, however, is not accurate. Beyond weighting collision events by their resulting change in momentum, τ_k^* also weights collisions based on the change in $\Omega_{\mathbf{k}}$, which causes spins to precess around new magnetic field axes.

Chapter 2

Ambipolar spin diffusion in GaAs quantum wells

The contents of this chapter were published as an article in Physical Review B on March 27, 2009.[20] The presentation here is derived from that article. For the sake of brevity, some experimental details are left out. The reader is asked to reference the article if interested in more information.

2.1 Introduction

Spin transport in semiconductors is conveniently studied using optical techniques. Optical spin injection and detection are very efficient due to well-established spin selection rules.[17] The injection of spin-polarized electrons is inevitably accompanied by the injection of an equal number of positively charged and spin-polarized holes.[21] In studies of n-type doped semiconductors, the optically injected holes quickly lose their polarization and recombine with majority carriers, leaving behind a purely electronic spin packet.[22–28] Similarly, in intrinsic samples with an externally applied electric field, holes are spatially separated from

electrons and the transport is dominated by the drift of spin-polarized electrons in the field.[29, 30] Since the influence of the holes is suppressed in each of these cases, spin transport is dominated by drift and diffusion of spin-polarized electrons, analogue to unipolar carrier transport.

In this chapter, we report theoretical and experimental studies of the diffusion of optically injected spin-polarized carriers in an intrinsic semiconductor without an externally applied electric field. In this case, spin diffusion is strongly influenced by the presence of holes. In the experiments, spin-polarized electron-hole pairs are excited in GaAs quantum wells by a tightly focused and circularly polarized laser pulse. Since hole spin relaxation is shorter than a few picoseconds,[31] after a short transient process, the carrier system has three components: spin-up electrons, spin-down electrons, and holes. This is illustrated in Fig. 2.1. All three species diffuse in the quantum well plane and interact with each other. Fig. 2.1b illustrates the carrier system at a later time. Although holes are unpolarized, they influence the diffusion of spin-polarized electrons via Coulomb attraction. Basically, the rate of diffusion is controlled by the slow holes, while the highly mobile electrons quickly adjust to neutralize the holes. This forces both spin-up and spin-down electrons to diffuse in the same direction, in marked opposition to unipolar spin packets in which electrons of opposite spin orientations diffuse in opposite directions.

Dr. Hui Zhao studied this triple-polar diffusion process using a pump-probe technique. Dynamics of electron density and spin density are spatially and temporally resolved by measuring carrier-induced changes of transmission of a linearly polarized probe pulse (Fig. 2.1b). A sub-linear expansion process of the area of the spin density packet is observed, while the simultaneously measured electron density packet expands linearly. This indicates that the spin transport cannot be described as a classical diffusion process with a constant diffusion coefficient. The spin diffusion is significantly slower than the ambipolar carrier diffusion, i.e. diffusion of holes screened by electrons. Our theoretical analysis, based on a three-component drift-diffusion equation, shows that the long-time behavior of the spin density

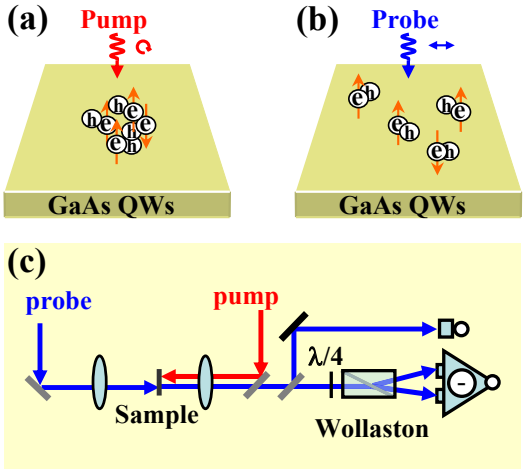

Figure 2.1: Experimental geometry (a) Spin-polarized electrons (e) and holes (h) are injected in GaAs quantum wells (QWs) by a circularly polarized pump pulse. Right after hole spin relaxation, the carrier system is composed of spin-up electrons, spin-down electrons, and holes, within the excitation spot. The orange arrows indicate the direction of electron spin. This is the initial state of the ambipolar carrier and spin diffusion process to be studied. (b) The carrier system at a later time. Diffusion of electron-hole pairs is driven by the density gradient, and is temporally and spatially resolved by measuring differential transmission of a linearly polarized probe pulse (c) Experimental set-up. The pump and probe pulses are counter-propagating and are focused on the sample by microscope objectives with numerical aperture of 0.4. A portion of the transmitted probe pulse is reflected by a beam splitter to a silicon photodiode to detect electron density. The spin density is detected by analyzing the polarization state of the other portion of the transmitted probe pulse by an optical bridge composed of a quarter-wave plate ($\lambda/4$), a Wollaston prism, and a balanced detector.

can be understood in terms of a spin relaxation rate that grows with decreasing density. This behavior is consistent with a model of Dyakonov-Perel spin relaxation limited by Coulomb scattering between carriers. However, the short-time behavior of spin diffusion remains for the time being beyond the reach of our drift-diffusion theory, and will have to be the subject of later investigation.

2.2 Experimental techniques

The GaAs multiple quantum well sample contains 40 periods of 10 nm GaAs layers sandwiched by 10 nm $Al_{0.7}Ga_{0.3}As$ barriers. During the measurements, the sample is cooled to 80 K. Spin-polarized carriers are excited by a circularly polarized 250 fs pump pulse with a central wavelength of 1550 nm. The pump pulse is tightly focused to excite carriers with a Gaussian spatial profile of w_0=1.5 μm (full width at half maximum) with an excitation excess energy of about 40 meV. The density of spin-up electrons excited $n_\uparrow$ is approximately three times higher than the density of spin-down electrons $n_\downarrow$ owing to the selection rules for two-photon absorption of circularly polarized light.[32]

The carrier and spin dynamics are monitored by simultaneously measuring electron and spin density profiles as functions of time by using a spatially and temporally resolved pump-probe technique. The total electron density $n = n_\uparrow + n_\downarrow$ is measured by focusing a linearly polarized 100 fs probe pulse on the sample with a spot size of 1.5 μm (Fig. 2.1c). The spin density $s = n_\uparrow - n_\downarrow$ is measured by analyzing carrier-induced circular dichroism of the same probe pulse, i.e. the absorption difference of right- and left-hand circularly polarized probe pulses in the presence of spin-polarized carriers.

2.3 Experimental results

Dr. Hui Zhao simultaneously measured electron density and spin density as functions of space by scanning the probe spot across the pump spot, and as functions of time by scanning the time-delay between the probe and the pump pulses. Fig. 2.2 summarizes the dynamics of electron density and spin density measured with a peak electron density of 2.3×10^{17} cm^{-3}. The contour map in Fig. 2.2a shows how electron density varies with time and space after injection. Here r is defined as the distance between the centers of the pump and probe spots, and t is the time delay of the probe pulse with respect to the pump pulse. Two normalized spatial profiles of electron density measured at t=5 ps (squares) and t =300 ps (circles) are plotted in Fig. 2.2b. The solid lines are Gaussian fits to the data. Clearly, the spatial profile of electron density remains Gaussian in shape, expanding due to electron transport. To quantitatively describe the transport, the time variation of the full width at half maximum of the electron density profile w_{n} was deduced by fitting the electron density profiles measured at all probe delays. In Fig. 2.2c, the squared width as a function of t is plotted.

According to the classical diffusion model with a constant diffusion coefficient, the squared width increases linearly in time as

$$w_{\mathrm{n}}^2(t) = w_0^2 + 16\ln(2) D_a t, \tag{2.1}$$

where D_a is the ambipolar carrier diffusion coefficient.[33, 34] With a linear fit to the data, we deduce $D_a = 21$ cm^{2}s^{-1}. It is worth mentioning that in the experiment, due to a finite size of the probe spot, the measured profiles shown in Fig. 2.2b are actually convolutions of the probe spot and the actual electron density profiles. However, since both the probe spot and the electron density profiles are Gaussian, the convolution doesn't influence the measurement of D_a.[35]

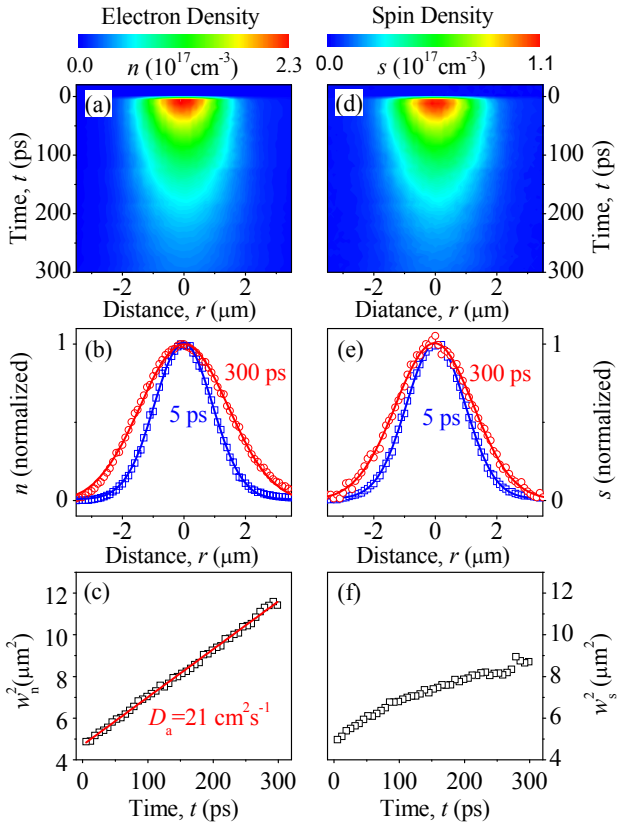

Figure 2.2: Spatio-temporal dynamics of electron (n) and spin (s) densities measured at a sample temperature of 80 K and a peak electron density of 2.3×10^{17} cm^{-3}. (a) Electron density as functions of time and space. The electron density is deduced from the measured $\Delta T/T_0$. (b) Spatial profiles of electron density measured at 5 ps (squares) and 300 ps (circles). The profiles are normalized in order to show the expansion caused by carrier diffusion. The solid lines are Gaussian fits. (c) Squared width of electron density profiles as a function of time obtained by Gaussian fit to profiles measured at various times. The linear fit (solid line) corresponds to an ambipolar carrier diffusion coefficient of $D_a = 21$ cm^{2}s^{-1}. (d)-(f) Spatio-temporal dynamics of spin density obtained in the same scans.

The right half of Fig. 2.2 shows the spin component of the diffusion process measured simultaneously with density. The contour map in Fig. 2.2d shows the spatio-temporal dynamics of spin density after optical excitation. Spin diffusion is evident by comparing the two profiles in Fig. 2.2e measured at t=5 ps (squares) and t =300 ps (circles). The profile remains Gaussian, as confirmed by the fits (solid lines). However, the spin density profile at t=300 ps is narrower than the electron density profile shown in Fig. 2.2b. This indicates different transport behavior of spin and electron densities. Quantitatively, the squared width of the spin density profile doesn't increase linearly, as shown in Fig. 2.2f, in striking contrast to the expansion of electron density profile obtained in the same measurement. Initially, the expansion rate of the spin density profile is similar to that of electron density profile. At later times, the spin diffusion slows down considerably relative to the density diffusion. The observed sub-linear expansion of spin density profile shows that spin diffusion cannot be described as a classical diffusion process with a *constant* diffusion coefficient.

The procedure summarized in Fig. 2.2 is used to systematically study the influence of electron density on the diffusion process. The sub-linear expansion of the spin density profile is observed at all densities and changes systematically with the peak electron density. In Fig. 2.3 we show several examples. The decrease of the slope with time is more pronounced at higher densities. Meanwhile, the simultaneously obtained expansions of the electron density profile (not shown) are all linear and similar to Fig. 2.2c. To approximately compare the rates of spin diffusion and carrier diffusion, we perform linear fits to the data with $t > 150$ ps (solid lines in Fig. 2.3). In this range the expansion is approximately linear. The spin diffusion coefficients deduced by the fits are plotted in Fig. 2.4 (circles) as a function of peak electron density. The ambipolar carrier diffusion coefficients are also plotted (squares) for comparison. In the density range studied, the ambipolar carrier diffusion coefficient is almost constant. In contrast, the spin diffusion coefficient decreases significantly with peak electron density.

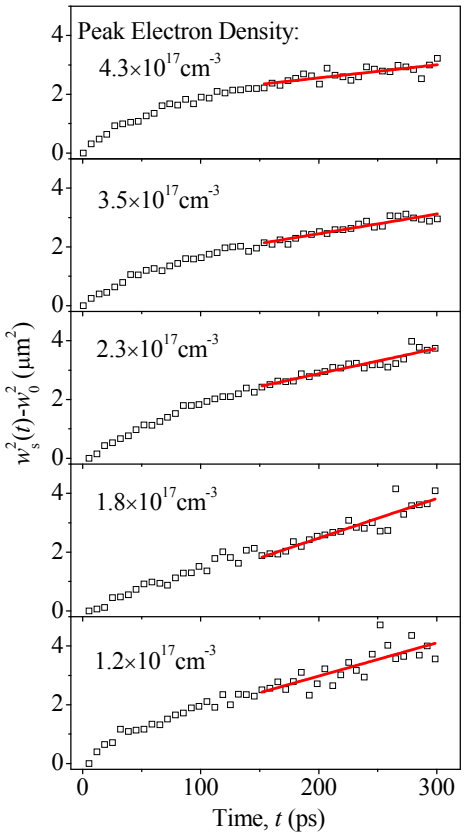

Figure 2.3: Expansions of spin density profiles at several peak electron densities as indicated in each panel, obtained by repeating the procedure summarized in Fig. 2.2. A sublinear expansion is generally observed. Linear fits to data with $t > 150$ ps (solid lines) are used in order to approximately illustrate the density dependence of spin diffusion.

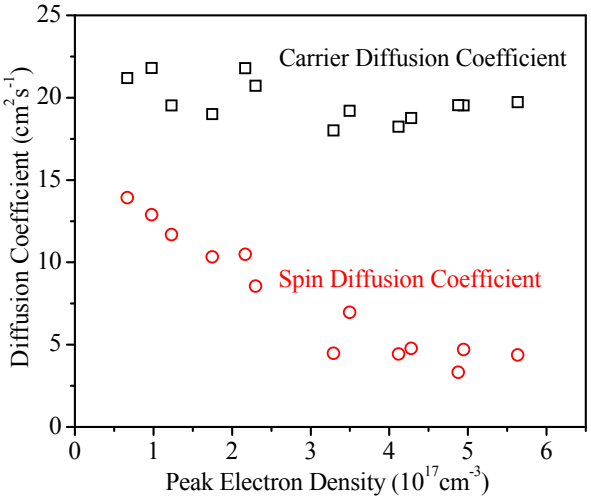

Figure 2.4: Ambipolar carrier diffusion coefficient (squares) and spin diffusion coefficient (circles) as functions of peak electron density obtained by repeating the procedure summarized in Fig. 2.2 at various electron densities. These coefficients are deduced by linear fits as shown in Figs. 2 and 3. A significant decrease of spin diffusion coefficient with peak electron density is observed. The carrier diffusion coefficient is almost constant.

2.4 Drift-diffusion theory

We denote the density of holes by p. The drift-diffusion equations for the three coupled densities $n_\uparrow$, $n_\downarrow$, and p are[36]

$$\frac{\partial n_\uparrow}{\partial t} = \boldsymbol{\nabla}\cdot\left[\frac{\sigma_\uparrow}{e}\mathbf{E} + D_{\uparrow\uparrow}\boldsymbol{\nabla}n_\uparrow + D_{\uparrow\downarrow}\boldsymbol{\nabla}n_\downarrow\right] + \frac{n_\downarrow}{\tau_{\downarrow\uparrow}} - \frac{n_\uparrow}{\tau_{\uparrow\downarrow}}, \tag{2.2}$$

$$\frac{\partial n_\downarrow}{\partial t} = \boldsymbol{\nabla}\cdot\left[\frac{\sigma_\downarrow}{e}\mathbf{E} + D_{\downarrow\downarrow}\boldsymbol{\nabla}n_\downarrow + D_{\downarrow\uparrow}\boldsymbol{\nabla}n_\uparrow\right] + \frac{n_\uparrow}{\tau_{\uparrow\downarrow}} - \frac{n_\downarrow}{\tau_{\downarrow\uparrow}}, \tag{2.3}$$

$$\frac{\partial p}{\partial t} = \boldsymbol{\nabla}\cdot\left[-\frac{\sigma_p}{e}\mathbf{E} + D_p\boldsymbol{\nabla}p\right], \tag{2.4}$$

where $\sigma_\uparrow$, $\sigma_\downarrow$ and σ_p are the ordinary conductivities of spin-up electrons, spin-down electrons and holes, respectively; $D_{\sigma\sigma'}$ is the spin-diffusion matrix for electrons; $\mathbf{E}$ is the electric field; $1/\tau_{\uparrow\downarrow}$ and $1/\tau_{\downarrow\uparrow}$ are the spin flip rates from up to down and down to up, respectively.

Several physical assumptions underlie the above equations. First, we have completely

neglected the hole spin polarization under the assumption that their spin relaxation time is very short. Second, we have neglected electron-hole recombination - an assumption well confirmed by experimental observation for the time scales of interest. Third, by keeping the off-diagonal elements of the spin-diffusion matrix (e.g. $D_{\uparrow\downarrow}$) we have allowed in principle for the effect of *spin Coulomb drag*[37], whereby a gradient of spin-up density can drive a current of spin down and vice-versa. The explicit form of this matrix is

$$\hat{D} = \frac{D_n}{1+\gamma\tau}\begin{bmatrix} 1+\frac{n_\uparrow}{n}\gamma\tau & \frac{n_\uparrow}{n}\gamma\tau \\ \frac{n_\downarrow}{n}\gamma\tau & 1+\frac{n_\downarrow}{n}\gamma\tau \end{bmatrix}, \tag{2.5}$$

where $D_n = \mu_n k_B T/e$ is the electron diffusion constant, τ is the momentum relaxation time for electrons, and γ is the spin Coulomb drag coefficient. The steps for deriving the spin diffusion matrix from the spin resistivity matrix are outlined in Appendix A.1.

The time rates of change of $n_\uparrow$ and $n_\downarrow$ can alternatively be written in terms of total density $n = n_\uparrow + n_\downarrow$ and spin density $s = n_\uparrow - n_\downarrow$ as follows:

$$\frac{\partial n}{\partial t} = \boldsymbol{\nabla}\cdot\left[\mu_n n\mathbf{E} + D_n\boldsymbol{\nabla}n\right], \tag{2.6}$$

$$\frac{\partial s}{\partial t} = \boldsymbol{\nabla}\cdot\left[\mu_n s\mathbf{E} + D_s\left(\boldsymbol{\nabla}s + s\gamma\tau\boldsymbol{\nabla}\ln n\right)\right] - \frac{s}{\tau_s}, \tag{2.7}$$

where μ_n and μ_p are the mobilities of electrons and holes, respectively, and we have used the standard relations: $\sigma_{\uparrow(\downarrow)} = n_{\uparrow(\downarrow)} e\mu_n$ and $\sigma_p = ep\mu_p$. In the second equation we have set

$$D_s = \frac{D_n}{1+\gamma\tau} \tag{2.8}$$

and have assumed $1/\tau_{\uparrow\downarrow} = 1/\tau_{\downarrow\uparrow}$. Finally, $1/\tau_{\uparrow\downarrow} + 1/\tau_{\downarrow\uparrow} = 1/\tau_s$, where $1/\tau_s$ is the spin relaxation rate.

The electric field $\mathbf{E}$ arises from the small charge imbalance that inevitably occurs as low-mobility holes try to keep up with high-mobility electrons. Even though the charge

imbalance is very small, it would not be legitimate to neglect this field, since the conductivity of the electrons is very high. Comparing the equations for n (2.6) and p (2.4), and making use of the approximate charge neutrality condition $p \cong n$, we identify the electric field as

$$\mathbf{E} = \frac{D_p - D_n}{\mu_p + \mu_n} \frac{\boldsymbol{\nabla} n}{n} \,. \tag{2.9}$$

Given the relative magnitudes of $D_p < D_n$, we can see that the electric field points away from high density regions. The impact of this small electric field is a slight resistance to the diffusion of electrons.

Substituting this into Eqs. (2.6) and (2.7) we arrive at our final diffusion equations:

$$\frac{\partial n}{\partial t} = D_a \nabla^2 n \,, \tag{2.10}$$

$$\frac{\partial s}{\partial t} = \boldsymbol{\nabla} \cdot [(D_a - D_s) s \boldsymbol{\nabla} \ln n + D_s \boldsymbol{\nabla} s] - \frac{s}{\tau_s} \,, \tag{2.11}$$

where

$$D_a = \frac{D_n \mu_p + D_p \mu_n}{\mu_n + \mu_p} \tag{2.12}$$

is the *ambipolar* diffusion constant, which is intermediate between D_n and D_p but numerically closer to the diffusion constant of the less mobile species (holes in this case). Eq. (2.10) is the standard electron diffusion equation with ambipolar diffusion constant. Assuming that the electron density packet at the initial time $t = 0$ has a Gaussian shape $n(r, 0) = N e^{-4 \ln(2) r^2 / w_0^2}$ we see that the solution at time t is given by

$$n(r, t) = N \left(\frac{w_0^2}{w_{\mathrm{n}}^2(t)} \right)^{3/2} e^{-4 \ln(2) r^2 / w_{\mathrm{n}}^2(t)}, \tag{2.13}$$

where $w_{\mathrm{n}}^2(t) = w_0^2 + 16 \ln(2) D_a t$. The linear growth in time of the area covered by the packet is in excellent agreement with the experimental observation, as shown in Fig. 2.2c.

Let us now consider Eq. (2.11) for the spin density. We assume that the initial spin

distribution is proportional to the density distribution, i.e., we have

$$s(r,0) = Cn(r,0)\,, \tag{2.14}$$

where C is a constant independent of position. For the present experiment the expected value of C is $1/2$. The number of spin-up electrons is three times larger than the number of spin-down electrons, owing to selection rules for two-photon absorption of circularly polarized light.[32] Then, *if the spin relaxation time is neglected* we see immediately, by direct substitution, that the solution of Eq. (2.11) is

$$s(r,t) = Cn(r,t)\,. \tag{2.15}$$

In other words, the spin density and the ordinary density diffuse at exactly the same rate, controlled by D_a.

It should be noted that this result holds irrespective of the value of the spin Coulomb drag coefficient. This is in sharp contrast with the case of *unipolar* spin packets[38] in which the same theory predicts the spin diffusion constant to be D_s, given by Eq. (2.8), which is evidently affected by spin Coulomb drag. The difference is easily understood if one considers that in the unipolar case the requirement of charge neutrality forces the electrons of opposite spin orientations to move in opposite directions: spin Coulomb drag arises from this relative motion. In the present case, charge neutrality is ensured by the holes. Thus, the electrons move in the same direction regardless of spin – there is no relative motion and therefore no spin Coulomb drag. The above solution (2.15) was found for the initial condition (2.14) but we have checked that, even if the spin density is not initially proportional to the density, it eventually becomes proportional to the density at sufficiently long times.

We conclude that the experimental observation of an apparently decreasing spin diffusion coefficient cannot be explained within the framework of the drift-diffusion theory, unless one

is willing to include the spin relaxation time. Further, it is easy to see that a *homogeneous* spin relaxation time ($1/\tau_s$ independent of density and hence of position) will not change the situation, for the solution of Eq. (2.11) in the presence of such a relaxation time is simply

$$s(r,t) = Cn(r,t)e^{-t/\tau_s}\,. \tag{2.16}$$

There is now a global decay of the spin in time, but still no change in the apparent rate of diffusion.

2.5 Inhomogeneous spin relaxation

In view of the above discussion we now examine the possibility of explaining the experimental data in terms of non-homogeneous spin relaxation. Suppose for instance, that the spin relaxation rate were larger at lower density, i.e. larger in the tails of the spin packet than at its center. This would produce the impression of slower spin diffusion, since the outward diffusion of the spin would be hidden by the more rapid decay of the spin at the edges (Fig. 2.5). To verify this idea, Dr. Hui Zhao measured the spin relaxation time as a function of peak electron density by using the same pump-probe technique. The results shown in Fig. 2.7 confirm this conjecture (see discussion below). The spin relaxation time is larger for packets of higher density, suggesting that $1/\tau_s$ increases with decreasing density. However, these are measurements of the lifetime of the spin packet as a whole, whereas in the drift-diffusion theory we need a position-dependent spin relaxation rate, determined by the local density.

We have developed a model for the position dependence of the spin relaxation rate along the following lines. First, we notice that electron-impurity effects or spin-orbit interactions with the lattice could not account for the spatial variation of $1/\tau_s$ within the packet, since the impurity environment and the crystalline environment are uniform over the region occupied

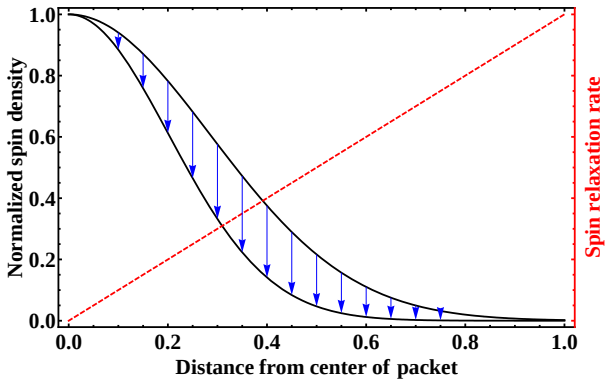

Figure 2.5: As electron density decreases, the spin relaxation rate increases (dashed line). A non-uniform spin relaxation rate across the packet gives the appearance of slower width increase. The length of the arrows is given by product of density and relaxation rate. (Linear $1/\tau_s$ for illustrative purposes only)

by the packet. What is not uniform is the frequency of electron-electron and electron-hole collisions. Because the Coulomb interaction is screened and thus effectively becomes of short range, we can say that the carriers near the center of the packet experience an electronic environment of higher density, and their scattering rate is accordingly higher than in the tails of the packet, where they experience an electronic environment of lower density.

How does the variation of the carrier-carrier scattering time translate into the observed spatial variation of the spin relaxation rate? A plausible answer comes from the Dyakonov-Perel spin relaxation mechanism[17, 39]. In this mechanism, spin relaxation is primarily due to spin-orbit interaction with the lattice. In GaAs the primary mechanism is the independent precession of each electron in the Dresselhaus k-dependent effective magnetic field[19]

$$\mathbf{\Omega_k} = \alpha_c \hbar^2 \left(2 {m_c}^3 E_g\right)^{-1/2} \boldsymbol{\kappa}\,, \tag{2.17}$$

$$\boldsymbol{\kappa} = \left\{ k_x \left(k_y^2 - k_z^2\right),\, k_y \left(k_z^2 - k_x^2\right),\, k_z \left(k_x^2 - k_y^2\right) \right\}\,, \tag{2.18}$$

where we apply the following parameters for GaAs: the spin orbit coupling is $\alpha_c \simeq 0.07$;

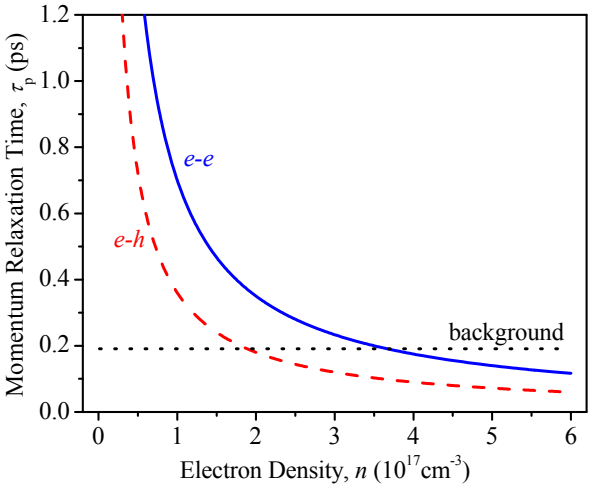

Figure 2.6: The momentum relaxation times due to e-e (solid line) and e-h (dashed line) scattering are on the same order of magnitude as the background scattering (dotted line) in high density regions ($> 10^{17}\text{cm}^{-3}$) but become quite long at lower densities. Under the present interaction model, the rate of carrier-carrier collisions is proportional to n. Here the relaxation time is calculated for wave vector $k = 1.43 \times 10^8$ m^{-1} and screening wave vector $k_0 = 1.89 \times 10^8 \text{m}^{-1}$.

the effective mass of conduction electrons is $m_c = 0.067 m_e$; the band gap energy is $E_g = 1.5eV$. Notice that the effective magnetic field depends on the momentum $\mathbf{k}$ of the electron. Electron-electron (e-e) and electron-hole (e-h) collisions change the momentum of the electron, and thus change the direction and magnitude of $\mathbf{\Omega_k}$. This hinders the process of spin relaxation, especially in regions where momentum-changing collisions are frequent, i.e. high-density regions. Referencing the derivation of Dyakonov-Perel spin relaxation in Chapter 1, the rate of spin relaxation can be approximated by the degenerate formula in Eq. (1.35) as

$$\frac{1}{\tau_s} = \tau^* \frac{32}{105} \frac{\alpha_c^2 \varepsilon_F^3}{\hbar^2 E_g}, \tag{2.19}$$

where τ^* is related to the momentum relaxation time by the effectiveness of the scattering event on the randomization of the precession axis of Ω_k.

We have evaluated the contribution of e-e and e-h interactions to the lifetime of a

momentum state in a homogeneous environment of density n according to standard formulas reported for example in reference [40], but evaluated at the parameters of the experiment. In order to simplify evaluation of the momentum relaxation time we use a screened Coulomb interaction model of the form

$$V(r) = \frac{e^2}{\epsilon_r r} e^{-k_0 r} \tag{2.20}$$

where k_0 is a fitting parameter on the order of the Debye screening wave vector at $n = 10^{17}$ cm^{-3} and Boltzmann statistics are used throughout. This is admittedly a significant approximation as the electrons are degenerate above $\sim 10^{17}$ cm^{-3}. While numerical accuracy may be improved, qualitative aspects are generalizable. Our results are shown in Fig. 2.6, where the momentum relaxation times due to e-e and e-h scattering are compared to the background scattering due to impurities, which is density independent. These values have been obtained for a typical thermal value of $k = 1.43 \times 10^8$ m^{-1} with a screening wave vector $k_0 = 1.89 \times 10^8$ m^{-1}. High density regions exhibit a higher rate of collisions which could potentially slow spin relaxation, whereas low density regions are governed primarily by lattice scattering.

Using Eq. (2.19), we arrive at τ_s shown in Fig. 2.7, where the calculated spin relaxation time (solid line) is shown to be in good agreement with experiment (circles). We remind the reader that the experimental τ_s is plotted as a function of peak electron density, while Eq. (2.19) is being applied on a microscopic scale. The results of the calculation give us confidence that the Dyakonov-Perel mechanism, limited by carrier-carrier scattering, can indeed produce a spin relaxation of the right order of magnitude and, more importantly for us, one that is faster in the tails of the packet. We note that our results are consistent with a recent study where electron spin relaxation time in bulk GaAs at room temperature was found to increase linearly with carrier density when the Dyakonov-Perel mechanism dominates.[41]

With the inhomogeneous spin relaxation time, the spatio-temporal evolution of a spin

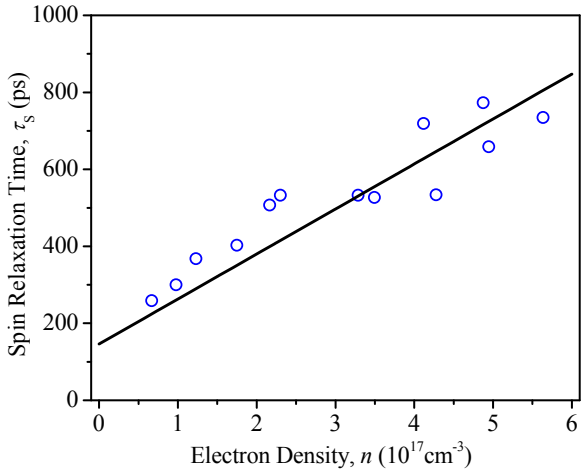

Figure 2.7: The spin relaxation time of electrons is inversely proportional to the momentum relaxation time and thus increases with density. Experimentally measured τ_s (circles) are plotted versus peak electron density.

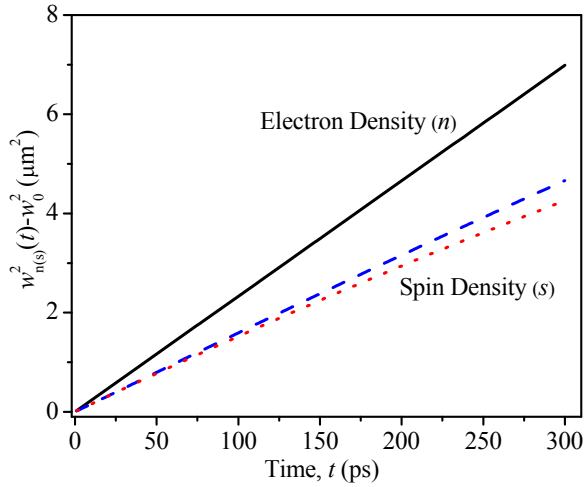

Figure 2.8: Squared width of the spin density packet calculated with (dotted line) and without (dashed line) taking into consideration spin Coulomb drag. These are considerably smaller than the squared width of a density packet (solid line). It is evident that spin Coulomb drag plays only a minor role in further reducing the apparent diffusion rate. Parameters used matched those of the experiment in Fig. 2.2.

polarized packet was evaluated using Eq. (2.11) with parameters similar to those used in Fig. 2.2. One dimensional dynamics were used for the simple goal of comparing diffusion rates. Fig. 2.8 illustrates the squared widths of the profiles of electron density and spin density over an interval of 300 ps, calculated by fitting a Gaussian curve at several times during the evolution. An interesting consequence of the inhomogeneous spin relaxation rate is that by breaking the trivial solution it "turns on" spin Coulomb drag, which would otherwise be completely inoperative. The spin diffusion rates with and without spin Coulomb drag are also compared. The differences are rather small, reflecting the fact that the slowing down of the spin is mostly apparent due to loss of spin in the edges of the packet rather than due to the relative motion of up- and down-spin components. Nonetheless, a small effect is visible and goes in the direction of further reducing the apparent spin diffusion.

2.6 Conclusion

We have studied, both theoretically and experimentally, diffusion of optically injected spin-polarized carriers in undoped GaAs quantum wells at 80 K. The experiment is performed with a high-resolution optical pump-probe technique. Spatio-temporal dynamics of locally injected spin-polarized carriers are directly resolved. By comparing expansions of electron and spin density profiles, we found that the spin diffusion cannot be described as a classical diffusion process with a constant diffusion coefficient. The spin diffusion appears to be slower than the ambipolar carrier diffusion. Our theoretical analysis, based on a three-component drift-diffusion equation, shows that the long time behavior of the spin density can be understood in terms of a spin relaxation rate that grows with decreasing density. This behavior is consistent with a model of Dyakonov-Perel spin relaxation limited by Coulomb scattering between carriers. However, the short time behavior of the spin-density remains for the time being beyond the reach of our drift-diffusion theory.

Acknowledgements

Hui Zhao acknowledges John Prineas of the University of Iowa for providing us with high-quality GaAs samples. This work was supported by NSF Grant No. DMR-0705460 and General Research Fund of The University of Kansas.

Chapter 3

Dyakonov-Perel spin relaxation in intrinsic GaAs

The contents of this chapter were published as an article in Physical Review B on April 14, 2011.[18] The presentation here is derived from that article.

3.1 Introduction

The most complete study of spin relaxation in semiconductors to date is by Wu *et al.*,[7] who made calculations of the spin relaxation time (SRT) due to each of the relevant spin relaxation mechanisms in III-V semiconductors: Bir-Aronov-Pikus (BAP) [14], Dyakonov-Perel (DP)[11], and Elliott-Yafet (EY)[12, 13]. Comparing the relative efficiencies of the mechanisms, their results suggest that Dyakonov-Perel spin relaxation is dominant for essentially all the electron densities and temperatures of experimental interest.[42] Although Teng *et al.* initially found cases where BAP spin relaxation dominates DP spin relaxation in intrinsic GaAs,[43] it was later pointed out by Jiang and Wu that non-degenerate statistics were being applied to degenerate electrons.[44] Also noted by Jiang *et al.*, Song and

Kim have investigated spin relaxation due to all of the relevant spin relaxation mechanisms in n- and p-type III-V semiconductors,[43] but their analytic expressions are again only applicable to the non-degenerate regime. Tamborenea *et al.*[15] have calculated EY SRTs due to electron-impurity and electron-electron collisions in n-doped GaAs for a wide range of temperatures and electron densities, finding that the EY mechanism alone is insufficient to explain experimental SRT measurements,[45] suggesting that DP spin relaxation may account for the discrepancies. These findings encourage us to continue looking at DP spin relaxation as the primary spin relaxation mechanism in GaAs and similar semiconductors of the zincblende structure.

The focus of the present study is on the role played by many-body interactions on the DP spin relaxation mechanism – a role that we would like to clearly disentangle from that of other scattering mechanisms. The theory of many-body effects in DP spin relaxation for electrons in semiconductors was formulated in several papers by Wu, Ning, and Weng,[46, 47] and separately by Glazov and Ivchenko.[48, 49] The basic idea is that electron-electron scattering causes the electron quasiparticle to perform a random walk in momentum space; this in turn causes random variations of the direction and magnitude of the spin precession axis. DP spin relaxation arises from the cumulative effect of many small precessions about randomly varying axes, and its main signature is that the spin relaxation rate is inversely proportional to the momentum scattering rate. In doped bulk semiconductors at low temperatures, however, it is difficult to disentangle the contribution of the electron-electron scattering rate from the similar but much larger contribution of electron-impurity scattering. An important exception arises in intrinsic semiconductors, when a non-equilibrium population of electrons *and holes* can be created by optical excitation. By using circularly polarized light it is possible to achieve a high degree of spin polarization of the electrons in the conduction band (the spins of the holes relax rapidly due to strong spin-orbit interactions in the valence band), and the time evolution of this spin polarization can be monitored in real time. Such a system is virtually impurity free, and thus offers a unique opportunity

to directly test the impact of many-body interactions on DP spin relaxation of electrons.[50, 51]

The initial motivation for the present study came from an experiment in which a density-dependent diffusion rate for spin polarized electrons was observed in a photo-excited electron-hole packet in bulk GaAs.[20] Zhao *et al.* found that the spin density in such a packet has a smaller diffusion constant than the carrier density. It was argued that this could be explained by a density dependent spin relaxation rate, where the electron spins in low density regions of the packet relax faster than in the high density regions, leading to the *appearance* of slow diffusion. This behavior is consistent with that of DP spin relaxation controlled by electron-electron scattering in the non-degenerate regime,[49] which is indeed expected to occur in the low density regions of the electron-hole packet. Remarkably, the *increase* of the spin relaxation rate with decreasing density in the non-degenerate regime is opposite to the behavior in the degenerate regime,[42] where the spin relaxation rate *decreases* with decreasing density. This means that the SRT has a maximum as a function of density at a density intermediate between the degenerate and the non-degenerate regime.[52]

The present study continues our efforts to develop a better microscopic understanding of the many-body effects in DP spin relaxation. We consider electron-electron, electron-impurity, and electron-hole interactions in the degenerate regime. In this regime, the presence of a large Fermi surface paves the way to an elegant analytical treatment of electron-electron and electron-hole scattering rates – a treatment pioneered by Abrikosov and Khalatnikov in their classic paper on the theory of the Fermi liquid.[53] The relevant scattering rates are similar to but not identical with the well-known momentum scattering rates which control, for example, the lifetime of quasiparticles. The difference arises because different collision events are not equally effective at changing the magnitude and direction of the spin precession: the contribution of different collision events must be weighted according to their effectiveness at changing the spin precession. (A similar "weighting" – this time

concerning the effectiveness of collisions at changing the current – is responsible for the replacement of the scattering cross section by the "transport cross section" in microscopic calculations of the electrical conductivity). Glazov, *et al.* had previously looked at the contribution of electron-electron collisions to DP spin relaxation in the degenerate regime, but limited themselves to qualitative estimates.[49] Jiang, *et al.* applied the powerful kinetic spin Bloch equation approach, including all relevant spin relaxation mechanisms, but their work was primarily numerical.[42] In the present study, analytic expressions are derived which are applicable to a variety of semiconductors of the zincblende structure. In particular, the calculation of the relevant electron-electron and electron-hole scattering rates is reduced to the evaluation of simple two-dimensional and one-dimensional integrals over the Fermi surface. We find that electron-hole scattering is the dominant mechanism of momentum randomization in these intrinsic semiconductors. Nevertheless, we emphasize that our mechanism of spin relaxation remains conceptually distinct from the BAP mechanism in which electrons transfer their spin polarization to the holes via interband matrix elements of the Coulomb interaction. In the BAP mechanism a conduction band electron drops into the valence band and is replaced by another electron coming from the valence band. In the present mechanism – that is in the DP mechanism – conduction band electrons remain in the conduction band, while transferring momentum to the holes. The relative effectiveness of DP and BAP mechanisms has been well studied,[7, 42] and it has been found that the BAP mechanism is unimportant in intrinsic samples, or in doped samples when the electron density is high.[7] Therefore, we are confident that DP spin relaxation is the dominant mechanism in the temperature and density regimes investigated in this study.

Another novel feature of the present work is that we include exchange and correlation effects in the calculation of the effective electron-electron and electron-hole interactions. In practice, this means that we are going beyond the basic RPA-screened interaction. Exchange and correlation effects are included via local field factors, and we will show that these effects cause an enhancement of the scattering rate – and a corresponding reduction of spin

relaxation rate – at low density and low temperature (still in the degenerate regime). In the opposite limit of high density, the scattering lifetime becomes very large. A cautionary note is included for the treatment of DP spin relaxation in this regime. Specifically, the common assumption that momentum-changing collisions are frequent on the scale of spin relaxation fails, since the two processes occur on comparable time scales. In this regime the quasiparticles are essentially non-interacting and the DP mechanism is superseded by the spin precession of individual quasiparticles of essentially constant momentum.

This chapter is organized as follows: in Section 3.2, we review the steps and the assumptions in the derivation of the standard formula for Dyakonov-Perel spin relaxation; in Section 3.3 we derive analytic expressions for the effective (i.e. weighted) scattering rates due to electron collisions with electrons, holes and impurities; Section 3.4 describes the effective scattering amplitudes used in our calculations; Section 3.5 discusses the effective scattering rates and SRTs for doped and intrinsic GaAs; Section 3.6 contains our concluding remarks.

3.2 Dyakonov-Perel spin relaxation for degenerate electrons

Derivation of Dyakonov-Perel spin relaxation was covered Section 1.2. The result from Eq. (1.34) is

$$\frac{1}{\tau_s} = \frac{2}{3}\frac{\sum_{\mathbf{k}} \tau_k^* f_k^0(1-f_k^0)\langle\Omega_{\mathbf{k}}^2\rangle}{\sum_{\mathbf{k}} f_k^0(1-f_k^0)}\,, \tag{3.1}$$

where we work with Fermi-Dirac distributions for unpolarized electrons at equilibrium.

In the degenerate limit, $k_B T \ll \varepsilon_F$, the factor $f_k^0(1-f_k^0)$ entering the integrals in Eq. (1.34) is strongly peaked at the Fermi level. Since the spin orbit field $\Omega_{\mathbf{k}}$ in Eq. (1.5) is a slowly varying function of k, it is legitimate to set $k = k_F$ and take it out of the integral.

As a result, the spin relaxation rate takes the following simple form:

$$\frac{1}{\tau_s} = \frac{2}{3}\tau^*_{\rm avg}\langle\Omega^2_{\mathbf{k}}\rangle|_{k\to k_F}\,, \tag{3.2}$$

where

$$\tau^*_{\rm avg} = \frac{\sum_{\mathbf{k}}\tau^*_k f^0_k(1-f^0_k)}{\sum_{\mathbf{k}} f^0_k(1-f^0_k)}\,. \tag{3.3}$$

Hence, in the degenerate limit, the spin relaxation time τ_s is completely determined by two parameters: the mean square of the spin-orbit field $\langle\Omega^2_{\mathbf{k}}\rangle$ at the Fermi energy and a properly averaged effective scattering time $\tau^*_{\rm avg}$. While calculation of $\langle\Omega^2_{\mathbf{k}}\rangle$ is straightforward, to find $\tau^*_{\rm avg}$ we normally need to solve a complicated integral equation. One of the goals of this study is to show that $\tau^*_{\rm avg}$, and thus τ_s, can be calculated rigorously using methods developed in the theory of Fermi liquids.[54]

3.3 The effective scattering time

In order to calculate the effective scattering time $\tau^*_{\mathbf{k}}$ we need to construct the collision integral. Naturally, the construction depends on the nature of the collision process. Let us begin with electron-electron scattering processes. Electron-hole scattering processes will then be easily handled. These two scattering mechanisms are all that is needed to treat DP spin relaxation in intrinsic, photo-excited semiconductors. For doped semiconductors, electron-impurity scattering needs to be included.

3.3.1 Electron-electron collisions

The collision integral for an interacting Fermi liquid has been derived by several authors.[49, 55, 56] The most direct derivation starts from the Kadanoff-Baym quantum kinetic equa-

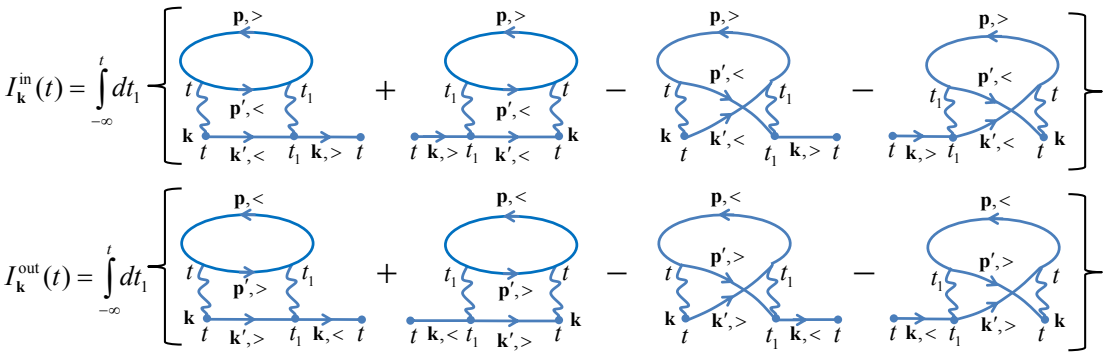

Figure 3.1: Contributions to the collision integral under the Born approximation.

tions.[57] The collision integral derived in this manner has the form

$$I_{\mathbf{k}}(t) = I^{\text{in}}_{\mathbf{k}}(t) - I^{\text{out}}_{\mathbf{k}}(t)\,, \tag{3.4}$$

where

$$I^{\text{in}}_{\mathbf{k}}(t) = \int_{-\infty}^{t} dt_1 \left\{\Sigma^{<}_{\mathbf{k}}(t,t_1)G^{>}_{\mathbf{k}}(t_1,t) + G^{>}_{\mathbf{k}}(t,t_1)\Sigma^{<}_{\mathbf{k}}(t_1,t)\right\}\,, \tag{3.5a}$$

$$I^{\text{out}}_{\mathbf{k}}(t) = \int_{-\infty}^{t} dt_1 \left\{\Sigma^{>}_{\mathbf{k}}(t,t_1)G^{<}_{\mathbf{k}}(t_1,t) + G^{<}_{\mathbf{k}}(t,t_1)\Sigma^{>}_{\mathbf{k}}(t_1,t)\right\}\,. \tag{3.5b}$$

Here, the lesser and greater Green's functions and the corresponding self-energies are all 2×2 matrices in spin space. For the self-energy function one adopts the Born approximation, in other words, second order in an effective electron-electron interaction. The scattering amplitude is denoted by $W_{\mathbf{kpk'p'}}$, where $\mathbf{k},\mathbf{p}$ are the momenta of the incoming particles and $\mathbf{k}',\mathbf{p}'$ those of the outgoing ones (Notice that one must have $\mathbf{k}+\mathbf{p}=\mathbf{k}'+\mathbf{p}'$ by momentum conservation). In the simplest approximation W is simply the Fourier transform of the Coulomb interaction:

$$W_{\mathbf{kpk'p'}} = \frac{4\pi e^2}{\epsilon|\mathbf{k}-\mathbf{k}'|^2}\delta_{\mathbf{k}+\mathbf{p},\mathbf{k}'+\mathbf{p}'}\,, \tag{3.6}$$

where ϵ is the background dielectric constant of the semiconductor and e is the electron charge. Here, we will include RPA screening and post-RPA screening via local field factors. In a more complete treatment, the effective interaction would also depend on the relative orientation of the spins; we will not consider such effects here, but simply assume that W is averaged over the relative spin orientations.

In Fig. 3.1, we show the diagrams that contribute to the collision integral in this approximation. As a further approximation, we adopt the generalized Kadanoff-Baym (GKB) ansatz[57, 58] relating the Green's functions to the distribution function:

$$G^<_{\mathbf{k}}(t,t') = \rho_{\mathbf{k}}(t)G^a_{\mathbf{k}}(t,t') - G^r_{\mathbf{k}}(t,t')\rho_{\mathbf{k}}(t')\,, \tag{3.7}$$

where

$$G^r_{\mathbf{k}}(t,t') = -i\theta(t-t')e^{-i\varepsilon_k(t-t')}\,, \tag{3.8a}$$

$$G^a_{\mathbf{k}}(t,t') = i\theta(t'-t)e^{-i\varepsilon_k(t-t')}\,, \tag{3.8b}$$

and $\varepsilon_k = \hbar^2k^2/2m^*$ is the single-electron energy in a parabolic band of effective mass m^*.[1] Notice that we are neglecting interaction contributions to the single particle energy, coming, for example, from exchange. It is assumed that these contributions are properly included in the effective mass. As a final approximation we ignore the difference between $\rho_{\mathbf{k}}(t_1)$ and $\rho_{\mathbf{k}}(t)$, i.e. we assume that the distribution function is slowly varying on the time scale probed by the integrals in Eq. (3.5). This is commonly referred to as the Markovian approximation, and is completely justified in the solution of a steady-state problem. Then, the remaining integral over time contains only a principle value term and a δ of conservation of energy. Retaining only the dissipative contribution (from the conservation of energy term), the final

[1] There is a sign correction in the exponential of Eq. (3.8b) compared to the published article [18].

expression is

$$I_{\mathbf{k}}(t)^{\text{e-e}} = -\frac{\pi}{\hbar}\sum_{\mathbf{k}'\mathbf{p}\mathbf{p}'}\delta\left(\varepsilon_k+\varepsilon_p-\varepsilon_{k'}-\varepsilon_{p'}\right)\delta_{\mathbf{k}+\mathbf{p},\mathbf{k}'+\mathbf{p}'}$$
$$\Big[\left|W_{\mathbf{k}\mathbf{p}\mathbf{k}'\mathbf{p}'}\right|^2\left(\left\{\rho_{\mathbf{k}},\hat{1}-\rho_{\mathbf{k}'}\right\}\mathrm{Tr}\left[\rho_{\mathbf{p}}\left(\hat{1}-\rho_{\mathbf{p}'}\right)\right]-\left\{\hat{1}-\rho_{\mathbf{k}},\rho_{\mathbf{k}'}\right\}\mathrm{Tr}\left[\left(\hat{1}-\rho_{\mathbf{p}}\right)\rho_{\mathbf{p}'}\right]\right)$$
$$-\left|W_{\mathbf{k}\mathbf{p}\mathbf{k}'\mathbf{p}'}W_{\mathbf{k}\mathbf{p}\mathbf{p}'\mathbf{k}'}\right|\left(\left\{\rho_{\mathbf{k}},\left(\hat{1}-\rho_{\mathbf{k}'}\right)\rho_{\mathbf{p}}\left(\hat{1}-\rho_{\mathbf{p}'}\right)\right\}-\left\{\hat{1}-\rho_{\mathbf{k}},\rho_{\mathbf{k}'}\left(\hat{1}-\rho_{\mathbf{p}}\right)\rho_{\mathbf{p}'}\right\}\right)\Big]\ . \quad (3.9)$$

We note that the collision integral in Eq. (3.9) can be shown to be exactly equivalent to the one presented in [49] by substituting $\rho_{\mathbf{k}} = f_{\mathbf{k}}\hat{1} + \mathbf{s}_{\mathbf{k}}\cdot\boldsymbol{\sigma}$ and carrying out some straightforward algebraic manipulations. However, at variance with Ref. [49], we only consider in the following the linearized form of the collision integral, take into account effects beyond RPA in the effective interaction, and neglect self-energy corrections which, when evaluated with properly screened interactions, can be shown to have negligible dependence on momentum.[40]

We now show that the relaxation-time approximation in Eq. (1.12) is consistent with this collision integral linearized in $\rho_{1\mathbf{k}}$. With $\delta\left(\varepsilon_k+\varepsilon_p-\varepsilon_{k'}-\varepsilon_{p'}\right)$, the quasi-equilibrium distributions make no contribution:

$$\left\{\rho_{0k},\left(\hat{1}-\rho_{0k'}\right)\right\}\mathrm{Tr}\left[\rho_{0p}\left(\hat{1}-\rho_{0p'}\right)\right] = \left\{\left(\hat{1}-\rho_{0k}\right),\rho_{0k'}\right\}\mathrm{Tr}\left[\left(\hat{1}-\rho_{0p}\right)\rho_{0p'}\right] \quad (3.10)$$

and

$$\left\{\rho_{0k},\left(\hat{1}-\rho_{0k'}\right)\rho_{0p}\left(\hat{1}-\rho_{0p'}\right)\right\} = \left\{\left(\hat{1}-\rho_{0k}\right),\rho_{0k'}\left(\hat{1}-\rho_{0p}\right)\rho_{0p'}\right\}\ . \quad (3.11)$$

Then, each term in the collision integral contains one ρ_1:

$$\begin{aligned}
&\left\{\rho_{\mathbf{k}}, \hat{1}-\rho_{\mathbf{k}'}\right\} \mathrm{Tr}\left[\rho_{\mathbf{p}}\left(\hat{1}-\rho_{\mathbf{p}'}\right)\right]-\left\{\hat{1}-\rho_{\mathbf{k}}, \rho_{\mathbf{k}'}\right\} \mathrm{Tr}\left[\left(\hat{1}-\rho_{\mathbf{p}}\right) \rho_{\mathbf{p}'}\right]= \\
&\quad\left\{\rho_{1\mathbf{k}}, \hat{1}-\rho_{0k'}\right\} \mathrm{Tr}\left[\rho_{0p}\left(\hat{1}-\rho_{0p'}\right)\right]+\left\{\rho_{1\mathbf{k}}, \rho_{0k'}\right\} \mathrm{Tr}\left[\left(\hat{1}-\rho_{0p}\right) \rho_{0p'}\right] \\
&-\left\{\rho_{0k}, \rho_{1\mathbf{k}'}\right\} \mathrm{Tr}\left[\rho_{0p}\left(\hat{1}-\rho_{0p'}\right)\right]-\left\{\hat{1}-\rho_{0k}, \rho_{1\mathbf{k}'}\right\} \mathrm{Tr}\left[\left(\hat{1}-\rho_{0p}\right) \rho_{0p'}\right] \\
&+\left\{\rho_{0k}, \hat{1}-\rho_{0k'}\right\} \mathrm{Tr}\left[\rho_{1\mathbf{p}}\left(\hat{1}-\rho_{0p'}\right)\right]+\left\{\hat{1}-\rho_{0k}, \rho_{0k'}\right\} \mathrm{Tr}\left[\rho_{1\mathbf{p}} \rho_{0p'}\right] \\
&-\left\{\rho_{0k}, \hat{1}-\rho_{0k'}\right\} \mathrm{Tr}\left[\rho_{0p} \rho_{1\mathbf{p}'}\right]-\left\{\hat{1}-\rho_{0k}, \rho_{0k'}\right\} \mathrm{Tr}\left[\left(\hat{1}-\rho_{0p}\right) \rho_{1\mathbf{p}'}\right]
\end{aligned} \tag{3.12}$$

and

$$\begin{aligned}
&\left\{\rho_{\mathbf{k}},\left(\hat{1}-\rho_{\mathbf{k}'}\right) \rho_{\mathbf{p}}\left(\hat{1}-\rho_{\mathbf{p}'}\right)\right\}-\left\{\hat{1}-\rho_{\mathbf{k}}, \rho_{\mathbf{k}'}\left(\hat{1}-\rho_{\mathbf{p}}\right) \rho_{\mathbf{p}'}\right\}= \\
&\quad\left\{\rho_{1\mathbf{k}},\left(\hat{1}-\rho_{0k'}\right) \rho_{0p}\left(\hat{1}-\rho_{0p'}\right)\right\}+\left\{\rho_{1\mathbf{k}}, \rho_{0k'}\left(\hat{1}-\rho_{0p}\right) \rho_{0p'}\right\} \\
&-\left\{\rho_{0k}, \rho_{1\mathbf{k}'} \rho_{0p}\left(\hat{1}-\rho_{0p'}\right)\right\}-\left\{\hat{1}-\rho_{0k}, \rho_{1\mathbf{k}'}\left(\hat{1}-\rho_{0p}\right) \rho_{0p'}\right\} \\
&+\left\{\rho_{0k},\left(\hat{1}-\rho_{0k'}\right) \rho_{1\mathbf{p}}\left(\hat{1}-\rho_{0p'}\right)\right\}+\left\{\hat{1}-\rho_{0k}, \rho_{0k'} \rho_{1\mathbf{p}} \rho_{0p'}\right\} \\
&-\left\{\rho_{0k},\left(\hat{1}-\rho_{0k'}\right) \rho_{0p} \rho_{1\mathbf{p}'}\right\}-\left\{\hat{1}-\rho_{0k}, \rho_{0k'}\left(\hat{1}-\rho_{0p}\right) \rho_{1\mathbf{p}'}\right\} .
\end{aligned} \tag{3.13}$$

These can be simplified a bit further, but at a loss of readability.

We assumed in Eq. (1.13) that the collision integral is proportional to $\rho_{1\mathbf{k}}$, which is in turn proportional to $[\mathbf{\Omega}_{\mathbf{k}} \cdot \boldsymbol{\sigma}, \rho_{0k}]$. Furthermore, each component of $\mathbf{\Omega}_{\mathbf{k}}$ gets all its angular dependencies from $l = 3$ spherical harmonics [e.g. $\Omega_{\mathbf{k},z}$ is expressed this way in Eq. (3.18)]. Obviously ρ_{0k} contains no such terms. Therefore $\rho_{1\mathbf{k}}$ must contain only $l = 3$ spherical harmonics. Viewing the collision integral as an integral operator,

$$\mathcal{L}\rho_{1\mathbf{k}} = \sum_{\mathbf{k}'} \mathcal{L}(\mathbf{k}, \mathbf{k}')\rho_{1\mathbf{k}'} , \tag{3.14}$$

it is apparent that $\mathcal{L}$, being rotationally invariant, has no means of changing the harmonic content of $\rho_{1\mathbf{k}'}$. Then, we reach the conclusion that the collision integral also contains only $l = 3$ harmonics. In other words, we see that the relaxation time approximation introduced

in Eq. (1.12) is consistent with the form of the linearized collision integral.

Clearly, $\rho_{1\mathbf{k}}$ is traceless; so then is the collision integral. We trace the linearized collision integral with $\boldsymbol{\sigma}$ to find a relationship between elements in $\rho_{1\mathbf{k}}$ and $I_{\mathbf{k}}$. In the limit of small spin polarization, $\rho_{\mathbf{k}}$ is expanded to first order in the polarization energy with the assumption that $\varepsilon_s \ll \varepsilon_k$. ρ_{0k} and $\rho_{1\mathbf{k}}$ then take the forms:

$$\rho_{0k} = f_k^0 \hat{1} + \beta\varepsilon_s f_k^0(1-f_k^0)\hat{\mathbf{s}}\cdot\boldsymbol{\sigma}\,, \tag{3.15}$$

$$\rho_{1\mathbf{k}} = \tau_{\mathbf{k}}^*\beta\varepsilon_s f_k^0(1-f_k^0)\left(\boldsymbol{\Omega}_{\mathbf{k}}\times\hat{\mathbf{s}}\right)\cdot\boldsymbol{\sigma}\,, \tag{3.16}$$

where f_k^0 is the unpolarized Fermi-Dirac distribution. Equating terms of first order in ε_s we find

$$\begin{aligned} &f_k^0(1-f_k^0)\boldsymbol{\Omega}_{\mathbf{k}}\times\hat{\mathbf{s}} = \\ &\quad\frac{4\pi}{\hbar}\frac{1}{(2\pi)^6}\sum_{\mathbf{p}'}\int d\mathbf{k}'\,d\mathbf{p}\,f_k^0(1-f_{k'}^0)f_p^0(1-f_{p'}^0)\delta\left(\varepsilon_k+\varepsilon_p-\varepsilon_{k'}-\varepsilon_{p'}\right)\delta_{\mathbf{k}+\mathbf{p},\mathbf{k}'+\mathbf{p}'} \\ &\quad\Big\{\left|W_{\mathbf{kpk'p'}}\right|^2\left[\tau_{\mathbf{k}}^*\boldsymbol{\Omega}_{\mathbf{k}}-\tau_{\mathbf{k}'}^*\boldsymbol{\Omega}_{\mathbf{k}'}\right] \\ &\qquad-\frac{1}{2}\left|W_{\mathbf{kpk'p'}}W_{\mathbf{kpp'k'}}\right|\left[\tau_{\mathbf{k}}^*\boldsymbol{\Omega}_{\mathbf{k}}-\tau_{\mathbf{k}'}^*\boldsymbol{\Omega}_{\mathbf{k}'}+\tau_{\mathbf{p}}^*\boldsymbol{\Omega}_{\mathbf{p}}-\tau_{\mathbf{p}'}^*\boldsymbol{\Omega}_{\mathbf{p}'}\right]\Big\}\times\hat{\mathbf{s}}\,. \end{aligned} \tag{3.17}$$

Cubic symmetry in III-V semiconductors permits us to consider only one component of this vector relation, $\boldsymbol{\Omega}_{\mathbf{k}}\times\hat{\mathbf{s}}\to\Omega_{\mathbf{k},z}$. The later quantity can be conveniently written in terms of spherical harmonics, $Y_l^m(\theta,\phi)$:

$$\Omega_{\mathbf{k},z} = \frac{\alpha_c\hbar^2k^3}{\sqrt{2m_c^3E_g}}\sqrt{\frac{8\pi}{105}}\left[Y_3^2(\vartheta_k,\varphi_k)+Y_3^{-2}(\vartheta_k,\varphi_k)\right]\,. \tag{3.18}$$

This fact, together with isotropy of the scattering, imply that the solution $\tau_{\mathbf{k}}^*$ of Eq. (3.17) does not depend on the direction of k. Indeed, assuming $\tau_{\mathbf{k}}^*=\tau_k^*$, we find that the presence of $\Omega_{\mathbf{k},z}$ [given by Eq. (3.18)] in the integrals in Eq. (3.17) already guarantees that the whole

right hand side has the proper angular dependences, consistent with that of the left hand side. As further evidence of this fact, it is easily demonstrated that integration of $\Omega_{\mathbf{q},z}$ (where $\mathbf{q}$ can be any of $\mathbf{k}'$, $\mathbf{p}$, or $\mathbf{p}'$) over $d\hat{\mathbf{q}}$ results in a term proportional to $\Omega_{\mathbf{k},z}$. This is shown in Appendix B.1.

As usual, further simplifications come in the degenerate limit because the factor $f_k^0(1-f_{k'}^0)f_p^0(1-f_{p'}^0)$ confines the momentum integrals to a narrow shell around the Fermi energy, where the density of states can be well approximated by a constant. In this case, $\tau_k^* = \tau^*(\xi)$ becomes a function of the dimensionless energy variable, $\xi = (\varepsilon_k - \mu)/(k_B T)$, which satisfies a one-dimensional integral equation of the following form:

$$B = \int_{-\infty}^{\infty} dx\, K(x,\xi)\left[\tau^*(\xi) - \lambda\tau^*(x)\right] . \tag{3.19}$$

The first term of the integral corresponds to the combination of each of the first terms in square brackets of Eq. (3.17); the second term in the integral picks up the remaining terms in the square brackets of Eq. (3.17). A detailed derivation of this equation, starting with Eq. (3.17), is given in Appendix B.2. The kernel $K(x,\xi)$ and the parameters B and λ

entering Eq. (3.19) are defined as follows:

$$K(x,\xi) = \frac{f^0(-x)}{f^0(-\xi)}\left[\frac{\xi - x}{1 - e^{x-\xi}}\right], \tag{3.20a}$$

$$B = \frac{\hbar^7 (2\pi)^4}{m_c^3 (k_B T)^2}\left(A_1 - \frac{A_2}{2}\right)^{-1}, \tag{3.20b}$$

$$\lambda = \frac{A_1\lambda_1 - A_2\lambda_2/2}{A_1 - A_2/2}, \tag{3.20c}$$

$$A_1 = \int d\Omega \, \frac{|W_{\mathbf{k}\mathbf{k}'}|^2}{\cos(\theta/2)}, \tag{3.20d}$$

$$A_2 = \int d\Omega \, \frac{|W_{\mathbf{k}\mathbf{k}'} W_{\mathbf{k}\mathbf{p}'}|}{\cos(\theta/2)}, \tag{3.20e}$$

$$\lambda_1 = \frac{1}{A_1}\int d\Omega \, \frac{|W_{\mathbf{k}\mathbf{k}'}|^2}{\cos(\theta/2)} P_3(\cos\theta_1), \tag{3.20f}$$

$$\lambda_2 = \frac{1}{A_2}\int d\Omega \, \frac{|W_{\mathbf{k}\mathbf{k}'} W_{\mathbf{k}\mathbf{p}'}|}{\cos(\theta/2)} \left[P_3(\cos\theta_1) - P_3(\cos\theta) + P_3(\cos\theta_2)\right]. \tag{3.20g}$$

$P_3(x)$ is the 3rd order Legendre polynomial. The solid angle $d\Omega = \sin\theta \, d\theta d\phi$ should not be confused with the Dresselhaus Larmor frequency. All of these angles (θ, ϕ, θ_1, θ_2) are described in Appendix B.2, but briefly: θ is the angle between $\mathbf{k}$ and $\mathbf{p}$; ϕ is the polar angle about the $\mathbf{k} + \mathbf{p}$ axis, between $\mathbf{k}'$ ($\mathbf{p}'$) and $\mathbf{k}$ ($\mathbf{p}$); $\cos\theta_1 = \hat{\mathbf{k}} \cdot \hat{\mathbf{k}}' = (1/2)(1 + \cos\theta + \cos\phi - \cos\theta\cos\phi)$; $\cos\theta_2 = \hat{\mathbf{k}} \cdot \hat{\mathbf{p}}' = (1/2)(1 + \cos\theta - \cos\phi + \cos\theta\cos\phi)$.

Integral equations of the type in Eq. (3.19) with a kernel of Eq. (3.20a) are common in the theory of transport coefficients of Fermi liquids.[53, 59] The general method of solution has been proposed by Sykes and Brooker.[54] This amounts to a clever Fourier transform utilizing the convolution theorem and ultimately changing the integral equation to a recognizable inhomogeneous differential equation. The solution to our Eq. (3.19) may then literally be read out from their paper:

$$\tau^*(\xi) = \frac{\cosh(\xi/2)}{2\pi}\int_{-\infty}^{\infty} d\omega \, e^{-i\omega\xi} \frac{B}{\pi} \sum_{l=0}^{\infty} \frac{(4l+3)\Phi_{2l}(\omega)}{\Lambda_{2l}(\Lambda_{2l} - \lambda)}, \tag{3.21}$$

where

$$\Phi_l(\omega) = p^1_{l+1}\left(\tanh \pi\omega\right) , \tag{3.22}$$

$$\Lambda_l = \frac{1}{2}(l+1)(l+2) , \tag{3.23}$$

and $p^m_l(x)$ are the associated Legendre polynomials.

In Section 3.2 we showed that the physical spin relaxation time is proportional to an average effective scattering time τ^*_{avg} given by Eq. (3.3). Expressing the summation over $\mathbf{k}$ in Eq. (3.3) in terms of a ξ-integral and using the solution of Eq. (3.21), we arrive at our final result:

$$\begin{aligned} \tau^*_{\text{avg}} &= \int_{-\infty}^{\infty} d\xi \left(-\frac{df^0_k}{d\xi}\right) \tau^*(\xi) \\ &= \frac{B}{2\pi^2} \sum_{l=0}^{\infty} \frac{4l+3}{\Lambda_{2l}\left[\Lambda_{2l} - \lambda\right]} . \end{aligned} \tag{3.24}$$

As it turns out, for all calculations performed in this study, the first two terms of the sum account for greater than 99% of total scattering time. The first term alone is about 95% of the sum at the lowest density examined ($n \sim 10^{16}\text{cm}^{-3}$) and the accuracy increases with increasing density.

For reference, we also mention the plane wave scattering time. This can be calculated readily from Eq. (B.24) by setting $P_3(x) \to 0$ and $\tau^*_k \to \tau_k$. The k-dependent scattering time is

$$\tau_k = 2B \left[\left(\frac{\varepsilon_k - \mu}{k_B T}\right)^2 + \pi^2\right]^{-1} \tag{3.25}$$

and the averaged scattering time is

$$\tau_{\text{avg}} = \frac{3B}{2\pi^2} . \tag{3.26}$$

Notice the close relationship between the plane wave scattering time and the $l = 0$ term of

the effective scattering time:

$$\tau^*_{\text{avg},l=0} = \frac{3B}{2\pi^2}\left(\frac{1}{1-\lambda}\right) . \tag{3.27}$$

For $0 < \lambda < 1$, the effective scattering time is enhanced (or the rate is decreased) compared to the plane wave scattering time. This range of λ is consistent with the calculations we make including the Dresselhaus field in Section 3.5.

3.3.2 Electron-hole collisions

The collision integral for electron-hole collisions is simply the direct-process-only portion of Eq. (3.9):

$$\begin{aligned} I_{\mathbf{k}}(t)^{\text{e-h}} = -\frac{\pi}{\hbar}\sum_{\mathbf{k}'\mathbf{p}\mathbf{p}'} \delta\left(\varepsilon_k + \varepsilon_p - \varepsilon_{k'} - \varepsilon_{p'}\right)\delta_{\mathbf{k}+\mathbf{p},\mathbf{k}'+\mathbf{p}'}\,|W_{\mathbf{k}\mathbf{k}'}|^2 \\ \left(\left\{\rho_{\mathbf{k}}, \hat{1}-\rho_{\mathbf{k}'}\right\}\text{Tr}\left[\rho^{(h)}_{\mathbf{p}}\left(\hat{1}-\rho^{(h)}_{\mathbf{p}'}\right)\right] - \left\{\hat{1}-\rho_{\mathbf{k}}, \rho_{\mathbf{k}'}\right\}\text{Tr}\left[\left(\hat{1}-\rho^{(h)}_{\mathbf{p}}\right)\rho^{(h)}_{\mathbf{p}'}\right]\right) , \end{aligned} \tag{3.28}$$

where $\rho^{(h)}$ is the hole density matrix. We consider equal densities of electrons and holes so that the Fermi momentum wavevectors are equal for the two species. This condition is likened to an intrinsic semiconductor under optical excitation. Additionally, the valence band energy for holes is considered parabolic.

The same logic used in solving the collision integral for electron-electron collisions (in Appendix B.2) can be applied here with the modification

$$d\mathbf{k}'\,d\mathbf{p} = \frac{m_c m_v^2}{2\hbar^6\cos(\theta/2)} d\varepsilon_{k'}\,d\varepsilon_p\,d\varepsilon_{p'}\,\sin\theta d\theta\,d\varphi\,d\varphi_p\,, \tag{3.29}$$

where m_v is the effective valence band hole mass. Following the same procedure used in e-e

scattering, the average effective scattering time for electron-hole collisions is

$$\tau_{\text{avg}}^{*(h)} = \frac{B^{(h)}}{2\pi^2} \sum_{l=0}^{\infty} \frac{4l+3}{\Lambda_{2l}\left[\Lambda_{2l} - \lambda_1\right]}\,, \tag{3.30}$$

where λ_1 is the same as in Eq. (3.20f), Λ_l is given by Eq. (3.23), and

$$B^{(h)} = \frac{\hbar^7 (2\pi)^4}{m_c m_v^2 \left(k_B T\right)^2} A_1^{-1}\,. \tag{3.31}$$

The plane wave scattering time is simply

$$\tau_k^{(h)} = 2B^{(h)} \left[\left(\frac{\varepsilon_k - \mu}{k_B T}\right)^2 + \pi^2\right]^{-1} \tag{3.32}$$

with an average of

$$\tau_{\text{avg}}^{(h)} = \frac{3B^{(h)}}{2\pi^2}\,. \tag{3.33}$$

3.3.3 Electron-impurity collisions

The collision integral for elastic collisions from impurities is considerably simpler:

$$I_{\mathbf{k}}(t)^{\text{e-i}} = -\frac{\pi}{\hbar} \sum_{\mathbf{k}'} \left|W_{\mathbf{k}\mathbf{k}'}\right|^2 \delta\left(\varepsilon_k - \varepsilon_{k'}\right)\left(\rho_{1\mathbf{k}} - \rho_{1\mathbf{k}'}\right)\,. \tag{3.34}$$

The resulting effective scattering rate is[5, 17]

$$\frac{1}{\tau_{k_F}^{*(i)}} = \frac{m_c k_F n_i}{4\pi\hbar^3} \int_{-1}^{1} d(\cos\theta)\ \left|W(\cos\theta)\right|^2 \left[1 - P_3(\cos\theta)\right]\,, \tag{3.35}$$

where n_i is the density of impurities.

3.4 Effective scattering amplitudes

We can apply the formulas derived in the previous section to the calculation of effective scattering times in both intrinsic and extrinsic semiconductors, provided they are in the degenerate regime ($k_BT \ll \varepsilon_F$). The intrinsic case will be considered first, since it is in this case that many-body effects play the dominant role. Electron-hole pairs are created in an intrinsic semiconductor by optical excitation and may, if the recombination time is sufficiently long, condense in a degenerate electron-hole liquid. The impurity concentration is negligible and electron-electron and, especially, electron-hole scattering plays the dominant role in controlling the DP mechanism of spin relaxation. We will also consider, for completeness, the electron liquid in extrinsic n-type doped semiconductors. In this case the doped electrons come from donor impurities and there is typically one impurity per electron. Furthermore, because we are considering a bulk semiconductor, the impurities are homogeneously distributed throughout the electron liquid, and thus provide the dominant scattering mechanism – far more important than electron-electron scattering, as we will see.

The crucial ingredient of the calculation is, of course, the effective interaction W to be used in Eqs. (3.24), (3.30), and (3.35). Here we have two options. The first option is to adopt a simple RPA-screened Coulomb interaction (also known as Lindhard screening); this leads to a parameter-free expression for the interaction, which should be exact in the high density limit. However, Lindhard screening is known to be inaccurate as the density decreases, and furthermore, the form of the RPA effective interaction misses important correlations between the electrons under consideration and the surrounding medium – correlations that become more and more important at low density. To counter these drawbacks, one may resort to a second option in which both the dielectric function and the effective interaction are modified by many-body local field factors which encapsulate exchange and correlation effects. (Discussion of these modified effective interactions can be found in Section 5.5 of reference [40].) Unfortunately, even this approach is not problem-free, since the local field

factors are imperfectly known in the electron liquid, and even more so in the electron-hole liquid. Nevertheless, the behavior of the many-body local field factors is constrained by exact sum rules and limiting cases which, taken together, allow us to form a qualitatively correct picture of the effective interaction at low density (still in the degenerate regime). We would like to point out that J. Zhou has also performed calculations of the spin relaxation time including Singwi-Tosi-Land-Sjölander local field corrections, but in 2D GaAs systems.[60]

We define the two-particle bare Coulomb interaction (v_{ij}) and static Lindhard function (χ_{0i}) ahead of time:

$$v_{ij}(q) = \frac{4\pi e_i e_j}{\epsilon_r q^2}\,, \tag{3.36}$$

$$\chi_{0i}(q) = -N_i(0)\left[\frac{1}{2} + \frac{1-x^2}{4x}\ln\left|\frac{1+x}{1-x}\right|\right]\,, \tag{3.37}$$

where $x = q/2k_F$, $N_i(0)$ is the density of states at the Fermi level for electrons or holes, and ϵ_r is the relative dielectric constant of the medium.

For the electron liquid, electron-electron interactions are handled by a spin averaged Kukkonen-Overhauser scattering amplitude:[61]

$$W^{\mathrm{EL}}_{e-e}(q) = v_{11}(q) + \left[v_{11}(q)\left(1 - G^s_{11}(q)\right)\right]^2 \chi_{11}(q)\,, \tag{3.38}$$

with the static density-density response function:

$$\chi_{11}(q) = \frac{\chi_{01}(q)}{1 - v_{11}(q)\left[1 - G^s_{11}(q)\right]\chi_{01}(q)}\,. \tag{3.39}$$

$G^s_{11}(q)$ is the spin symmetric local field factor for electron liquids. The scattering amplitude has the following physical interpretation: The first term $v_{11}(q)$ is the bare Coulomb interaction between electrons while the second term has an electron interacting with the density

induced in the electron liquid which in turn acts on another electron (each with a reduced Coulomb interaction). Our calculations in the following section use a fit for $G^s_{11}(q)$ from Moroni, *et al.*[62] (also reviewed in [63]) which is based on diffusive Monte Carlo studies of the static density-density response function. It should be noted that $G^s_{11}(q)$ used in these calculations is intended for use with $2 < r_s < 10$ and $0 < q < 3k_F$, but limiting behavior and graphical analysis suggests the fit is still qualitatively reasonable for the range of r_s examined in this study, $0.4 < r_s < 2$ (r_s is the average inter-particle distance in units of the effective Bohr radius.). Since we are restricted to the Fermi surface, the range of q is not a concern, $0 < q < 2k_F$. Setting $G^s_{11}(q) = 0$ amounts to using the random phase approximation (RPA).

Impurity scattering rates in the electron liquid are calculated with the electron-test charge effective scattering amplitude:

$$W^{\mathrm{EL}}_{e-i}(q) = v_{21}(q) + v_{21}(q)\chi_{11}(q)v_{11}(q)\left[1 - G^s_{11}(q)\right] , \tag{3.40}$$

where $\chi_{11}(q)$ is as in Eq. (3.39) and we are assuming a uniform distribution of impurities. The physical interpretation is similar to that described for Eq. (3.38), except now the impurity interacts with the density induced in the electron liquid with the bare Coulomb interaction.

For the electron-hole liquid, a multicomponent scattering amplitude analogous to the Kukkonen-Overhauser formula is necessary:

$$W^{\mathrm{EHL}}_{ij}(q) = v_{ij}(q) + \sum_{kl=1}^{2} v_{ik}(q)\left[1 - G^s_{ik}(q)\right]\chi_{kl}(q)v_{lj}(q)\left[1 - G^s_{lj}(q)\right] . \tag{3.41}$$

Electron-electron scattering is represented by W^{EHL}_{11}, and electron-hole scattering by W^{EHL}_{12}.

The density response function is found from[64]

$$[(\underline{\chi})^{-1}]_{ij}(q) = [\chi_{0i}(q)]^{-1}\,\delta_{i,j} - v_{ij}(q)\left(1 - G^s_{ij}(q)\right)\,, \tag{3.42}$$

where $\underline{\chi}$ is the spin symmetric density response function in matrix form. The local field factors for electron-hole liquids (which should not be confused to be the same as those for the electron liquid) have not been well studied to the best of our knowledge. We opt to use an approximate form of $G^s_{ij}(q)$ from [64] with parameters based on a hole-to-electron mass ratio of $m_h/m_e = 6$, which is actually not too far from the value of the ratio in GaAs. Again, setting $G^s_{ij}(q) = 0$ amounts to using RPA.

3.5 Calculations of the effective scattering rates and spin relaxation times

According to Eq. (3.2), to calculate the spin relaxation time τ_s we need two ingredients: the average scattering time τ^*_{avg} and the mean square of the spin-orbit field $\langle\Omega^2_{\mathbf{k}}\rangle_{k_F}$. The former has been calculated in Section 3.3 and is given by Eq. (3.24) for electron-electron scattering and Eq. (3.30) for electron-hole scattering. The later can be found straightforwardly using the explicit form of $\Omega_{\mathbf{k}}$ in Eq. (1.5):

$$\frac{2}{3}\langle\Omega^2_{\mathbf{k}}\rangle_{k_F} = \frac{32}{105}\frac{\alpha_c^2\varepsilon_F^3}{\hbar^2 E_g}\,. \tag{3.43}$$

Inserting this result into Eq. (3.2), we get for the spin relaxation time

$$\frac{1}{\tau_s} = \tau^*_{\text{avg}}\frac{32}{105}\frac{\alpha_c^2\varepsilon_F^3}{\hbar^2 E_g}\,. \tag{3.44}$$

While the above results are valid for generic zincblende III-V semiconductors, we opt to include results for GaAs with the following properties: $m_c = 0.067m_e$, $m_v = 0.47m_e$,

$E_g = 1.43$eV, $\epsilon_r = 13.2$, and $\alpha_c = 0.07$. In Fig. 3.2, panel (a), the electron scattering rates from electrons and impurities in the electron liquid (EL) are plotted as functions of density. Panel (b) shows scattering from electrons and holes in the electron-hole liquid (EHL). Recalling that the SRT is proportional to the scattering rate, we can see immediately via application of Matthiesen's rule that between electron-electron (e-e) collisions and electron-impurity (e-i) collisions, the SRT will be controlled by e-i collisions in n-GaAs. Only at low densities do e-e collisions begin to make a significant contribution, and at that point degeneracy diminishes so that one should be more careful about including non-degenerate effects. In the electron-hole liquid (intrinsic GaAs), e-e collisions are downplayed even more and electron-hole collisions (e-h) dominate the effective scattering rate. The physical reason for this is that holes, with their large mass and concurrently high density of states provide effective screening of the electron-electron interaction, which thus turns out to be much smaller than in the electron liquid. On the other hand, the presence of e-h scattering more than makes up for what is lost in the e-e scattering strength.

When compared to the scattering rates of plane waves, the effective scattering rates are found to be generally smaller: see again Fig. 3.2. Approximating the effective scattering time by the plane wave lifetime can lead to a difference in the SRT of between 0 and 1 order of magnitude. As discussed in the introduction, this happens because some collision processes cause a large change in momentum but a small change in the Dresselhaus field (consider for example a collision that takes us from a point in **k**-space where the Dresselhaus field vanishes to another symmetry-related point where it also vanishes); such a process contributes to the plane wave lifetime, but has no effect on spin relaxation. The use of the effective scattering rate rather than the plane wave approximation appears to be of utmost importance for high densities, but one must be cautious that the rate of spin relaxation does not approach the order of magnitude of the momentum scattering rate, as we will see momentarily.

In Fig. 3.3 the effect of local field factors on the effective scattering rates is apparent

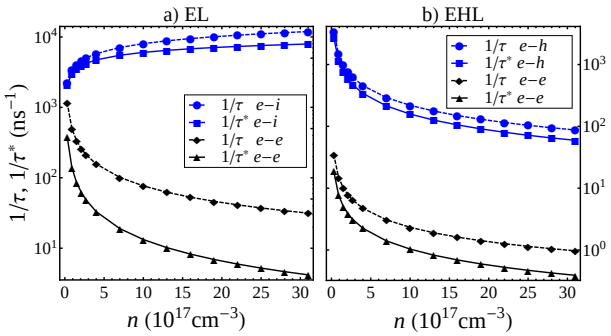

Figure 3.2: The plane wave and effective scattering rates in the a) electron liquid (EL) and b) electron-hole liquid (EHL) have been calculated with RPA at $T = 20$K.

especially at low densities. While the local field factors for the electron-hole liquid are rough approximations based on $m_v/m_c = 6$, and so their results might not be quantitatively accurate, they likely reflect the qualitative trends as functions of density. Additionally, while the local field factors for the electron liquid have been calculated using modern quantum Monte Carlo analyses of the density response function, they were designed for the pure electron liquid (no impurities) and considerably smaller densities. Disclaimers aside, we see that the inclusion of the local field factor generally enhances the effective scattering rates, and therefore suppresses the spin relaxation rate (e-e scattering in the EHL is a bit of an anomaly here). The enhancement of the interaction is expected on physical grounds since, as the density is lowered, the electron-hole liquid becomes increasingly "soft" – meaning a large density of low-lying excitations – and has a strong tendency to develop inhomogeneous density waves. The strong effective interaction arising from this softening was recognized long ago as a possible mechanism of superconductivity in the electron-hole liquid.[64] However, the precise value of r_s (the average inter-particle distance in units of the effective Bohr radius) at which the transition would occur, as well as the actual degree of enhancement at a given r_s, are still quite uncertain.

With regard to Zhao's work mentioned in the introduction, the claims argued there are still relevant. The spin polarized packets in Zhao's experiment consist of a degenerate center

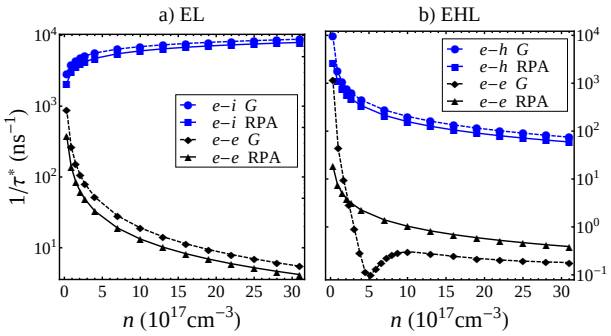

Figure 3.3: a) Local field factors for the electron liquid (EL) are derived from fits by Moroni, *et al.*[62] and their inclusion in the scattering amplitude has the overall effect of enhancing the scattering rate. b) Local field factors for the electron-hole liquid (EHL) are based on a hole-to-electron mass ratio of 6 and are found in Vignale, *et al.*[64] The G signifies inclusion of local field factors while RPA sets local field factors equal to 0. All rates have been calculated at $T = 20$K.

and non-degenerate tails. In the tails, e-i collisions are reduced in liu of e-e collisions so that the effective scattering rate is generally smaller than in the center of the packet. The net effect is that spins relax faster in the tails than in the center.

The spin relaxation times for n-GaAs and intrinsic GaAs are plotted in Fig. 3.4. As n-GaAs is largely dominated by e-i collisions, it can be understood why past theoretical curves fit the experimental data in references [65] and [66] so well. Caution should be taken when calculating the SRT for electrons in the electron-hole liquid. A region of validity becomes apparent for the relaxation time approximation in Eq. (1.13). As pointed out earlier, SRTs shorter than the plane wave scattering time break the derivation of the effective scattering time. The plane wave lifetime in n-GaAs is sufficiently short to avoid this problem for all densities examined here, but e-h scattering has a comparatively long scattering lifetime which results in unfeasibly short SRTs. Admittedly, the overall effective scattering rate ought to take into account all scatterers (phonons, impurities, etc.) which may ultimately lengthen the SRT. The intrinsic GaAs example here is an idealized electron-hole liquid.

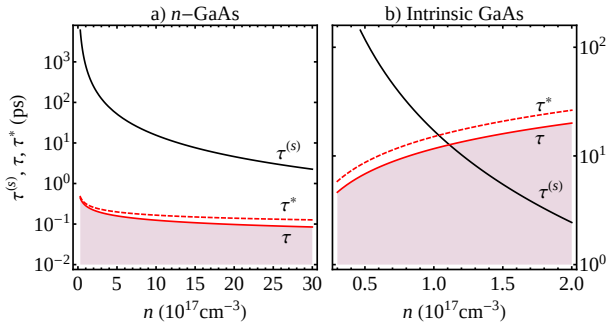

Figure 3.4: The spin relaxation time in a) n-GaAs and b) intrinsic GaAs. Calculations were performed with RPA at $T = 20$K. n-GaAs is modeled by the EL and includes contributions from electron-electron and electron-impurity collisions. Impurity collisions dominate the SRT for the degenerate electron liquid. Intrinsic GaAs is modeled by the EHL and includes contributions from electron-electron and electron-hole collisions. Electron-hole collisions dominate the SRT for the degenerate electron-hole liquid. Where the SRT crosses the scattering time marks the beginning of the breakdown of the standard DP assumptions. From this point on, spin relaxation and momentum relaxation occur on similar time scale and can no longer be separated. Eventually, at very high density, momentum relaxation becomes extremely slow and spin and momentum dynamics become decoupled again, this time with each spin performing an independent precession in the Dresselhaus field at a given point $\mathbf{k}$.

3.6 Conclusion

We have derived simple one- and two-dimensional integrals for the effective scattering rate of electrons in the many body system, valid in the degenerate regime. The energy dependence has been handled according to exact expressions by Sykes/Brooker[54] and the angular dependence is a result of a Dresselhaus field acting as an addition spin-axis re-orientation mechanism. In general, scattering events with the Dresselhaus field present are less effective in randomizing the momentum axis than without a field present.

In highly degenerate systems, the contribution of electron-electron scattering to the spin relaxation time is minimal in comparison to electron-impurity or electron-hole contributions. For the case of high degeneracy in intrinsic GaAs, we observe a limitation of the assumption that the timescale of spin relaxation is long compared to the scattering lifetime. In this regime, the quasiparticles are essentially non-interacting and the DP mechanism is superseded by the spin precession of individual quasiparticles of essentially constant momentum.

Local field factors, taking into account exchange and correlation effects, have been introduced into the scattering rate calculations. Scattering rates are generally enhanced compared to using RPA, more-so at low densities, for both electron-electron interactions and electron-hole interactions. Significant improvements to the accuracy of the scattering rates could be made with new local field factors tailored to the densities of typical intrinsic and n-type III-V semiconductors.

Acknowledgements

This work was supported by the National Science Foundation under grant number DMR-0705460 and the Department of Energy under grant number DE-FG02-05ER46203. The work of IVT was supported by Spanish MEC (FIS2007-65702-C02-01), "Grupos Consoli-

dados UPV/EHU del Gobierno Vasco" (IT-319-07), and the European Union through e-I3 ETSF project (Contract No. 211956). We are indebted to Ming-Wei Wu for a crucial discussion on the relevancy of many-body effects in the photo-excited electron-hole liquid in intrinsic semiconductors.

Chapter 4

Spin relaxation near a ferromagnetic transition

4.1 Introduction

The draw of magnetic semiconductors is readily apparent from the name; they offer an opportunity to blend magnetic and semiconducting properties in a single material. In spintronics, this is especially relevant because of the additional means of interaction through the magnetic and electrical properties of carriers. While ferromagnetism in dilute magnetic semiconductors[67–71] remains relegated to low temperatures, these systems have proven useful to better understand critical phenomena and some of the physics has potential application in metallic ferromagnets.[72–74]

In this chapter, we examine the impact of a ferromagnetic transition on carrier spin lifetimes. Strong spin fluctuations are expected for the constituents driving a ferromagnetic phase change.[75] These fluctuations can manifest themselves through enhanced carrier scattering. In the Dyakonov-Perel (DP) spin relaxation mechanism,[11] spin lifetimes are typically inversely related to scattering lifetimes. Then, in the DP mechanism, enhanced

scattering due to spin fluctuations can inhibit the rate of spin relaxation. Under these circumstances, we can find a crossover in dominant spin relaxation mechanism to Elliott-Yafet[7, 12, 13] or simply spin flips in scattering, both of which scale with the rate of scattering as opposed to inversely.

The model we use to simulate this ferromagnetic transition is a dilute magnetic semiconductor with itinerant carriers interacting via spin exchange with localized magnetic impurities. GaMnAs is the prototypical material to which this model is often applied, though not without controversy over the hole transport mechanism.[73, 76, 77] GaGdN is another example with s-f exchange driving the ferromagnetic transition.[7, 78, 79] We keep the discussion fairly generic, applying parameters related to a GaMnAs system for the sake of calculations and analysis, but noting that the model is meant more as an example of critical phenomena than an exact description of GaMnAs. Other articles have examined the critical behavior of GaMnAs in more detail.[77, 80–84] Our treatment is mean-field-like in that we replace the many-body interactions by an average self-consistent field generated by all the particles in the system. Still, we give it substance by considering dynamic spin fluctuations of the particles.

Derivations of spin relaxation times resulting from spin dependent scattering are presented for two mechanisms: spin flips in scattering and the DP mechanism. We find some interesting features not seen before with spin-independent scattering. The results are applicable to dynamic, spin-polarized systems and focus primarily on the contribution of carrier-carrier interactions mediated by the spin fluctuations of magnetic impurities. We apply common Fermi liquid theory techniques, beginning with the Kadanoff-Baym kinetic equation. In utilizing the GW approximation for the carriers' self-energy, the resulting expressions are generic to a wide variety of effective interactions. The results derived here follow previous analytic[7, 18, 47–49] and computational[42, 85, 86] studies, but extend on them significantly via inclusion of dynamics and dissipative spin-dependent interactions. The results have been reduced to relatively easy to calculate two dimensional integrals,

making them accessible to quick calculations.

This chapter is organized as follows: in Section 4.2, we present an effective interaction that can be used to generate a ferromagnetic transition and which will be used to calculate carrier scattering rates; in Section 4.3, we discuss the ferromagnetic phase change and the behavior of the scattering amplitude near the transition; in Section 4.4 we derive analytic expressions for the rate of spin relaxation due to spin-flips in scattering and the DP mechanism; in Section 4.5, we analyze some results of spin relaxation across a ferromagnetic transition; Section 4.6 contains our concluding remarks.

4.2 Effective spin-spin interaction

We first introduce the model dilute magnetic semiconductor on which we base calculations. Our model resembles the Zener model of ferromagnetism, with a ferromagnetic transition being driven by spin-exchange interactions between itinerant carriers and localized magnetic impurities.[84, 87] The Hamiltonian has the following contributions:

$$\mathcal{H}_\sigma = \int d\mathbf{r} \left(\frac{p(\mathbf{r})^2}{2m_c} + \mu_B g_\sigma \boldsymbol{\sigma}(\mathbf{r}) \cdot \mathbf{B}_\sigma(\mathbf{r}) \right) , \tag{4.1a}$$

$$\mathcal{H}_S = \int d\mathbf{R}\, \mu_B g_S \mathbf{S}(\mathbf{R}) \cdot \mathbf{B}_S(\mathbf{R}) \,, \tag{4.1b}$$

$$\mathcal{H}_{\sigma S} = \int d\mathbf{r} \int d\mathbf{R}\, J\delta\left(\mathbf{r} - \mathbf{R}\right) \boldsymbol{\sigma}(\mathbf{r}) \cdot \mathbf{S}(\mathbf{R}) \,. \tag{4.1c}$$

The carrier contribution to the Hamiltonian $\mathcal{H}_\sigma$ contains kinetic and magnetic terms, where m_c is the effective mass of the carriers, g_σ is their g-factor, and the field $\mathbf{B}_\sigma$ acts only on carriers. The magnetic impurities are localized, so their contribution to the Hamiltonian $\mathcal{H}_S$ has only a magnetic term, where g_S is the impurity g-factor and $\mathbf{B}_S$ is the field acting only on impurities. The impurities are taken to be sufficiently dilute that they do not interact with each other directly. The interaction between carriers and impurities is included in

$\mathcal{H}_{\sigma S}$. In its bare form, this is a contact type interaction $J\delta(\mathbf{r}-\mathbf{R})$, where J is the unit cell averaged interaction strength.

The alignment of spins with a magnetic field is linearized as $\mu_B g\langle\mathbf{s}\rangle = \chi\langle\mathbf{B}\rangle$, where χ is the magnetic susceptibility. We adopt the convention that spins align themselves anti-parallel to an applied magnetic field, or in other words, the magnetic moment prefers parallel alignment with a magnetic field. We create effective fields $\mathbf{B}_S^{\text{eff}}$ and $\mathbf{B}_\sigma^{\text{eff}}$ by combining the interaction J from Eq. (4.1c) with the bare fields:

$$\mu_B g_S \mathbf{B}_S^{\text{eff}}(\mathbf{R}) = \mu_B g_S \mathbf{B}_S(\mathbf{R}) + J\boldsymbol{\sigma}(\mathbf{R})\,, \tag{4.2}$$

$$\mu_B g_\sigma \mathbf{B}_\sigma^{\text{eff}}(\mathbf{r}) = \mu_B g_\sigma \mathbf{B}_\sigma(\mathbf{r}) + J\mathbf{S}(\mathbf{r})\,. \tag{4.3}$$

Later we will introduce a spin-orbit field that acts only on carriers to calculate the DP spin relaxation time. While it would be possible to include this term in Eq. (4.3), the spin-orbit field we consider is weak and its inclusion at this point would not appreciably affect the effective field. The magnetic fields in Eqs. (4.2) and (4.3) are specific to each specie, so it is cleanest to absorb $\mu_B g$ into these fields and write

$$\langle\mathbf{S}\rangle = \chi_{SS}^{(0)}\langle\mathbf{B}_S^{\text{eff}}\rangle\,, \tag{4.4}$$

$$\langle\boldsymbol{\sigma}\rangle = \chi_{\sigma\sigma}^{(0)}\langle\mathbf{B}_\sigma^{\text{eff}}\rangle\,, \tag{4.5}$$

where $\chi_{SS}^{(0)}$ and $\chi_{\sigma\sigma}^{(0)}$ are non-interacting (with regards to J) spin-spin susceptibilities for magnetic impurities and carriers, respectively. They have dimensions of inverse energy-volume. To be explicit, these fields relate to the physical magnetic field by $\mathbf{B}_s = g_s\mu_B\mathbf{B}$ and the susceptibilities are related to textbook magnetic susceptibilities by $\chi_{ss} = \chi/(g\mu_B)^2$.

The non-interacting spin susceptibility of the magnetic impurities is defined by assuming

$\langle S_z \rangle$ follows the Brillouin function $\mathcal{B}_J(x)$,

$$\langle S_z \rangle = -\mathrm{S}_S n_S \mathcal{B}_{\mathrm{S}_S}\left[\frac{\mathrm{S}_S \langle B_{S,z} \rangle}{k_B T}\right], \tag{4.6}$$

where S_S is the magnitude of the impurity spin and n_S is the density of magnetic impurities. Then, the longitudinal and transverse components of the susceptibility are calculated from

$$\chi^{(0)}_{S_z S_z} = \partial \langle S_z \rangle / \partial \langle B_{S,z} \rangle \,, \tag{4.7}$$

$$\chi^{(0)}_{S_\pm S_\mp} = 2\langle S_z \rangle / \langle B_{S,z} \rangle \,. \tag{4.8}$$

The non-interacting spin response of carriers coincides with Lindhard response:

$$\chi^{(0)}_{\sigma_z \sigma_z}(q,\omega) = \mathrm{S}_\sigma^2 \sum_{\mathbf{k},\alpha} \frac{f^0_{k\alpha} - f^0_{\mathbf{k}+\mathbf{q}\alpha}}{\hbar\omega + \varepsilon_{k\alpha} - \varepsilon_{\mathbf{k}+\mathbf{q}\alpha} + i\eta} \,, \tag{4.9}$$

$$\chi^{(0)}_{\sigma_+ \sigma_-}(q,\omega) = 4\mathrm{S}_\sigma^2 \sum_{\mathbf{k}} \frac{f^0_{k\uparrow} - f^0_{\mathbf{k}+\mathbf{q}\downarrow}}{\hbar\omega + \varepsilon_{k\uparrow} - \varepsilon_{\mathbf{k}+\mathbf{q}\downarrow} + i\eta} \,, \tag{4.10}$$

where S_σ is the magnitude of the carrier spin, $f^0_{k\alpha}$ is the equilibrium Fermi-Dirac distribution, and $\chi^{(0)}_{\sigma_-\sigma_+}(q,\omega) = [\chi^{(0)}_{\sigma_+\sigma_-}(q,-\omega)]^*$.

Alternative to defining effective fields, we can shift the interaction J into the spin susceptibilities to generate effective response functions. This is accomplished by solving the coupled linear Eqs. (4.4) and (4.5) for $\langle \boldsymbol{\sigma} \rangle$ and $\langle \mathbf{S} \rangle$ and identifying the effective response function as the proportionality between average spin and bare field. As we work on both sides of the ferromagnetic transition, it is necessary to break Eqs. (4.4) and (4.5) into longitudinal and transverse relations:

$$\begin{bmatrix} \langle S_z \rangle \\ \langle \sigma_z \rangle \end{bmatrix} = \underline{\underline{\chi_l}} \begin{bmatrix} \langle B_{S,z} \rangle \\ \langle B_{\sigma,z} \rangle \end{bmatrix}, \tag{4.11}$$

and

$$\begin{bmatrix} \langle S_+ \rangle \\ \langle S_- \rangle \\ \langle \sigma_+ \rangle \\ \langle \sigma_- \rangle \end{bmatrix} = \frac{1}{2} \underline{\underline{\chi_t}} \begin{bmatrix} \langle B_{S+} \rangle \\ \langle B_{S-} \rangle \\ \langle B_{\sigma+} \rangle \\ \langle B_{\sigma-} \rangle \end{bmatrix} , \tag{4.12}$$

where $s_\pm = s_x \pm i s_y$ and $B_{s\pm} = B_{s,x} \pm i B_{s,y}$. The effective susceptibilities are found to be

$$\underline{\underline{\chi_l}} = \begin{bmatrix} \chi_{S_z S_z} & \chi_{S_z \sigma_z} \\ \chi_{\sigma_z S_z} & \chi_{\sigma_z \sigma_z} \end{bmatrix} = \begin{bmatrix} 1/\chi^{(0)}_{S_z S_z} & -J \\ -J & 1/\chi^{(0)}_{\sigma_z \sigma_z} \end{bmatrix}^{-1} \tag{4.13}$$

and

$$\underline{\underline{\chi_t}} = \begin{bmatrix} \chi_{S_+S_-} & \chi_{S_+S_+} & \chi_{S_+\sigma_-} & \chi_{S_+\sigma_+} \\ \chi_{S_-S_-} & \chi_{S_-S_+} & \chi_{S_-\sigma_-} & \chi_{S_-\sigma_+} \\ \chi_{\sigma_+S_-} & \chi_{\sigma_+S_+} & \chi_{\sigma_+\sigma_-} & \chi_{\sigma_+\sigma_+} \\ \chi_{\sigma_-S_-} & \chi_{\sigma_-S_+} & \chi_{\sigma_-\sigma_-} & \chi_{\sigma_-\sigma_+} \end{bmatrix} = \begin{bmatrix} 1/\chi^{(0)}_{S_+S_-} & 0 & -J/2 & 0 \\ 0 & 1/\chi^{(0)}_{S_-S_+} & 0 & -J/2 \\ -J/2 & 0 & 1/\chi^{(0)}_{\sigma_+\sigma_-} & 0 \\ 0 & -J/2 & 0 & 1/\chi^{(0)}_{\sigma_-\sigma_+} \end{bmatrix}^{-1} , \tag{4.14}$$

where $\chi^{(0)}_{ss}$ are the non-interacting susceptibilities. Rather than give explicit expressions for every effective response function in Eqs. (4.13) and (4.14), we write only those which are used in this chapter. Namely, the effective impurity spin-spin response functions are

$$\chi_{S_z S_z}(q,\omega) = \frac{\chi^{(0)}_{S_z S_z}}{1 - J^2 \chi^{(0)}_{S_z S_z} \chi^{(0)}_{\sigma_z \sigma_z}(q,\omega)} , \tag{4.15}$$

$$\chi_{S_+ S_-}(q,\omega) = \frac{\chi^{(0)}_{S_+ S_-}}{1 - (J/2)^2 \chi^{(0)}_{S_+ S_-} \chi^{(0)}_{\sigma_+ \sigma_-}(q,\omega)} , \tag{4.16}$$

where $\chi_{S_- S_+}(q,\omega) = [\chi_{S_+ S_-}(q,-\omega)]^*$.

The interaction that interests us is the effective carrier-carrier interaction. This interaction is shown schematically in Fig. 4.1. By using the previously derived effective spin-spin

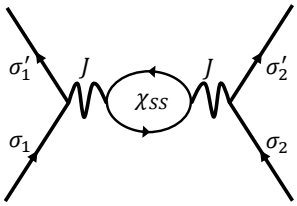

Figure 4.1: The effective spin-spin interaction between carriers. While carriers do not interact directly with each other via spin, the spin interaction J can be mediated by impurities through the effective spin-spin susceptibility χ_{SS}. Here, σ and σ' are the incoming and outgoing carrier spins, respectively.

susceptibility for impurities, we capture the effect of *collective* impurity spin fluctuations on scattering. Notice that although the non-interacting impurity spin response is frequency independent, the effective spin response is dynamic due to the inclusion of carrier dynamics. The longitudinal and transverse components of this interaction are

$$W_{\parallel}(q,\omega) = J^2 \chi_{S_z S_z}(q,\omega)\,, \tag{4.17}$$

$$W_{\perp}(q,\omega) = (J/2)^2 \left[\chi_{S_+ S_-}(q,\omega) + \chi_{S_- S_+}(q,\omega)\right]\,. \tag{4.18}$$

It can be verified that these effective interactions are equivalent to an infinite sum of all possible bare interactions mediated by non-interacting susceptibilities, e.g.

$$W = \sum_{n=1}^{\infty} J^{2n} \left[\chi_{SS}^{(0)}\right]^n \left[\chi_{\sigma\sigma}^{(0)}\right]^{n-1}\,.$$

4.3 Ferromagnetic transition and phase

An applied field will generate magnetization, subject to the average spins in Eqs. (4.4) and (4.5). By including the interaction J between carriers and impurities in the effective fields, we admit the possibility of magnetization in the absence of external fields. The transition is controlled by temperature and signaled by critical behavior in the previously derived

effective longitudinal response functions $\underline{\underline{\chi_l}}$. In the static, long wavelength limit, each of these response functions resembles a Curie-Weiss susceptibility with the form $(T - T_c)^{-1}$. Then, the paramagnetic $\leftrightarrow$ ferromagnetic phase change occurs when

$$\begin{aligned} 1 - J^2 \chi^{(0)}_{S_z S_z}(T_c) \lim_{q \to 0} \chi^{(0)}_{\sigma_z \sigma_z}(q, 0) &= 0 \\ \Rightarrow \quad T_c &= \frac{\mathrm{S}_S(\mathrm{S}_S + 1)}{3k_B} J^2 n_S \mathrm{S}_\sigma^2 N(0)\,, \end{aligned} \tag{4.19}$$

where $N(0)$ is the carrier density of states at the Fermi level.

We can self-consistently solve for the polarizations of, and average fields acting on, magnetic impurities and carriers below T_c. The polarization of the magnetic impurities is defined by the Brillouin function $\mathcal{B}_J(x)$:

$$P_S = \mathcal{B}_{\mathrm{S}_S}\left[\frac{\mathrm{S}_S\,|\langle B_{S,z}\rangle|}{k_B T}\right]. \tag{4.20}$$

To a good approximation, the field acting on carriers is equivalent to the first order interaction with magnetic impurities:

$$|\langle B_{\sigma,z}\rangle| \cong J \mathrm{S}_S n_S P_S\,. \tag{4.21}$$

The field acting on carriers also defines the spin splitting energy $\varepsilon_{F\uparrow} - \varepsilon_{F\downarrow}$ about the Fermi energy ε_F:

$$|\langle B_{\sigma,z}\rangle| = \varepsilon_F\left[(1 + P_\sigma)^{2/3} - (1 - P_\sigma)^{2/3}\right]. \tag{4.22}$$

Finally, we ensure self-consistency in the generated fields through expectation of a Goldstone mode on the ferromagnetic side of the transition. Effectively a long-range interaction, the polarized spins can all rotate together without any energy cost (a broken symmetry state). This mode is identified by setting $q = \omega = 0$ in the effective transverse susceptibility and

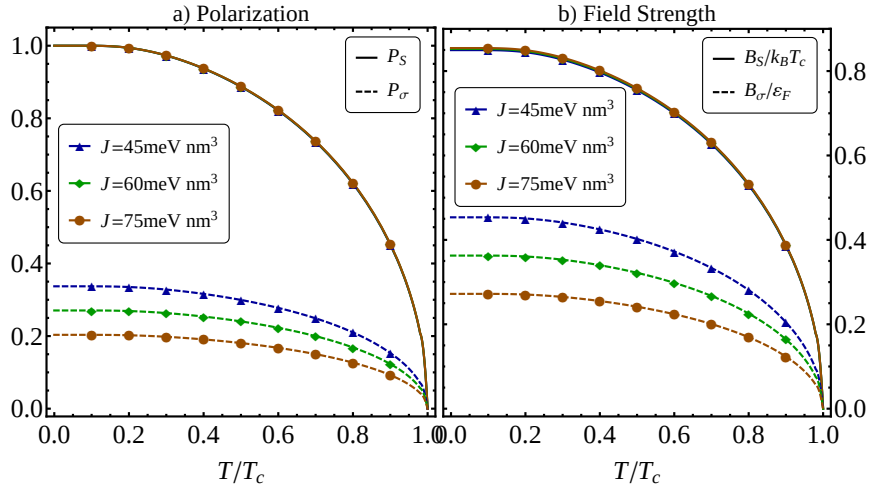

Figure 4.2: Polarizations and fields have been calculated using GaMnAs parameters for holes with effective mass $m_c = 0.5m_e$ and density $n_\sigma = 5 \times 10^{20}\text{cm}^{-3}$. The Mn acceptors have spin $\text{S}_S = 5/2$ and density $n_S = 0.05/\Omega_0$, where $\Omega_0 = 0.45 \times 10^{-22}\text{cm}^3$ is the unit cell volume in GaAs. a) The carrier and impurity spins closely follow the approximation $P_s(T) = P_s(0)\sqrt{1-(T/T_c)^2}$ from Ref. [88]. The carrier polarization does not saturate due to a significantly smaller magnetic susceptibility than for the impurities. b) As the fields are self-generated, their behavior parallels the $\sqrt{1-(T/T_c)^2}$ shape of polarization. The field acting on magnetic impurities is largely due to the second order RKKY-like interaction mediated by carriers, and scales with T_c for varying interaction strengths.

stipulating a divergence:

$$1-(J/2)^2\chi^{(0)}_{S_+S_-}(T)\lim_{q\to 0}\chi^{(0)}_{\sigma_+\sigma_-}(q,0) = 1-(J/2)^2\frac{2\langle S_z\rangle}{\langle B_{S,z}\rangle}\frac{2\langle\sigma_z\rangle}{\langle B_{\sigma,z}\rangle} = 0\,. \tag{4.23}$$

The resulting polarizations and fields for several values of J are plotted in Fig. 4.2.

It is instructive to examine the strength of the singularity in the effective interactions when T_c is approached. Approximating the non-interacting carrier susceptibility in the paramagnetic phase by its static, small-q form $\chi_{\sigma_z\sigma_z}(q,\omega) \cong -\text{S}_\sigma^2 N(0)\left(1-q^2/12k_F^2\right)$, we

can write the denominator of the scattering amplitude in Eq. (4.17) as

$$1 - J^2 \chi^{(0)}_{S_z S_z}(T) \chi^{(0)}_{\sigma_z \sigma_z}(q, 0) \propto \left[\frac{T - T_c}{T_c} + \frac{q^2}{12 k_F^2} \right] . \tag{4.24}$$

Then as $T \to T_c$, we have the same q^{-2} divergence in the interaction strength as a bare Coulomb interaction.

4.4 Spin relaxation

Typically, spin relaxation is understood to be the evolution of polarized spins into an unpolarized state. In a ferromagnetic system where there is an equilibrium spin polarization, spin relaxation refers to the evolution of spins into a polarized state. Thus, rather than picturing the process as decay of polarization, it's better to understand it as restoration of equilibrium polarization.

We focus on two mechanisms of spin relaxation: spin flips in scattering and Dyakonov-Perel (DP). Under a wide variety of temperatures, scattering sources, and degeneracy, the DP mechanism dominates in III-V semiconductors.[7, 42] Thus, we find it relevant to include derivations for this spin relaxation mechanism here. As will become evident, the inverse relationship between scattering and spin relaxation in the DP mechanism hinders its effectiveness when scattering becomes frequent, leading to a change in dominant mechanism. Both spin flips in scattering and the Elliott-Yafet mechanism depend proportionally on the scattering rate. Of these two, we opt to include only the simpler example of spin flips in scattering due to the the transverse component of the previously derived effective interaction. The Elliott-Yafet mechanism would only slightly correct this dominant mechanism by including more opportunities for spin flips in interaction due to spin-orbit, which is typically weak.

4.4.1 Spin flips in scattering

We previously introduced effective carrier-carrier interactions in Eqs. (4.17) and (4.18). In both cases, the bare interaction J is mediated by an effective impurity spin response. While the longitudinal interaction is clearly spin conserving, the transverse interaction involves a transfer of spin from carriers to impurities. Then, this interaction alone can act as a spin relaxation mechanism where carriers relax to a state where total spin $\langle\sigma_z\rangle + \langle S_z\rangle$ has been conserved, but the individual spins have not. The rate of this relaxation is calculated in detail using Keldysh formalism for the collisions. We work within the degenerate regime, so scattering events take place on the Fermi surface.

The time rate of change of the average spin density $\langle\sigma_{\mathbf{k}}\rangle = n_\sigma \mathrm{S}_\sigma \,\mathrm{Tr}[\hat{\rho}_{\mathbf{k}}\hat{\sigma}_z]$ is

$$\frac{\partial\langle\sigma_{\mathbf{k}}\rangle}{\partial t} = n_\sigma \mathrm{S}_\sigma \,\mathrm{Tr}\left[\frac{\partial\hat{\rho}_{\mathbf{k}}}{\partial t}\hat{\sigma}_z\right], \tag{4.25}$$

where $\hat{\rho}_{\mathbf{k}}$ is a 2x2 density matrix in spin space for carriers, $\hat{\sigma}_z$ is the z-Pauli matrix, and $\mathbf{z}$ has been chosen for the direction of spin polarization. Taking advantage of the relaxation time approximation for $\partial_t\langle\sigma_{\mathbf{k}}\rangle$ and averaging over all wavevectors $\mathbf{k}$, the spin relaxation time τ_s is calculated from

$$\frac{1}{\tau_s} = -\frac{\sum_{\mathbf{k}} \mathrm{Tr}\left[\partial_t\hat{\rho}_{\mathbf{k}}\hat{\sigma}_z\right]}{\sum_{\mathbf{k}} \mathrm{Tr}\left[\hat{\rho}^1_{\mathbf{k}}\hat{\sigma}_z\right]}, \tag{4.26}$$

where $\hat{\rho}^1_{\mathbf{k}}$ is the first order non-equilibrium correction to the linearized density matrix. In the absence of spin-orbit and other external fields, the density matrix evolves according to

$$\frac{\partial\hat{\rho}_{\mathbf{k}}}{\partial t} = \hat{I}_{\mathbf{k}}, \tag{4.27}$$

where $\hat{I}_{\mathbf{k}}$ is the 2x2 collision integral in spin space for carriers.

Starting from the Kadanoff-Baym quantum kinetic equation,[57, 58] the collision integral

is

$$\hat{I}_{\mathbf{k}} = \frac{1}{2}\sum_{\omega}\left[\left\{\hat{\Sigma}^{<}_{\mathbf{k}}(\omega),\hat{G}^{>}_{\mathbf{k}}(\omega)\right\} - \left\{\hat{\Sigma}^{>}_{\mathbf{k}}(\omega),\hat{G}^{<}_{\mathbf{k}}(\omega)\right\}\right], \tag{4.28}$$

where $\hat{\Sigma}_{\mathbf{k}}(\omega)$ is the carrier self-energy and $\hat{G}_{\mathbf{k}}(\omega)$ is its Green's function. We use sum notation for ω, but it should be understood that $\sum_{\omega} = \int d\omega/2\pi$. In the absence of spin-orbit, small deviations from the equilibrium spin polarization only show up on the diagonal elements of the density matrix. Then, we know *a priori* that $\hat{G}_{\mathbf{k}}(\omega)$ and $\hat{\Sigma}_{\mathbf{k}}(\omega)$ are diagonal and can write the collision integral per spin-α as

$$I_{\mathbf{k}\alpha} = \sum_{\omega}\left[G^{>}_{\mathbf{k}\alpha}(\omega)\Sigma^{<}_{\mathbf{k}\alpha}(\omega) - \Sigma^{>}_{\mathbf{k}\alpha}(\omega)G^{<}_{\mathbf{k}\alpha}(\omega)\right]. \tag{4.29}$$

We evaluate the self-energy in the GW approximation,[40, 89]

$$\Sigma^{\lessgtr}_{\mathbf{k}\alpha}(\omega) = i\hbar\sum_{\mathbf{q},\Omega} G^{\lessgtr}_{\mathbf{k}-\mathbf{q}\alpha}(\omega-\Omega)W^{\lessgtr}_{\mathbf{q}}(\Omega)\,. \tag{4.30}$$

In allowing for arbitrary spin polarization, we should separate the GW spin-space operator into longitudinal and transverse components according to Fig. 4.3: $\widehat{GW} = W_{\parallel}\hat{\sigma}_z\hat{G}\hat{\sigma}_z + W_{\perp}(\hat{\sigma}_x\hat{G}\hat{\sigma}_x + \hat{\sigma}_y\hat{G}\hat{\sigma}_y)$. This amends Eq. (4.30) to

$$\Sigma^{\lessgtr}_{\mathbf{k}\alpha}(\omega) = i\hbar\sum_{\mathbf{q},\Omega}\left[W^{\lessgtr}_{\parallel\mathbf{q}}(\Omega)G^{\lessgtr}_{\parallel\mathbf{k}-\mathbf{q}\alpha}(\omega-\Omega) + 2W^{\lessgtr}_{\perp\mathbf{q}}(\Omega)G^{\lessgtr}_{\perp\mathbf{k}-\mathbf{q}\alpha}(\omega-\Omega)\right], \tag{4.31}$$

where $W_{\parallel}$ and $W_{\perp}$ are scalar longitudinal and transverse interactions, respectively, and

$$\hat{G}_{\parallel\mathbf{k}} = \hat{\sigma}_z\hat{G}_{\mathbf{k}}\hat{\sigma}_z\,, \tag{4.32}$$

$$\hat{G}_{\perp\mathbf{k}} = \hat{\sigma}_x\hat{G}_{\mathbf{k}}\hat{\sigma}_x + \hat{\sigma}_y\hat{G}_{\mathbf{k}}\hat{\sigma}_y\,. \tag{4.33}$$

The GKB ansatz is utilized to relate the lesser and greater Green's functions to the

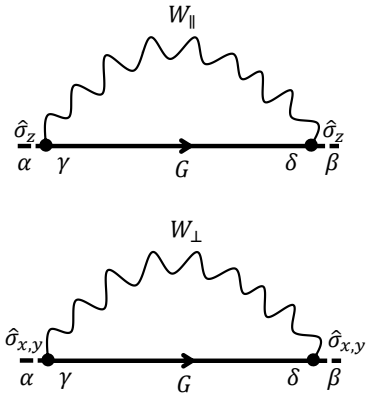

Figure 4.3: The GW self-energy includes separate contributions from longitudinal $W_\parallel$ and transverse $W_\perp$ interactions. Here, α, β, γ, and δ are spin states on which the interactions $\hat{\sigma}_i W \hat{\sigma}_i$ operate.

density matrices $\hat{\rho}^<_{\mathbf{k}} = \hat{\rho}_{\mathbf{k}}$ and $\hat{\rho}^>_{\mathbf{k}} = \hat{1} - \hat{\rho}_{\mathbf{k}}$, where $\hat{1}$ is the 2x2 identity matrix:

$$G^{\lessgtr}_{\mathbf{k}\alpha}(\omega) = \mp G^r_{\mathbf{k}\alpha}(\omega)\rho^{\lessgtr}_{\mathbf{k}\alpha} \pm \rho^{\lessgtr}_{\mathbf{k}\alpha} G^a_{\mathbf{k}\alpha}(\omega)\,. \tag{4.34}$$

Notice that we are neglecting retardation effects in the density matrix by making it frequency independent. This is commonly referred to as the Markovian approximation. We let all non-equilibrium properties reside in $\hat{\rho}_{\mathbf{k}}$, so $\hat{G}^r_k(\omega)$ and $\hat{G}^a_k(\omega)$ are taken to be equilibrium Green's functions. Furthermore, given that we hope to achieve a Boltzmann-like collision integral, we retain only the singularities in $\hat{G}^{r,a}_k(\omega)$, as those are the parts which conserve energy in collisions.[90] Under these circumstances, the lesser and greater Green's functions become

$$G^{\lessgtr}_{\mathbf{k}\alpha}(\omega) = \pm i 2\pi\delta(\hbar\omega - \varepsilon_{k\alpha})]\rho^{\lessgtr}_{\mathbf{k}\alpha}\,. \tag{4.35}$$

Being diagonal, it is perhaps more familiar to denote the diagonal elements of $\hat{\rho}_{\mathbf{k}}$ by Fermi-Dirac distributions: $\rho_{\mathbf{k}\alpha} = f_{\mathbf{k}\alpha}$. Similar to the GKB ansatz, we can relate the lesser and

greater interactions $W^{\lessgtr}_{\mathbf{q}}(\omega)$ to their retarded counterpart $W^{r}_{\mathbf{q}}(\omega)$ using the relation

$$W^{\lessgtr}_{\mathbf{q}}(\omega) = \mp i 2 n_B(\pm\omega) \Im W^{r}_{\mathbf{q}}(\omega)\,, \tag{4.36}$$

where $n_B(\omega) = (e^{\beta\hbar\omega} - 1)^{-1}$ is the Bose-Einstein distribution, $\beta = (k_B T)^{-1}$.

The result of inserting Eqs. (4.30)-(4.36) into the collision integral, Eq. (4.29), is

$$\begin{aligned} I_{\mathbf{k}\alpha} = 2(2\pi) \sum_{\mathbf{q},\omega} & \\ \Big\{ \Im W^{r}_{\parallel\mathbf{q}}(\omega) \delta(\varepsilon_{k\alpha} - \varepsilon_{\mathbf{k}-\mathbf{q}\alpha} - \hbar\omega) \left[n_B(\omega)(1 - f_{\mathbf{k}\alpha}) f_{\mathbf{k}-\mathbf{q}\alpha} + n_B(-\omega) f_{\mathbf{k}\alpha}(1 - f_{\mathbf{k}-\mathbf{q}\alpha}) \right] & \\ + 2 \Im W^{r}_{\perp\mathbf{q}}(\omega) \delta(\varepsilon_{k\alpha} - \varepsilon_{\mathbf{k}-\mathbf{q}\bar{\alpha}} - \hbar\omega) \left[n_B(\omega)(1 - f_{\mathbf{k}\alpha}) f_{\mathbf{k}-\mathbf{q}\bar{\alpha}} + n_B(-\omega) f_{\mathbf{k}\alpha}(1 - f_{\mathbf{k}-\mathbf{q}\bar{\alpha}}) \right] \Big\}\,. \end{aligned} \tag{4.37}$$

If we prepare a spin polarization such that $f_{\mathbf{k}\alpha}$ is slightly out-of-equilibrium, it can be linearized as

$$f_{\mathbf{k}\alpha} = f^0_{k\alpha} + \alpha\beta\varepsilon_s f^0_{k\alpha}(1 - f^0_{k\alpha})\,, \tag{4.38}$$

where ε_s is a small spin perturbation energy, $\alpha = +1$ for spin-up, and $\alpha = -1$ for spin-down. From a physical standpoint, it should be clear that longitudinal interactions will preserve spin polarization, and so we should see that portion of the collision integral vanish upon insertion of Eq. (4.38) into Eq. (4.37). Indeed, this is the case and we only need to evaluate

$$I_{\mathbf{k}\alpha} = -16\pi\alpha\beta\varepsilon_s \sum_{\mathbf{q},\omega} \Im W^{r}_{\perp\mathbf{q}}(\omega) \delta(\varepsilon_{k\alpha} - \varepsilon_{\mathbf{k}-\mathbf{q}\bar{\alpha}} - \hbar\omega) \frac{f^0_{k\alpha} - f^0_{\mathbf{k}-\mathbf{q}\bar{\alpha}}}{4\sinh^2(\beta\hbar\omega/2)}\,. \tag{4.39}$$

Returning to Eq. (4.26), we can insert expressions for $\hat{\rho}_{\mathbf{k}}$ and $\hat{I}_{\mathbf{k}}$. The rate of spin relaxation from transverse spin scattering events is

$$\frac{1}{\tau_s} = \frac{16\beta}{N_\uparrow(0) + N_\downarrow(0)} \sum_{\mathbf{q},\omega,\alpha} \Im W^{r}_{\perp\mathbf{q}}(\omega) \frac{\Im \chi^{(0)}_{\bar{\alpha}\alpha}(q,\omega)}{4\sinh^2(\beta\hbar\omega/2)}\,, \tag{4.40}$$

where

$$\Im\chi^{(0)}_{\alpha\beta}(q,\omega) = \pi \sum_{\mathbf{k}} \delta(\varepsilon_{\mathbf{k}+\mathbf{q}\beta} - \varepsilon_{k\alpha} - \hbar\omega) \left[f^0_{\mathbf{k}+\mathbf{q}\beta} - f^0_{k\alpha} \right] . \tag{4.41}$$

4.4.2 Dyakonov-Perel mechanism

In the DP mechanism, spins relax due to precession around axes defined by a magnetic field which varies in **k**-space. The obvious example of a **k**-dependent magnetic field in semiconductors is the spin-orbit field, which for III-V semiconductors usually includes the Dresselhaus and/or Rashba fields. The effect of scattering on this process is usually to inhibit spin relaxation as spins are unable to make full precessions before being relocated in momentum space. This sets a timescale, where the rate of scattering must be faster than the rate of spin precession for spin relaxation to be inhibited, otherwise spins enter a regime of free precessions and the rate of relaxation is directly proportional to the rate of precession. In the limit of fast scattering, spins are unable to make appreciable precessions around the spin-orbit field's axes and spin relaxation is entirely suppressed. This is the scenario we encounter.

The derivation of DP spin relaxation was reviewed in Ch. 1. When the Hamiltonian includes a contribution from a spin-orbit field $\mathbf{\Omega_k}$ of the form

$$\mathcal{H}^1_{\mathbf{k}} = \frac{\hbar}{2} \mathbf{\Omega_k} \cdot \hat{\boldsymbol{\sigma}} \,, \tag{4.42}$$

where $\hat{\boldsymbol{\sigma}}$ is the Pauli matrix vector, the rate of spin relaxation $1/\tau_s$ for carriers due to the DP mechanism is

$$\frac{1}{\tau_s} = \frac{2}{3} \frac{\sum_{\mathbf{k}} \tau^*_k \langle \Omega^2_{\mathbf{k}} \rangle \, \mathrm{Tr} \left[\hat{\rho}^0_k \hat{\sigma}_z \right]}{\sum_{\mathbf{k}} \mathrm{Tr} \left[\hat{\rho}^0_k \hat{\sigma}_z \right]} \,. \tag{4.43}$$

τ^*_k is an effective scattering time that weights collisions based on the randomization of momentum relative to a spin-orbit field's wavevector dependence. $\langle \Omega^2_{\mathbf{k}} \rangle$ is the angular averaged spin-orbit field which we've taken to be isotropic. It should be noted that while

Eq. (4.43) would seem to have a ratio of 0/0 in the paramagnetic phase due to the traces over $\hat{\rho}_k^0\hat{\sigma}_z$, there is an implicit assumption that a small polarization has been prepared which will relax. This is the reason for the *quasi* qualifier when describing ρ_k^0; it is stable on the time scale of scattering but changes on the time scale of spin relaxation. The calculations performed in this chapter use the Dresselhaus spin-orbit field in a bulk III-V semiconductor which has an angular average defined by

$$\langle\Omega_{\mathbf{k}}^2\rangle = \frac{16}{35}\frac{\alpha_c^2\varepsilon_k^3}{\hbar^2 E_g}\,, \tag{4.44}$$

where α_c is the spin-orbit coupling constant and E_g is the band gap energy. The challenge in evaluating Eq. (4.43) comes from the effective scattering rate $1/\tau^*$. An oft-made approximation is to substitute the rate of momentum relaxation in its place. The validity of this approximation in the context of spin-scattering is discussed at the end of this section.

The spin-orbit field makes small non-equilibrium contributions to the carrier density matrix, appearing as spin mixing elements on the off-diagonal. In this case, when we linearize the density matrix

$$\hat{\rho}_{\mathbf{k}} = \hat{\rho}_k^0 + \hat{\rho}_{\mathbf{k}}^1\,, \tag{4.45}$$

the quasi-equilibrium part $\hat{\rho}_k^0$ is diagonal and the non-equilibrium part $\hat{\rho}_{\mathbf{k}}^1$ is off-diagonal. Written in terms of the Fermi-Dirac distribution, the quasi-equilibrium density matrix $\hat{\rho}_k^0$ is

$$\hat{\rho}_k^0 = \begin{cases} \left(\frac{f_{k\uparrow}^0+f_{k\downarrow}^0}{2}\right)\hat{1} + \left(\frac{f_{k\uparrow}^0-f_{k\downarrow}^0}{2}\right)\hat{\sigma}_z + \left(\frac{f_{k\uparrow}^1-f_{k\downarrow}^1}{2}\right)\hat{\sigma}_z & \text{Ferromagnetic phase} \\ \left(\frac{f_{k\uparrow}^0+f_{k\downarrow}^0}{2}\right)\hat{1} + \left(\frac{f_{k\uparrow}^1-f_{k\downarrow}^1}{2}\right)\hat{\sigma}_z & \text{Paramagnetic phase,} \end{cases} \tag{4.46}$$

where $f_{k\alpha}^1 = \alpha\beta\varepsilon_s f_{k\alpha}^0(1-f_{k\alpha}^0)$. Alluded to earlier in this section, the reason for the distinct

ferromagnetic and paramagnetic forms of $\hat{\rho}^0_k$ is that a small non-equilibrium spin polarization is necessary for spin relaxation to occur. Thus, the factors in front of $\hat{\sigma}_z$ are the lowest order, out-of-equilibrium spin distributions. In fact, this distinction is really only needed in Eq. (4.43), where $\mathrm{Tr}[\hat{\rho}^0_k \hat{\sigma}_z]$ should not vanish. When we use Eq. (4.46) in a linearized collision integral, every term will contain $\rho^1_{\mathbf{k}}$ and thus we can drop any first order corrections from $\hat{\rho}^0_k$ and simply use

$$\rho^0_{k\alpha} = f^0_{k\alpha} \,. \tag{4.47}$$

The non-equilibrium part of the density matrix $\hat{\rho}_{1\mathbf{k}}$ arises from interaction with the spin-orbit field:[18]

$$\hat{\rho}^1_{\mathbf{k}} = \tau^*_k \left(\frac{f^1_{k\uparrow} - f^1_{k\downarrow}}{2} \right) (\boldsymbol{\Omega}_{\mathbf{k}} \times \hat{\mathbf{z}}) \cdot \hat{\boldsymbol{\sigma}} \,, \tag{4.48}$$

where $\hat{\boldsymbol{\sigma}} = \{\hat{\sigma}_x, \hat{\sigma}_y, \hat{\sigma}_z\}$ is the Pauli spin vector. Inserting the linearized expression for $f^1_{k\alpha}$ it is easily verified that $\hat{\rho}^1_{\mathbf{k}}$ satisfies $\rho^*_{\downarrow\uparrow} = \rho_{\uparrow\downarrow}$:

$$\rho^1_{\mathbf{k}\alpha\bar{\alpha}} = \tau^*_k (\beta\varepsilon_s/2)(\Omega_{\mathbf{k},y} + \alpha i \Omega_{\mathbf{k},x}) \sum_\gamma f^0_{k\gamma}(1 - f^0_{k\gamma}) \,. \tag{4.49}$$

We use a relaxation time approximation to relate $\hat{\rho}^1_{\mathbf{k}}$ and τ^*_k to the collision integral $\hat{I}_{\mathbf{k}}$,

$$-\frac{\hat{\rho}^1_{\mathbf{k}}}{\tau^*_k} = \hat{I}_{\mathbf{k}} \,, \tag{4.50}$$

and note that $\hat{I}_{\mathbf{k}}$ is not diagonal in spin space,

$$\hat{I}_{\mathbf{k}} = \frac{1}{2} \sum_\omega \left[\left\{ \hat{\Sigma}^<_{\mathbf{k}}(\omega), \hat{G}^>_{\mathbf{k}}(\omega) \right\} - \left\{ \hat{\Sigma}^>_{\mathbf{k}}(\omega), \hat{G}^<_{\mathbf{k}}(\omega) \right\} \right] . \tag{4.51}$$

As in Eq. (4.31), we evaluate the self-energy $\hat{\Sigma}^{\lessgtr}_{\mathbf{k}}$ in the GW approximation, making a

distinction between longitudinal and transverse components:

$$\hat{\Sigma}^{\lessgtr}_{\mathbf{k}}(\omega) = i\hbar \sum_{\mathbf{q},\Omega} \left[W^{\lessgtr}_{\parallel \mathbf{q}}(\Omega) \hat{G}^{\lessgtr}_{\parallel \mathbf{k}-\mathbf{q}}(\omega - \Omega) + 2 W^{\lessgtr}_{\perp \mathbf{q}}(\Omega) \hat{G}^{\lessgtr}_{\perp \mathbf{k}-\mathbf{q}}(\omega - \Omega) \right] . \tag{4.52}$$

While the formal GKB ansatz is used to relate lesser and greater Green's functions to their corresponding density matrices, a physical argument removes spurious terms for a Boltzmann type collision integral. Formally, we have

$$\hat{G}^{\lessgtr}_{\mathbf{k}}(\omega) = \mp \hat{G}^{r}_{\mathbf{k}}(\omega) \hat{\rho}^{\lessgtr}_{\mathbf{k}} \pm \hat{\rho}^{\lessgtr}_{\mathbf{k}} \hat{G}^{a}_{\mathbf{k}}(\omega) . \tag{4.53}$$

Retaining only the singularities in $\hat{G}^{r,a}_{\mathbf{k}}(\omega)$, the equilibrium Green's functions are

$$G^{0\lessgtr}_{\mathbf{k}\alpha\alpha} = \pm i 2\pi \delta \left(\hbar\omega - \varepsilon_{k\alpha} \right) f^{0\lessgtr}_{k\alpha} . \tag{4.54}$$

For the first order non-equilibrium Green's function, we will find products of the form $\delta(\hbar\omega - \varepsilon_{k\alpha})(f^{1}_{k\alpha} + f^{1}_{k\bar{\alpha}})$ resulting from Eq. (4.53). From a physical perspective we should only associate a spectral distribution with its corresponding distribution function, thus we discard $\delta(\hbar\omega - \varepsilon_{k\alpha}) f^{1}_{k\bar{\alpha}}$ terms and write the non-equilibrium Green's function as

$$G^{1\lessgtr}_{\mathbf{k}\alpha\bar{\alpha}} = i\pi \tau^{*}_{k} (\beta\varepsilon_{s}/2)(\Omega_{\mathbf{k},y} + \alpha i \Omega_{\mathbf{k},x}) \sum_{\gamma} \delta \left(\hbar\omega - \varepsilon_{k\gamma} \right) f^{0}_{k\gamma} (1 - f^{0}_{k\gamma}) . \tag{4.55}$$

Inserting the linearized expressions for the Green's functions from Eqs. (4.54)-(4.55) and the self-energy from Eq. (4.52), the collision integral in Eq. (4.51) becomes off-diagonal. Tracing both sides of Eq. (4.50) with $\hat{\sigma}_x$ reduces the equality to a scalar relation without

losing any information:

$$\sum_{\gamma} f^0_{k\gamma}(1-f^0_{k\gamma})\Omega_{\mathbf{k},y} = \pi \sum_{\mathbf{q},\omega,\alpha,\gamma} \Bigg[\Im W^r_{\parallel \mathbf{q}}(\omega) \frac{\delta(\varepsilon_{k\gamma} - \varepsilon_{\mathbf{k}-\mathbf{q}\alpha} - \hbar\omega)}{4\sinh^2(\beta\hbar\omega/2)} \left[f^0_{k\gamma} - f^0_{\mathbf{k}-\mathbf{q}\alpha}\right] \left[\tau^*_k \Omega_{\mathbf{k},y} + \tau^*_{\mathbf{k}-\mathbf{q}} \Omega_{\mathbf{k}-\mathbf{q},y}\right] + 2\Im W^r_{\perp \mathbf{q}}(\omega) \frac{\delta(\varepsilon_{k\gamma} - \varepsilon_{\mathbf{k}-\mathbf{q}\alpha} - \hbar\omega)}{4\sinh^2(\beta\hbar\omega/2)} \left[f^0_{k\gamma} - f^0_{\mathbf{k}-\mathbf{q}\alpha}\right] \tau^*_k \Omega_{\mathbf{k},y} \Bigg] . \tag{4.56}$$

This integral equation can be solved exactly using the methods of Sykes and Brooker,[54] but given the slowly varying nature of τ^*_k around the Fermi level in the degenerate regime, it is a reasonable approximation to treat it as a constant evaluated at ε_F and extract it from the collision integral. Then, we only need to specify the spin-orbit field and solve for the effective scattering rate.

The y-component of the Dresselhaus field[19] is

$$\Omega_{\mathbf{k},y} = \frac{i\alpha_c \hbar^2 k^3}{\sqrt{2m_c^3 E_g}} \left[\sqrt{\frac{\pi}{21}} \left(Y_{3,1}(\vartheta,\varphi) + Y_{3,-1}(\vartheta,\varphi)\right) - \sqrt{\frac{\pi}{35}} \left(Y_{3,3}(\vartheta,\varphi) + Y_{3,-3}(\vartheta,\varphi)\right) \right] , \tag{4.57}$$

where $Y_{l,m}(\vartheta,\varphi)$ are the spherical harmonics. By writing the spin-orbit field in terms of spherical harmonics, we can take advantage of their orthogonality and especially the addition theorem for spherical harmonics. Ultimately, we have the following useful identity:

$$\int \frac{d\Omega'}{4\pi} V_{\mathbf{k}-\mathbf{k}'} \Omega_{\mathbf{k}',j} = \Omega_{\mathbf{k},j} \left(\frac{k'}{k}\right)^3 \int \frac{d\Omega'}{4\pi} V_{\mathbf{k}-\mathbf{k}'} P_3(\cos\vartheta') , \tag{4.58}$$

where $d\Omega' = d(\cos\vartheta')d\varphi'$ and j can be any of x, y, or z. Pushing $\sum_{\mathbf{k}} \Omega_{\mathbf{k},y}/k^6$ onto both sides of Eq. (4.56), we can extract the following modified Lindhard imaginary response function (analytic solution in Appendix C.1):

$$\Im\chi^{(n)}_{3\alpha\beta}(q,\omega) = \pi \sum_{\mathbf{k}} \delta(\varepsilon_{\mathbf{k}+\mathbf{q}\beta} - \varepsilon_{k\alpha} - \hbar\omega) \left[f^0_{\mathbf{k}+\mathbf{q}\beta} - f^0_{k\alpha}\right] z_n(\mathbf{k},\mathbf{q}) , \tag{4.59}$$

where

$$z_n(\mathbf{k},\mathbf{q}) = \left(\frac{k}{|\mathbf{k}+\mathbf{q}|}\right)^n P_n\left(\frac{\mathbf{k}\cdot(\mathbf{k}+\mathbf{q})}{k\,|\mathbf{k}+\mathbf{q}|}\right). \tag{4.60}$$

The final result for the effective scattering rate due to a spin dependent interaction in the degenerate regime is

$$\frac{1}{\tau^*_{k_F}} = \frac{\beta}{N_\uparrow(0)+N_\downarrow(0)} \sum_{\mathbf{q},\omega,\alpha,\gamma} \left\{ \Im W^r_\parallel(q,\omega) \frac{\Im\chi^{(0)}_{\alpha\gamma}(q,\omega) + \Im\chi^{(3)}_{3\alpha\gamma}(q,\omega)}{4\sinh^2(\beta\hbar\omega/2)} + 2\Im W^r_\perp(q,\omega) \frac{\Im\chi^{(0)}_{\alpha\gamma}(q,\omega)}{4\sinh^2(\beta\hbar\omega/2)} \right\}. \tag{4.61}$$

By comparison, the effective scattering rate obtained when a spin-independent interaction is used is

$$\frac{1}{\tau^*_{k_F}} = \frac{\beta}{N_\uparrow(0)+N_\downarrow(0)} \sum_{\mathbf{q},\omega,\alpha,\gamma} \Im W^r_c(q,\omega) \frac{\Im\chi^{(0)}_{\alpha\gamma}(q,\omega) - \Im\chi^{(3)}_{3\alpha\gamma}(q,\omega)}{4\sinh^2(\beta\hbar\omega/2)}. \tag{4.62}$$

4.4.3 Comparison to momentum relaxation

To get a feel for the effective scattering rate, we compare it to momentum relaxation. Derivation is analogous to Sec. 4.4.1 since the non-equilibrium density matrix is diagonal.

We use the Drude model and Matthiessen's rule to define the momentum relaxation rate for spin-α carriers $1/\tau_\alpha$ in terms of the resistivity $\rho_{\alpha\beta}$:

$$\frac{1}{\tau_\alpha} = \sum_\beta \frac{n_\beta e^2}{m_c} \rho_{\alpha\beta}. \tag{4.63}$$

Notice the resistivity is not necessarily diagonal in the ferromagnetic regime, where mobilities between spin-up and spin-down carriers may differ. The resistivity is in turn defined by a proportionality between the drift velocity $\mathbf{v}_\alpha$ and the average time rate of change of

momentum $\sum_{\mathbf{k}} \hbar \mathbf{k} I_{\mathbf{k}}$:

$$\sum_{\beta} \rho_{\alpha\beta} n_\beta \mathbf{v}_\beta = -\frac{1}{e^2 n_\alpha} \sum_{\mathbf{k}} \hbar \mathbf{k} I_{\mathbf{k}\alpha} \,. \tag{4.64}$$

Again, starting from the Kadanoff-Baym kinetic equation, the collision rate $I_{\mathbf{k}\alpha}$ is defined by

$$I_{\mathbf{k}\alpha} = \sum_{\omega} \left[G^{>}_{\mathbf{k}\alpha}(\omega) \Sigma^{<}_{\mathbf{k}\alpha}(\omega) - \Sigma^{>}_{\mathbf{k}\alpha}(\omega) G^{<}_{\mathbf{k}\alpha}(\omega) \right] . \tag{4.65}$$

Applying the same techniques as in Section 4.4.1 (GKB ansatz, GW self-energy, $W^{\lessgtr} \to \Im W^r$), but with a linearization in the drift velocity $f^1_{\mathbf{k}\alpha} = \beta\hbar \mathbf{k} \cdot \mathbf{v}_\alpha f^0_{k\alpha}(1 - f^0_{k\alpha})$ rather than spin energy, we obtain for the momentum relaxation rate

$$\frac{1}{\tau_{k_F}} = \frac{4\beta}{N_\uparrow(0) + N_\downarrow(0)} \sum_{\mathbf{q},\omega,\alpha} \left\{ \Im W^r_{\parallel q}(\omega) \frac{\bar{q}_\alpha^2 \Im \chi^{(0)}_{\alpha\alpha}(q,\omega) + \bar{q}_\alpha \Im \chi^{(1,\alpha)}_{1\alpha\alpha}(q,\omega)}{4 \sinh^2(\beta\hbar\omega/2)} \right.$$
$$\left. + 2 \Im W^r_{\perp q}(\omega) \frac{\bar{q}_\alpha^2 \Im \chi^{(0)}_{\bar{\alpha}\alpha}(q,\omega) + \bar{q}_\alpha \Im \chi^{(1,\alpha)}_{1\bar{\alpha}\alpha}(q,\omega)}{4 \sinh^2(\beta\hbar\omega/2)} \right\} , \tag{4.66}$$

where $\bar{q}_\gamma = q/k_{F\gamma}$ and the modified response function (with analytic solution in Appendix C.1) is

$$\Im \chi^{(n,\gamma)}_{1\alpha\beta}(q,\omega) = \frac{\pi}{k^n_{F\gamma}} \sum_{\mathbf{k}} \delta(\varepsilon_{\mathbf{k}+\mathbf{q}\beta} - \varepsilon_{k\alpha} - \hbar\omega) \left[f^0_{\mathbf{k}+\mathbf{q}\beta} - f^0_{k\alpha} \right] (\mathbf{k} \cdot \hat{\mathbf{q}})^n \,. \tag{4.67}$$

4.5 Analysis

The result for the effective scattering rate in the DP mechanism has some interesting differences from previous derivations. In particular, notice there is a sign difference in the vertex correction $\Im \chi^{(0)}_{\alpha\gamma}(q,\omega) \pm \Im \chi^{(3)}_{3\alpha\gamma}(q,\omega)$ of the longitudinal contribution to the scattering rate in Eq. (4.61) and the spin-independent scattering rate in Eq. (4.62). The significance of this sign is perhaps easier to understand if we look back to Eq. (4.56). In the longitudinal term, after extracting τ^* as a constant, we have a factor $(\Omega_{\mathbf{k},y} + \Omega_{\mathbf{k}-\mathbf{q},y})$. This should be

compared to $(\Omega_{\mathbf{k},y} - \Omega_{\mathbf{k}-\mathbf{q},y})$ which appears when a spin-independent interaction is used. The minus sign in the vertex correction due to a spin-independent interaction has previously been compared to the $(1 - \cos\theta)$ factor in momentum relaxation; a similar factor can be extracted from $(\Omega_{\mathbf{k},y} - \Omega_{\mathbf{k}-\mathbf{q},y})$ and has the form $[1 - P_3(\cos\theta)]$, where $P_3(x)$ is the $n = 3$ Legendre polynomial.[5, 17, 18] For the case of momentum relaxation, when there is no relative angle θ between two particles in a scattering event, there is no contribution to momentum relaxation. The analogy for the effective scattering rate is that zero momentum transfers do not relocate particles in a $\mathbf{k}$-dependent magnetic field, so spins can continue to precess around the same magnetic field axis and those scattering events do not inhibit the rate of spin relaxation. This analogy is not appropriate for spin-dependent scattering, where even in direct processes spins may change orientation for zero momentum transfers. In fact, what we find is a sort of generalized DP spin relaxation, where spin- and momentum-dependent scattering has a significantly greater chance of disrupting spin relaxation than momentum-only scattering. This is why we see a sum, rather than difference, in $(\Omega_{\mathbf{k},y} + \Omega_{\mathbf{k}-\mathbf{q},y})$.

The effective scattering rate from Eq. (4.61) is compared to the momentum relaxation rate from Eq. (4.66) in Fig. 4.4 for varying interaction strengths and carrier densities. Unlike previous reports, the effective scattering rate is found to generally be larger than the momentum relaxation rate.[18] This is consistent with the idea that more scattering events disrupt spin relaxation than affect momentum relaxation. Especially near the critical temperature T_c, notice that momentum relaxation has a finite peak whereas the effective scattering rate does not – there is no vanishing vertex correction in the effective scattering rate to control this divergence. This is an indication that spin exchange and spin flip processes become very important near the critical temperature.

An interesting consequence of the effective interaction used in this chapter is the height of the scattering peaks only indirectly depend on J through the hyperbolic sine in Eqs. (4.61) and (4.66), and not through the interaction $W(q, \omega)$. This can be shown by writing the non-

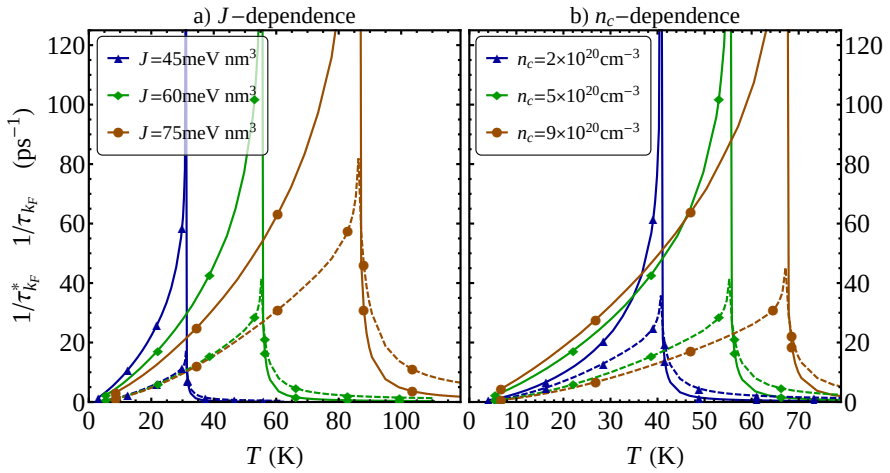

Figure 4.4: The effective scattering rate used in Dyakonov-Perel spin relaxation calculations (solid lines) is compared to the momentum relaxation rate (dashed lines) for varying a) interaction strengths and b) carrier densities. Since zero-momentum transfer processes can still contribute to inhibiting Dyakonov-Perel spin relaxation when spin flips are taken into account, the effective scattering rate does not have any factors to compensate for the diverging interaction at T_c.

interacting paramagnetic spin response for impurities as $\chi^{(0)}_{S_zS_z}(T) = -(T_c/T)[J^2\mathrm{S}^2_\sigma N(0)]^{-1}$, then the effective interaction in the paramagnetic phase reduces to

$$W(q,\omega) = -\left[\mathrm{S}^2_\sigma N(0)(T/T_c) + \chi^{(0)}_{\sigma_z\sigma_z}(q,\omega)\right]^{-1} . \tag{4.68}$$

At $T = T_c$, there is neither an explicit dependence on J nor on T_c; we are left with an interaction that only depends on the non-interacting carrier response. In the paramagnetic phase, the scattering rates derived in this chapter contain $\Im W(q,\omega)\Im\chi^{(0)}_{\sigma_z\sigma_z}(q,\omega)/\sinh^2(\beta\hbar\omega/2)$ as part of their integrand. In the small frequency limit, this term reduces to $\sim T^2$. Then, higher critical temperatures have greater scattering rates associated with them; this is verified by Fig. 4.4a.

The height of the scattering peaks are largely independent of the carrier density n_σ, seen in Fig. 4.4b. Combining the interaction in Eq. (4.68) with the imaginary response functions

$\Im\chi^{(n,\gamma)}_{N\alpha\alpha}(q,\omega)$ rids the integrand of density of state factors. The primary contribution of carrier density comes from the cut-off frequency $\hbar\omega < \varepsilon_{F\alpha}$ in each of $\Im\chi^{(n,\gamma)}_{N\alpha\alpha}(q,\omega)$.

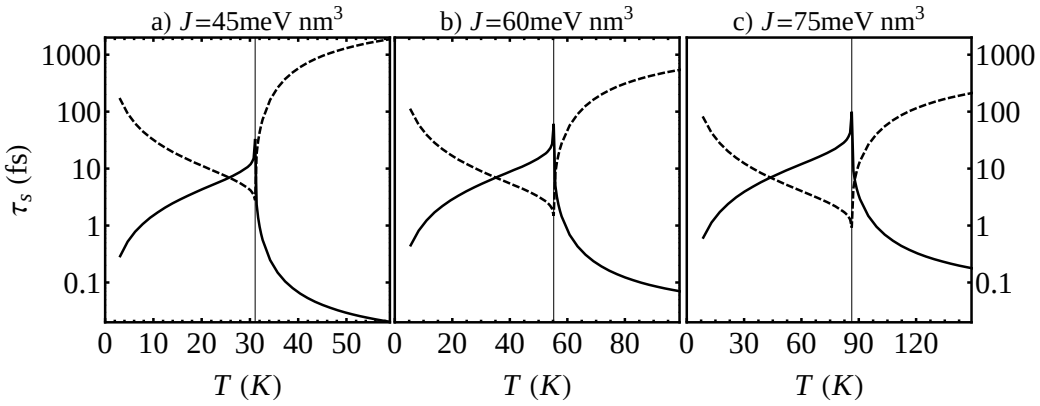

Figure 4.5: The Dyakonov-Perel spin relaxation time (solid lines) is compared to spin-flip based spin relaxation (dashed lines) resulting from a spin dependent interaction. For calculations, we used GaAs parameters for holes: $m_c = 0.5m_e$, $\alpha_c = 0.34$, and $E_g = 1.5$eV. The vertical lines mark the critical temperature in each plot. The peak in scattering rate near the ferromagnetic transition correlates with short spin relaxation times in the spin-flip mechanisms and enhanced spin relaxation times in the Dyakonov-Perel mechanism. Away from the ferromagnetic transition, we see Dyakonov-Perel spin relaxation becoming dominant as is often found in III-V semiconductors.

Turning our attention to spin relaxation, the earlier discussion about the effect of spin-dependent interactions on inhibiting spin precession in the DP mechanism sounds like a novel way to squelch spin relaxation. This is especially relevant for hole spins in III-V semiconductors, which usually relax very quickly compared to electrons due to a stronger spin-orbit coupling.[31] In fact, the expressions derived for DP spin relaxation rely on the assumption that scattering lifetimes are shorter (by roughly an order of magnitude) than spin lifetimes.[5, 6] Strong spin orbit coupling leads to fast spin precessions in the spin-orbit field, which in turn requires even faster scattering events to disrupt precession. In Fig. 4.5, we plot several spin relaxation rates for different interaction strengths J. It can be quickly verified by a comparison of timescales that the scattering rates in Fig. 4.4 are

indeed fast enough to affect spin relaxation in the DP mechanism. Unfortunately, this form of scattering comes at the cost of introducing spin-flips via transverse interactions. As scattering becomes strong, so does the frequency of spin flips, cumulating a very effective spin-flip based spin relaxation. This point is in agreement with Morandi, *et al.*[91], who find that spin-flip-based spin relaxation mechanisms (including Elliott-Yafet) are important when spin-dependent scattering is dominant.

An interesting consequence of fast carrier spin relaxation due to spin-flips in scattering is that while the total spin of carriers and magnetic impurities is conserved in collisions, the spin of carriers alone is not necessarily conserved. Scattering of carriers from impurity spin fluctuations allows for transfer of spin from carriers to impurities. Near the ferromagnetic transition, this spin transfer is very efficient. This could have an impact on the overall magnetism of the system which is not proportional to $\langle \mathbf{S} \rangle + \langle \boldsymbol{\sigma} \rangle$, but rather weights each spin by a g-factor. We suggest this could lead to an interesting study on the relationship between magnetism and spin polarization when one spin population changes rapidly.

Further comparing the DP mechanism to spin-flip spin relaxation, a reasonable question to ask is whether the rates can be summed according to Matthiessen's rule. This would not be appropriate, as each mechanism relaxes spins to different equilibrium states. For the case of spin-flip spin relaxation, the total spin of carriers and impurities is conserved. This is not true in the DP mechanism, where spin is lost to the spin-orbit field instead of transferred to impurities. Especially considering the timescales at which each spin relaxation mechanism operates near the ferromagnetic transition, it makes more sense to order the events as spin-flip spin relaxation to reach an intermediate equilibrium state, and then DP spin relaxation brings the system to its final equilibrium state where the total spin in the system will have declined.

4.6 Conclusion

We derived analytic expressions for spin relaxation in Zener model dilute magnetic semiconductors. Two spin relaxation mechanisms were considered: spin flips in scattering and Dyakonov-Perel. The expressions are valid for degenerate carriers with arbitrary spin polarization and can be used with a variety of spin-dependent dynamic interactions.

We demonstrate the relative effectiveness of these spin relaxation mechanisms near a ferromagnetic instability. In the Dyakonov-Perel mechanism, spin-dependent scattering turns out to significantly inhibit spin relaxation, due to both spin- and momentum-transfer processes disrupting spin precession in a spin-orbit field. When Dyakonov-Perel spin relaxation is suppressed, spin-flip spin relaxation becomes dominant. The two spin relaxation mechanisms do not relax spins to the same final state, though. While total spin is conserved in spin-flip scattering, spin is dissipated by a spin orbit field in the Dyakonov-Perel mechanism. We argue that Elliott-Yafet spin relaxation would only slightly modify the rate of spin relaxation due to transverse interactions which are already very strong near a ferromagnetic instability.

Our investigation demonstrates some interesting features of the mean-field model utilized. Namely, the height of the carrier scattering rate peak at a ferromagnetic transition depends only indirectly on the interaction strength, through the critical temperature. Furthermore, the peak's height has a weak dependence on carrier density. We should acknowledge that mean-field theory is not ideal to describe critical phenomena, but argue that this model was sufficient to reproduce scattering enhancements and their impact on spin relaxation *near* an instability.

Acknowledgements

This work was supported by the National Science Foundation under grant number DMR-1104788. We would like to thank Dr. Ilya Tokatly for extensive and enlightening discussions on spin-dependent interactions in the collision integral for a Fermi liquid.

Chapter 5

Summary

The viability of a material for use in spintronics applications depends critically on the spin lifetimes of particles in the material. For some applications, nanosecond timescales are sufficient to propagate a signal across a short junction before depolarization and decoherence set in. For others, years are needed to ensure stored information is not corrupted. Understanding spin relaxation mechanisms and how they might be manipulated in various materials is then fundamental to the field of spintronics.

The study of spin lifetimes in even well understood materials like gallium arsenide and silicon goes beyond the field of spintronics by severely testing our ability to describe interactions in the solid state. Theoretical descriptions of effective charge or spin based interactions and scattering at the microscopic level are still challenging research topics. As well as the materials studied in this report are understood for electronics applications, their magnetic properties continue to produce interesting spin phenomena. For instance, the Dresselhaus and Rashba spin-orbit fields are responsible for countless research papers on spin dynamics in semiconductors. It is in these well known semiconductors that we get secure footing before applying the theories to more novel materials.

In this dissertation, three theoretical studies of spin relaxation in III-V type semicon-

ductors have been presented. In Chapter 2, we showed how spin relaxation led to the appearance of diminished diffusion rates for spin polarized electrons in optically excited packets in GaAs. This was a collaborative study with experimentalist Dr. Hui Zhao at the University of Kansas, who shared measurements with us to help provide theoretical backing. Ultimately, the rate of scattering dictated how fast electrons were able to depolarize due to spin precessions in a spin-orbit field. In a spin packet, the electrons on the outermost edges scattered less often so that their spins were able to relax faster than those in the center of the packet. The time evolution of the packet made it appear as if spins were diffusing slower than charge, but a more apt description would be that polarization was diminishing at the packet edges faster than in the center.

In Chapter 3, we took a more in-depth look at GaAs and the contribution of many-body interactions to Dyakonov-Perel spin relaxation. Analytic results were obtained for spin relaxation inhibited by electron-electron and electron-hole collisions. We also studied the effect of including local-field factors in the scattering amplitude, which had some pronounced effects as the system moved away from high degeneracy via temperature or electron density. The results obtained in this chapter enable experimentalists to make quick theoretical predictions without significant computational power or time investment.

In Chapter 4, we studied spin relaxation near a ferromagnetic transition in dilute magnetic semiconductors. We used the Zener model to describe a system of itinerant carriers and localized magnetic impurities interacting via spin-exchange. As in Chapter 3, we derived analytic results for spin relaxation inhibited by scattering, but we also derived results for spin-flip based spin relaxation. We found that near a ferromagnetic transition, where impurity spin fluctuations become strong, carriers quickly lose any non-equilibrium spin polarization by transferring spin to the impurities.

Each of the projects completed in this dissertation have answered questions about the microscopic behavior of electrons and holes in III-V semiconductors. They have also generated new questions. For instance, in Chapter 2, while Dyakonov-Perel spin relaxation was

able to describe the long timescale behavior of diminished spin diffusion, there is a short time period at the beginning of measurements where the theory could not fit the fast initial diffusion. Is there another effect that should be taken into account for very short timescales? In Chapter 4, while we were careful to only include scattering events where total spin was conserved, this involved two distinct particles, carriers and magnetic impurities. The carriers lose non-equilibrium spin polarization very quickly via the transverse interaction with impurities. What impact does this fast spin relaxation have on total magnetization, which is not proportional to the total spin but rather weights each spin by a g-factor?

In summary, the effect of many-body collisions on spin relaxation has shown to not only be a significant factor, but sometimes the driving force behind the presence or absence of spin relaxation. The Dyakonov-Perel mechanism is a major contributor to spin relaxation in III-V semiconductors. By including all relevant scattering sources for carriers, this mechanism can be the basis of a challenging theoretical calculation at the microscopic level.

Appendix A

Ambipolar spin diffusion in GaAs quantum wells

A.1 Spin diffusion matrix

The spin diffusion matrix is derived from the resistivity matrix by application of Einstein's relations. The resistivity matrix is given by[37]

$$\hat{\rho} = \frac{m^*}{ne^2\tau}\begin{bmatrix} \frac{n}{n_\uparrow} + \frac{n_\downarrow}{n_\uparrow}\tau\gamma & -\tau\gamma \\ -\tau\gamma & \frac{n}{n_\downarrow} + \frac{n_\uparrow}{n_\downarrow}\tau\gamma \end{bmatrix} \tag{A.1}$$

where we have assumed no external electric field. In addition, the momentum relaxation rate due to electron-impurity collisions which flip the spin was taken as negligible in comparison to non-flip processes. τ is essentially the Drude scattering time.

Inverting the resistivity to find conductivity ($\hat{\sigma}$), Einstein's relation gives the diffusion matrix

$$e^2 D_{\alpha\beta} = \sum_\gamma \sigma_{\alpha\gamma}\left[\chi^{-1}\right]_{\gamma\beta} \tag{A.2}$$

where the spin susceptibility matrix $\hat{\chi}$ is approximated as

$$\hat{\chi} = \begin{bmatrix} \frac{\partial n_\uparrow}{\partial \mu_{c\uparrow}} & \frac{\partial n_\uparrow}{\partial \mu_{c\downarrow}} \\ \frac{\partial n_\downarrow}{\partial \mu_{c\uparrow}} & \frac{\partial n_\downarrow}{\partial \mu_{c\downarrow}} \end{bmatrix} \cong \begin{bmatrix} \frac{n_\uparrow}{kT} & 0 \\ 0 & \frac{n_\downarrow}{kT} \end{bmatrix} . \tag{A.3}$$

The diffusion matrix is finally,

$$\hat{D} = \frac{D_n}{1+\gamma\tau} \begin{bmatrix} 1+\frac{n_\uparrow}{n}\tau\gamma & \frac{n_\uparrow}{n}\tau\gamma \\ \frac{n_\downarrow}{n}\tau\gamma & 1+\frac{n_\downarrow}{n}\tau\gamma \end{bmatrix} \tag{A.4}$$

where the following relation was used,

$$D_n = \mu_n \frac{k_B T}{e} = \frac{e\tau}{m^*} \frac{k_B T}{e} . \tag{A.5}$$

Appendix B

Dyakonov-Perel spin relaxation in intrinsic GaAs

B.1 Equivalence of harmonics

It is relatively straightforward to demonstrate that integration of $W\Omega_{\mathbf{q},z}$ (where $\mathbf{q}$ can be any of $\mathbf{k}'$, $\mathbf{p}$, or $\mathbf{p}'$) over $d\hat{\mathbf{q}} = \sin\vartheta_q d\vartheta_q d\varphi_q$ in Eq. (3.17) results in a term proportional to $\Omega_{\mathbf{k},z}$. Let us write $\mathbf{\Omega}_{\mathbf{q},z}$ in terms of spherical harmonics:

$$\Omega_{\mathbf{q},z} = Cq^3\sqrt{\frac{8\pi}{105}}\left[Y_3^2(\vartheta_q,\varphi_q) - Y_3^{-2}(\vartheta_q,\varphi_q)\right] , \tag{B.1}$$

where C is a constant.

The angular portion of the collision integral in Eq. (3.17) has each $\Omega_{\mathbf{q},z}$ integrated with a scattering probability. These scattering probabilities can be expanded in Legendre polynomials of argument $\cos\alpha = \hat{\mathbf{k}}\cdot\hat{\mathbf{q}}$:

$$W = \sum_l w_l P_l\left(\cos\alpha\right) , \tag{B.2}$$

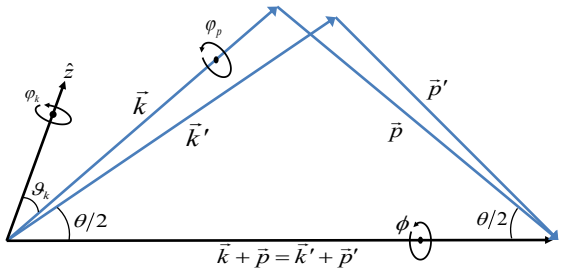

Figure B.1: For an arbitrary direction of $\mathbf{k}$ with respect to $\hat{\mathbf{z}}$, the direction of each momentum vector can be put entirely in terms of $\mathbf{k}$ and the angles θ, ϕ, and φ_p. Angle ϕ defines the planes in which $\mathbf{k}$,$\mathbf{p}$ and $\mathbf{k}'$,$\mathbf{p}'$ lie.

where W can represent either $\left|W_{\mathbf{kpk'p'}}\right|^2$ or $\left|W_{\mathbf{kpk'p'}}W_{\mathbf{kpp'k'}}\right|$. The coefficients can later be found with

$$w_l = \frac{2l+1}{2}\int_{-1}^{1} d\left(\cos\alpha\right) W P_l\left(\cos\alpha\right) . \tag{B.3}$$

The addition theorem for spherical harmonics expands P_l in spherical harmonics:

$$P_l\left(\cos\alpha\right) = \frac{4\pi}{2l+1}\sum_m Y_l^{*m}\left(\vartheta_q,\varphi_q\right) Y_l^m\left(\vartheta_k,\varphi_k\right) . \tag{B.4}$$

Then, integration over $d\hat{\mathbf{q}}$ is easy due to the orthogonality of spherical harmonics:

$$\begin{aligned}\int d\hat{\mathbf{q}}\, W\Omega_{\mathbf{q},z} =& w_3\frac{4\pi}{7}\Omega_{\mathbf{k},z} \\ =& 2\pi\Omega_{\mathbf{k},z}\int_{-1}^{1} d(\cos\alpha)\, W P_3(\cos\alpha) .\end{aligned} \tag{B.5}$$

That $\Omega_{\mathbf{k},z}$ can be extracted from each term in Eq. (3.17) goes to show that the relaxation time approximation in Eq. (1.12) and an angular-independent τ_k^* are both reasonable claims.

B.2 Reduction of the integral equation

We begin our solution for τ_k^* by working from Eq. (3.17) with the replacements discussed, cubic symmetry allows $\mathbf{\Omega_k} \times \hat{\mathbf{s}} \to \Omega_{\mathbf{k},z}$ and angular independence in $\tau_{\mathbf{k}}^*$ allows $\tau_{\mathbf{k}}^* \to \tau_k^*$:

$$
\begin{aligned}
& f_k^0(1-f_k^0)\Omega_{\mathbf{k},z} = \\
& \quad \frac{4\pi}{\hbar}\frac{1}{(2\pi)^6}\sum_{\mathbf{p}'}\int d\mathbf{k}'\, d\mathbf{p}\, f_k^0(1-f_{k'}^0)f_p^0(1-f_{p'}^0)\delta\left(\varepsilon_k+\varepsilon_p-\varepsilon_{k'}-\varepsilon_{p'}\right)\delta_{\mathbf{k}+\mathbf{p},\mathbf{k}'+\mathbf{p}'} \\
& \quad \Big\{ \left|W_{\mathbf{kpk'p'}}\right|^2 \left[\tau_k^*\Omega_{\mathbf{k},z}-\tau_{k'}^*\Omega_{\mathbf{k}',z}\right] \\
& \qquad -\frac{1}{2}\left|W_{\mathbf{kpk'p'}}W_{\mathbf{kpp'k'}}\right|\left[\tau_k^*\Omega_{\mathbf{k},z}-\tau_{k'}^*\Omega_{\mathbf{k}',z}+\tau_p^*\Omega_{\mathbf{p},z}-\tau_{p'}^*\Omega_{\mathbf{p}',z}\right]\Big\}. \qquad \text{(B.6)}
\end{aligned}
$$

The sum over $\mathbf{p}'$ can be evaluated immediately using conservation of momentum. Then, following a method introduced by Abrikosov and Khalatnikov[53] (or for an alternative derivation, Baym and Pethick[59]), at low temperatures the integral over momentum space can be re-expressed as

$$
d\mathbf{k}'\, d\mathbf{p} = \frac{m_c^3}{2\hbar^6\cos(\theta/2)} d\varepsilon_{k'}\, d\varepsilon_p\, d\varepsilon_{p'}\, \sin\theta d\theta\, d\phi\, d\varphi_p\,, \qquad \text{(B.7)}
$$

where θ is the angle between $\mathbf{k}$ and $\mathbf{p}$, and ϕ is a polar angle about the $\mathbf{k}+\mathbf{p}$ axis (See Fig. B.1). Aside from spin dependence, the scattering amplitudes are functions of only θ and ϕ.

At this point our kinetic equation has the form

$$\Omega_{\mathbf{k},z} = \frac{2m_c^3}{\hbar^7(2\pi)^5}\int_{-\infty}^{\infty}d\varepsilon_{k'}\int_{-\infty}^{\infty}d\varepsilon_p\int_{-\infty}^{\infty}d\varepsilon_{p'}\left(\frac{1-f^0_{k'}}{1-f^0_k}\right)f^0_p(1-f^0_{p'})\delta\left(\varepsilon_k+\varepsilon_p-\varepsilon_{k'}-\varepsilon_{p'}\right)$$
$$\times\int_0^{2\pi}d\phi\int_0^{\pi}d\theta\int_0^{2\pi}d\varphi_p\sin(\theta/2)\Big\{\left|W_{\mathbf{kpk'p'}}\right|^2\left[\Omega_{\mathbf{k},z}\tau^*_k-\Omega_{\mathbf{k'},z}\tau^*_{k'}\right]$$
$$-\frac{1}{2}\left|W_{\mathbf{kpk'p'}}W_{\mathbf{kpp'k'}}\right|\left[\Omega_{\mathbf{k},z}\tau^*_k-\Omega_{\mathbf{k'},z}\tau^*_{k'}+\Omega_{\mathbf{p},z}\tau^*_p-\Omega_{\mathbf{p'},z}\tau^*_{p'}\right]\Big\}. \tag{B.8}$$

The spherical harmonic definition of $\Omega_{\mathbf{k},z}$ from Eq. (3.18) is useful at this point. The orthogonality associated with the spherical harmonic functions is exploited by multiplying through by $\Omega_{\mathbf{k},z}$ in Eq. (B.8) and integrating over $\sin\vartheta_k d\vartheta_k\, d\varphi_k$. The left hand side reduces with use of

$$\int_0^{\pi}d\vartheta_k\int_0^{2\pi}d\varphi_k\,\sin\vartheta_k\Omega^2_{\mathbf{k},z}=C^2k^6\frac{16\pi}{105}\,, \tag{B.9}$$

where $C^2=\alpha_c^2\hbar^4/(2m_c^3E_g)$.

There is still the matter of putting the angles corresponding to vectors $\mathbf{p}$, $\mathbf{k}'$, and $\mathbf{p}'$ in in terms of the integration variables. This is accomplished by introducing a right hand orthonormal basis of vectors:

$$\hat{\mathbf{k}}=\{\sin\vartheta_k\cos\varphi_k,\sin\vartheta_k\sin\varphi_k,\cos\vartheta_k\}\,, \tag{B.10a}$$

$$\hat{\mathbf{t}}=\{\cos\vartheta_k\cos\varphi_k,\cos\vartheta_k\sin\varphi_k,-\sin\vartheta_k\}\,, \tag{B.10b}$$

$$\hat{\mathbf{n}}=\hat{\mathbf{k}}\times\hat{\mathbf{t}}\,. \tag{B.10c}$$

Aligning $\hat{\mathbf{k}}$ along $\hat{\mathbf{z}}$, it is seen that

$$\hat{\mathbf{p}}=\cos\theta\hat{\mathbf{k}}+\sin\theta\cos\varphi_p\hat{\mathbf{t}}+\sin\theta\sin\varphi_p\hat{\mathbf{n}}\,. \tag{B.11}$$

A rotation formula can be applied so that vectors $\mathbf{k}$ and $\mathbf{p}$ are turned about the $\mathbf{k}+\mathbf{p}$ axis

to find $\hat{\mathbf{k}}'$ and $\hat{\mathbf{p}}'$:

$$\hat{\mathbf{k}}' = \frac{\hat{\mathbf{k}}+\hat{\mathbf{p}}}{2} + \frac{\hat{\mathbf{k}}-\hat{\mathbf{p}}}{2}\cos\phi + \left(\frac{\hat{\mathbf{k}}\times\hat{\mathbf{p}}}{|\hat{\mathbf{k}}+\hat{\mathbf{p}}|}\right)\sin\phi\,, \tag{B.12}$$

$$\hat{\mathbf{p}}' = \frac{\hat{\mathbf{k}}+\hat{\mathbf{p}}}{2} - \frac{\hat{\mathbf{k}}-\hat{\mathbf{p}}}{2}\cos\phi - \left(\frac{\hat{\mathbf{k}}\times\hat{\mathbf{p}}}{|\hat{\mathbf{k}}+\hat{\mathbf{p}}|}\right)\sin\phi\,. \tag{B.13}$$

Standard relations are used to put the angular components of $\hat{\mathbf{k}}'$, $\hat{\mathbf{p}}$, and $\hat{\mathbf{p}}'$ in terms of the integration variables:

$$\cos\vartheta_q = q_z\,, \tag{B.14}$$

$$\cos\varphi_q = \frac{q_x}{\sqrt{1-q_z^2}}\,. \tag{B.15}$$

This concludes the needed angular transformations. Let us define the angular-only portion of $\Omega_{\mathbf{k},z}$ with $\kappa(\vartheta_k,\varphi_k)$. In other words

$$\begin{aligned}\kappa(\vartheta_k,\varphi_k) =& \cos\vartheta_k \sin^2\vartheta_k \cos(2\varphi_k)\\ =&(\cos\vartheta_k - \cos^3\vartheta_k)(2\cos^2\varphi_k - 1)\,,\end{aligned} \tag{B.16}$$

where identities have been used to write κ in terms of cosine functions for direct use of Eqs. (B.14) and (B.15). This leaves us with

$$\frac{16\pi}{105} = \frac{2m_c^3}{\hbar^7(2\pi)^5}$$
$$\times \int_{-\infty}^{\infty} d\varepsilon_{k'} \int_{-\infty}^{\infty} d\varepsilon_p \int_{-\infty}^{\infty} d\varepsilon_{p'} \left(\frac{1-f_{k'}^0}{1-f_k^0}\right) f_p^0(1-f_{p'}^0)\delta\left(\varepsilon_k+\varepsilon_p-\varepsilon_{k'}-\varepsilon_{p'}\right)$$
$$\times \int_0^{2\pi} d\varphi_k \int_0^{\pi} d\vartheta_k \int_0^{2\pi} d\phi \int_0^{\pi} d\theta \int_0^{2\pi} d\varphi_p \sin\vartheta_k \sin(\theta/2)\kappa\left(\vartheta_k,\varphi_k\right)$$
$$\times \left\{ |W_{\mathbf{kk'}}|^2 \left[\kappa\left(\vartheta_k,\varphi_k\right)\tau_k^* - \frac{\kappa\left(\vartheta_{k'},\varphi_{k'}\right)}{(k/k')^3}\tau_{k'}^*\right] - \frac{1}{2}\left|W_{\mathbf{kk'}}W_{\mathbf{kp'}}\right| \right.$$
$$\left. \times \left[\kappa\left(\vartheta_k,\varphi_k\right)\tau_k^* - \frac{\kappa\left(\vartheta_{k'},\varphi_{k'}\right)}{(k/k')^3}\tau_{k'}^* + \frac{\kappa\left(\vartheta_p,\varphi_p\right)}{(k/p)^3}\tau_p^* - \frac{\kappa\left(\vartheta_{p'},\varphi_{p'}\right)}{(k/p')^3}\tau_{p'}^*\right] \right\}. \tag{B.17}$$

Here, we have made use of the fact that the scattering amplitude in the direct portion of the collision integral only depends on the momentum transfer $\mathbf{k} \to \mathbf{k'}$, whereas the exchange portion includes the possibilities of $\mathbf{k} \to \mathbf{k'}$ and $\mathbf{k} \to \mathbf{p'}$. For scattering near the Fermi surface, the scattering amplitudes only vary with the angle between incoming and outgoing momenta. These angles can be written in terms of just θ and ϕ with the following relations:

$$\cos\theta_1 = \hat{\mathbf{k}}\cdot\hat{\mathbf{k}}' = \frac{1}{2}(1+\cos\theta+\cos\phi-\cos\theta\cos\phi)\,, \tag{B.18}$$
$$\cos\theta_2 = \hat{\mathbf{k}}\cdot\hat{\mathbf{p}}' = \frac{1}{2}(1+\cos\theta-\cos\phi+\cos\theta\cos\phi)\,. \tag{B.19}$$

The scattering amplitudes written as functions of θ_1 and θ_2 are

$$W_{\mathbf{kk'}} = W(\cos\theta_1)\,, \tag{B.20}$$
$$W_{\mathbf{kp'}} = W(\cos\theta_2)\,. \tag{B.21}$$

For reference, the dimensionless momentum transfers are

$$\widetilde{q}_1 = |\mathbf{k} - \mathbf{k}'|/\left(2k_F\right) = \sin\left(\theta/2\right)\sin\left(\phi/2\right) \ , \tag{B.22}$$

$$\widetilde{q}_2 = |\mathbf{k} - \mathbf{p}'|/\left(2k_F\right) = \sin\left(\theta/2\right)\left|\cos\left(\phi/2\right)\right| \ . \tag{B.23}$$

The absolute value is a result of the range of integration, $0 < \phi < 2\pi$.

Integration over $d\varphi_p$, $d\vartheta_k$ and $d\varphi_k$ can be done immediately with the result

$$\begin{aligned}
&\frac{\hbar^7(2\pi)^4}{m_c^3} = \\
&\int_{-\infty}^{\infty} d\varepsilon_{k'} \int_{-\infty}^{\infty} d\varepsilon_p \int_{-\infty}^{\infty} d\varepsilon_{p'} \left(\frac{1-f_{k'}^0}{1-f_k^0}\right) f_p^0(1-f_{p'}^0)\delta\left(\varepsilon_k + \varepsilon_p - \varepsilon_{k'} - \varepsilon_{p'}\right) \\
&\times \int d\Omega \Bigg\{ \frac{|W_{\mathbf{kk'}}|^2}{\cos(\theta/2)} \left[\tau_k^* - \frac{P_3\left(\cos\theta_1\right)}{(k/k')^3}\tau_{k'}^*\right] \\
&\quad -\frac{1}{2}\frac{\left|W_{\mathbf{kk'}}W_{\mathbf{kp'}}\right|}{\cos(\theta/2)} \left[\tau_k^* - \frac{P_3\left(\cos\theta_1\right)}{(k/k')^3}\tau_{k'}^* + \frac{P_3\left(\cos\theta\right)}{(k/p)^3}\tau_p^* - \frac{P_3\left(\cos\theta_2\right)}{(k/p')^3}\tau_{p'}^*\right] \Bigg\} ,
\end{aligned} \tag{B.24}$$

where $d\Omega = \sin\theta\, d\theta d\phi$ should not be confused with the Dresselhaus Larmor frequency.

Notice that without the Legendre polynomial terms, the scattering time could be factored out of the integral and we would have exactly the scattering rate of plane waves, as can be referenced in [40]. Given that well known solution, we are led to believe τ_k^* will have even dependences on energy and temperature.

The ratios $(k/k')^3$, $(k/p)^3$, and $(k/p')^3$ vary slowly across the Fermi surface when compared to the Fermi-Dirac functions and anticipated $\varepsilon_k - \mu$ dependence in τ_k^*. They are all set to 1. We shall consider only static screening in the scattering amplitudes, a reasonable assumption at low temperature. The resulting integral equation for τ_k^* has been exactly solved by Sykes and Brooker.[54] We will reproduce a simplified version of the solution here.

The energy integrals are written in terms of unitless variables:

$$\xi = (\varepsilon_k - \mu)/k_B T\,, \tag{B.25}$$

$$x = (\varepsilon_{k'} - \mu)/k_B T\,, \tag{B.26}$$

$$y = (\varepsilon_{p'} - \mu)/k_B T\,, \tag{B.27}$$

and the δ-function evaluated for $(\varepsilon_p - \mu)/k_B T$ to give

$$\begin{aligned}
&\frac{\hbar^7 (2\pi)^4}{m_c^3 \left(k_B T\right)^2} = \\
&\quad \int_{-\infty}^{\infty} dx \int_{-\infty}^{\infty} dy \left[\frac{f^0(-x)}{f^0(-\xi)}\right] f^0(x+y-\xi) f^0(-y) \int d\Omega \\
&\quad \times \left\{ \frac{|W_{\mathbf{kk'}}|^2}{\cos(\theta/2)} \left[\tau^*(\xi) - P_3\left(\cos\theta_1\right) \tau^*(x)\right] - \frac{1}{2} \frac{\left|W_{\mathbf{kk'}} W_{\mathbf{kp'}}\right|}{\cos(\theta/2)} \right. \\
&\qquad \left. \times \left[\tau^*(\xi) - P_3\left(\cos\theta_1\right) \tau^*(x) + P_3\left(\cos\theta\right) \tau^*(x+y-\xi) - P_3\left(\cos\theta_2\right) \tau^*(y)\right] \right\}.
\end{aligned} \tag{B.28}$$

The equilibrium Fermi-Dirac functions are now described by

$$f^0(x) = \frac{1}{1+e^x}\,. \tag{B.29}$$

Integration of $\tau^*(x+y-\xi)$ over dy is equivalent to integration of $\tau^*(-y)$ over dy. This relation, along with a simple swap of $x \leftrightarrow y$ variables in terms which have $\tau^*(\pm y)$, allows the integration over dy to be performed:

$$\int_{-\infty}^{\infty} dy\, f^0(x+y-\xi) f^0(-y) = \frac{\xi - x}{1 - e^{x-\xi}}\,. \tag{B.30}$$

With an even dependence on x, we can also let $\tau^*(-x) \to \tau^*(x)$. To simplify the form of the integral equation, the angular integrals are represented by constants B and λ, and the

remaining x-dependent factor by $K(x,\xi)$:

$$K(x,\xi) = \frac{f^0(-x)}{f^0(-\xi)}\left[\frac{\xi - x}{1 - e^{x-\xi}}\right], \tag{B.31a}$$

$$A_1 = \int d\Omega \, \frac{|W_{\mathbf{kk'}}|^2}{\cos(\theta/2)}, \tag{B.31b}$$

$$A_2 = \int d\Omega \, \frac{|W_{\mathbf{kk'}} W_{\mathbf{kp'}}|}{\cos(\theta/2)}, \tag{B.31c}$$

$$\lambda_1 = \frac{1}{A_1}\int d\Omega \, \frac{|W_{\mathbf{kk'}}|^2}{\cos(\theta/2)} P_3(\cos\theta_1), \tag{B.31d}$$

$$\lambda_2 = \frac{1}{A_2}\int d\Omega \, \frac{|W_{\mathbf{kk'}} W_{\mathbf{kp'}}|}{\cos(\theta/2)} \left[P_3(\cos\theta_1) - P_3(\cos\theta) + P_3(\cos\theta_2)\right], \tag{B.31e}$$

$$B = \frac{\hbar^7 (2\pi)^4}{m_c^3 (k_B T)^2}\left(A_1 - \frac{A_2}{2}\right)^{-1}, \tag{B.31f}$$

$$\lambda = \frac{A_1\lambda_1 - A_2\lambda_2/2}{A_1 - A_2/2}. \tag{B.31g}$$

The remaining integral equation for $\tau^*(\xi)$ is exactly of the form in Sykes and Brooker:

$$B = \int_{-\infty}^{\infty} dx \, K(x,\xi)\left[\tau^*(\xi) - \lambda\tau^*(x)\right]. \tag{B.32}$$

Notice that the kernel of this integral equation involves only two-dimensional angular integrals on the Fermi surface. In fact, since A_1 and λ_1 do not contain any exchange terms, they can actually be simplified to one-dimensional integrals of the momentum transfer $\widetilde{q}_1$ in Eq. (B.22):

$$A_1 = 8\pi \int_0^1 d\widetilde{q}_1 \, |W(\widetilde{q}_1)|^2, \tag{B.33}$$

$$\lambda_1 = 8\pi \int_0^1 d\widetilde{q}_1 \, |W(\widetilde{q}_1)|^2 P_3(1 - 2\widetilde{q}_1^2)). \tag{B.34}$$

The solution for $\tau^*(\xi)$ is found by converting the integral equation to a differential equation via Fourier transform, utilizing the convolution theorem. For $\tau^*(\xi)$ with an even

dependence on ξ,

$$\tau^*(\xi) = \frac{\cosh(\xi/2)}{2\pi} \int_{-\infty}^{\infty} d\omega \, e^{-i\omega\xi} \frac{B}{\pi} \sum_{l=0}^{\infty} \frac{(4l+3)\Phi_{2l}(\omega)}{\Lambda_{2l}\left(\Lambda_{2l} - \lambda\right)} \,, \tag{B.35}$$

where

$$\Phi_l(\omega) = p_{l+1}^1 \left(\tanh \pi\omega\right) \,, \tag{B.36}$$

$$\Lambda_l = \frac{1}{2}(l+1)(l+2) \,, \tag{B.37}$$

and $p_l^m(x)$ are the associated Legendre polynomials.

Appendix C

Spin relaxation near a ferromagnetic transition

C.1 Modified Lindhard response functions

The modified Lindhard imaginary response functions presented in Chapter 4 have easily derivable analytic solutions. They are most compactly written in terms of the following dimensionless variables:

$$\bar{q}_\gamma = q/k_{F\gamma}\,, \tag{C.1}$$

$$\nu_{\gamma\pm} = \frac{\hbar\omega + (\beta-\alpha)\Delta/2}{\hbar q v_{F\gamma}} \pm \frac{q}{2k_{F\gamma}}\,, \tag{C.2}$$

$$\eta_\gamma = \frac{\hbar\omega + (\beta-\alpha)\Delta/2}{\varepsilon_{F\gamma}}\,. \tag{C.3}$$

The response function that enters momentum relaxation calculations is

$$\begin{aligned}\Im\chi^{(n,\gamma)}_{1\alpha\beta}(q,\omega) &= \frac{\pi}{k^n_{F\gamma}}\sum_{\mathbf{k}}\delta(\varepsilon_{\mathbf{k}+\mathbf{q}\beta}-\varepsilon_{k\alpha}-\hbar\omega)\left[f^0_{\mathbf{k}+\mathbf{q}\beta}-f^0_{k\alpha}\right](\mathbf{k}\cdot\hat{\mathbf{q}})^n \\ &= \nu^n_{\gamma-}\left\{\frac{\pi N_\beta(0)}{4\bar{q}_\beta}\Theta\left[1-\nu^2_{\beta+}\right]\left(1-\nu^2_{\beta+}\right)-\frac{\pi N_\alpha(0)}{4\bar{q}_\alpha}\Theta\left[1-\nu^2_{\alpha-}\right]\left(1-\nu^2_{\alpha-}\right)\right\}.\end{aligned} \tag{C.4}$$

The response function used in effective scattering rate calculations for spin relaxation is

$$\begin{aligned}\Im\chi^{(n)}_{3\alpha\beta}(q,\omega) &= \pi\sum_{\mathbf{k}}\delta(\varepsilon_{\mathbf{k}+\mathbf{q}\beta}-\varepsilon_{k\alpha}-\hbar\omega)\left[f^0_{\mathbf{k}+\mathbf{q}\beta}-f^0_{k\alpha}\right]\frac{k^n}{|\mathbf{k}+\mathbf{q}|^n}P_n\left[\hat{\mathbf{k}}\cdot\frac{\mathbf{k}+\mathbf{q}}{|\mathbf{k}+\mathbf{q}|}\right] \\ &= \frac{\pi N_\beta(0)}{4\bar{q}_\beta}\Theta\left[1-\nu^2_{\beta+}\right]\left[\mathcal{Z}_n\left(1,\eta_\beta,\bar{q}_\beta\right)-\mathcal{Z}_n\left(\nu^2_{\beta+},\eta_\beta,\bar{q}_\beta\right)\right] \\ &\quad -\frac{\pi N_\alpha(0)}{4\bar{q}_\alpha}\Theta\left[1-\nu^2_{\alpha-}\right]\left[\mathcal{Z}_n\left(1+\eta_\alpha,\eta_\alpha,\bar{q}_\alpha\right)-\mathcal{Z}_n\left(\nu^2_{\alpha-}+\eta_\alpha,\eta_\alpha,\bar{q}_\alpha\right)\right],\end{aligned} \tag{C.5}$$

where

$$\mathcal{Z}_n\left(x,\eta,\bar{q}\right)=\int dx\left|\frac{x-\eta}{x}\right|^{n/2}P_n\left[\frac{2x-\eta-\bar{q}^2}{2\sqrt{x^2-x\eta}}\right]. \tag{C.6}$$

In the case of a Dresselhaus spin-orbit field, $\Im\chi^{(3)}_{3\alpha\beta}(q,\omega)$ is the relevant response function with

$$\mathcal{Z}_3\left(x,\eta,\bar{q}\right)=\frac{5(\bar{q}^2+\eta)^3}{32x^2}-\frac{3(5\bar{q}^4+8\bar{q}^2\eta+3\eta^2)}{8x}+x-\frac{3(2\bar{q}^2+\eta)}{2}\ln(x). \tag{C.7}$$

For both of the above response functions, $n=0$ reduces them to standard Lindhard imaginary response. Comparisons of the relevant modified response functions are plotted in Fig. C.1. They obey the same cutoff frequencies and electron-hole continuum boundaries as Lindhard imaginary response. The property that $\Im\chi(q,\omega)$ be negative for positive frequencies does not necessarily hold for odd n though.

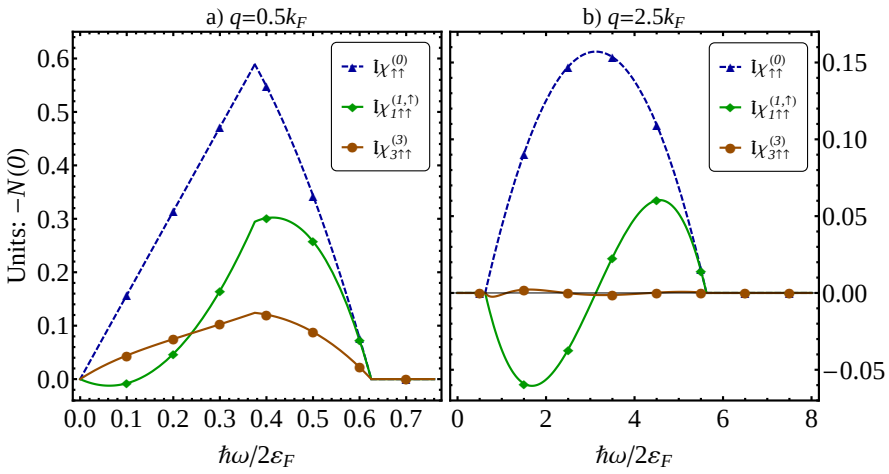

Figure C.1: The modified response functions (solid lines) compared to Lindhard imaginary response (dashed line) for a) $q = 0.5k_F$ and b) $q = 0.5k_F$ at zero polarization.

Bibliography

[1] D. D. Awschalom, D. Loss, and N. Samarth. *Semiconductor Spintronics and Quantum Computation*. Verlag Berlin Heidelberg New York: Springer, 2002. ISBN: 978-3-540-42176-4. URL: http://www.springer.com/978-3-540-42176-4.

[2] D. D. Awschalom and M. E. Flatté. "Challenges for semiconductor spintronics". In: *Nat. Phys.* 3 (Mar. 2007), p. 153. DOI: 10.1038/nphys551.

[3] S. A. Wolf et al. "Spintronics: A Spin-Based Electronics Vision for the Future". In: *Science* 294.5546 (2001), pp. 1488–1495. DOI: 10.1126/science.1065389.

[4] I. Žutić, J. Fabian, and S. Das Sarma. "Spintronics: Fundamentals and applications". In: *Rev. Mod. Phys.* 76 (2 Apr. 2004), pp. 323–410. DOI: 10.1103/RevModPhys.76.323. URL: http://link.aps.org/doi/10.1103/RevModPhys.76.323.

[5] J. Fabian et al. "Semiconductor Spintronics". In: *Acta physica Slovaca* 57 (4&5 July 2007), pp. 565–907. URL: http://www.physics.sk/aps/pub.php?y=2007&pub=aps-07-04.

[6] M. I. Dyakonov. *Spin Physics in Semiconductors*. Verlag Berlin Heidelberg: Springer, 2008. ISBN: 978-3-540-78819-5. URL: http://www.springer.com/978-3-540-78819-5.

[7] M.W. Wu, J.H. Jiang, and M.Q. Weng. "Spin dynamics in semiconductors". In: *Phys. Rep.* 493.2-4 (2010), pp. 61–236. ISSN: 0370-1573. DOI: http://dx.doi.org/10.1016/j.physrep.2010.04.002. URL: http://www.sciencedirect.com/science/article/pii/S0370157310000955.

[8] M. I. Dyakonov. "Introduction to spin physics in semiconductors". In: *Physica E* 35.2 (2006), pp. 246–250. ISSN: 1386-9477. DOI: 10.1016/j.physe.2006.08.024. URL: http://www.sciencedirect.com/science/article/pii/S1386947706004723.

[9] R. Hanson et al. “Spins in few-electron quantum dots”. In: *Rev. Mod. Phys.* 79 (Oct. 2007), pp. 1217–1265. DOI: 10.1103/RevModPhys.79.1217. URL: http://link.aps.org/doi/10.1103/RevModPhys.79.1217.

[10] K. C. Nowack et al. “Coherent Control of a Single Electron Spin with Electric Fields”. In: *Science* 318.5855 (2007), pp. 1430–1433. DOI: 10.1126/science.1148092. URL: http://www.sciencemag.org/content/318/5855/1430.abstract.

[11] M. I. D’yakonov and V. I. Perel’. “Spin relaxation of conduction electrons in noncentrosymmetric semiconductors”. In: *Zh. Eksp. Teor. Fiz.* 60 (1971). [Sov. Phys. JETP **33**, 1053 (1971)], p. 1954.

[12] R. J. Elliott. “Theory of the Effect of Spin-Orbit Coupling on Magnetic Resonance in Some Semiconductors”. In: *Phys. Rev.* 96 (2 Oct. 1954), pp. 266–279. DOI: 10.1103/PhysRev.96.266. URL: http://link.aps.org/doi/10.1103/PhysRev.96.266.

[13] Y. Yafet. “Calculation of the g Factor of Metallic Sodium”. In: *Phys. Rev.* 85 (3 Feb. 1952), pp. 478–478. DOI: 10.1103/PhysRev.85.478. URL: http://link.aps.org/doi/10.1103/PhysRev.85.478.

[14] G.L. Bir, A.G. Aronov, and G.E. Pikus. “Spin relaxation of electrons scattered by holes”. In: *Zh. Eksp. Teor. Fiz.* 69 (1975). [Sov. Phys. JETP **42**, 705 (1975)], p. 1382. URL: http://www.jetp.ac.ru/cgi-bin/e/index/r/69/4/p1382?a=list.

[15] P. I. Tamborenea, M. A. Kuroda, and F. L. Bottesi. “Spin relaxation in n-doped GaAs due to impurity and electron-electron Elliot-Yafet scattering”. In: *Phys. Rev. B* 68 (24 Dec. 2003), p. 245205. DOI: 10.1103/PhysRevB.68.245205. URL: http://link.aps.org/doi/10.1103/PhysRevB.68.245205.

[16] J. -N. Chazalviel. “Spin relaxation of conduction electrons in n-type indium antimonide at low temperature”. In: *Phys. Rev. B* 11 (4 Feb. 1975), pp. 1555–1562. DOI: 10.1103/PhysRevB.11.1555. URL: http://link.aps.org/doi/10.1103/PhysRevB.11.1555.

[17] G.E. Pikus and A.N. Titkov. “CHAPTER 3 - Spin Relaxation under Optical Orientation in Semiconductors”. In: *Optical Orientation*. Ed. by F. Meier and B.P. Zakharchenya. Vol. 8. Modern Problems in Condensed Matter Sciences. Elsevier, 1984, pp. 73–131. DOI: 10.1016/B978-0-444-86741-4.50008-1. URL: http://www.sciencedirect.com/science/article/pii/B9780444867414500081.

[18] Matthew D. Mower, G. Vignale, and I. V. Tokatly. “Dyakonov-Perel spin relaxation for degenerate electrons in the electron-hole liquid”. In: *Phys. Rev. B* 83 (15 Apr. 2011), p. 155205. DOI: 10.1103/PhysRevB.83.155205. URL: http://link.aps.org/doi/10.1103/PhysRevB.83.155205.

[19] G. Dresselhaus. "Spin-Orbit Coupling Effects in Zinc Blende Structures". In: *Phys. Rev.* 100 (2 Oct. 1955), pp. 580–586. DOI: 10.1103/PhysRev.100.580. URL: http://link.aps.org/doi/10.1103/PhysRev.100.580.

[20] Hui Zhao, Matt Mower, and G. Vignale. "Ambipolar spin diffusion and D'yakonov-Perel' spin relaxation in GaAs quantum wells". In: *Phys. Rev. B* 79 (11 Mar. 2009), p. 115321. DOI: 10.1103/PhysRevB.79.115321. URL: http://link.aps.org/doi/10.1103/PhysRevB.79.115321.

[21] Michael E. Flatté and Jeff M. Byers. "Spin Diffusion in Semiconductors". In: *Phys. Rev. Lett.* 84 (18 May 2000), pp. 4220–4223. DOI: 10.1103/PhysRevLett.84.4220. URL: http://link.aps.org/doi/10.1103/PhysRevLett.84.4220.

[22] D. D. Awschalom and J. M. Kikkawa. In: *Nature* 397.6715 (Jan. 1999), pp. 139–141. DOI: 10.1038/16420. URL: http://dx.doi.org/10.1038/16420.

[23] I. Malajovich et al. "Persistent sourcing of coherent spins for multifunctional semiconductor spintronics". In: *Nature* 411.6839 (June 2001), pp. 770–772. DOI: 10.1038/35081014. URL: http://dx.doi.org/10.1038/35081014.

[24] S. A. Crooker and D. L. Smith. "Imaging Spin Flows in Semiconductors Subject to Electric, Magnetic, and Strain Fields". In: *Phys. Rev. Lett.* 94 (23 June 2005), p. 236601. DOI: 10.1103/PhysRevLett.94.236601. URL: http://link.aps.org/doi/10.1103/PhysRevLett.94.236601.

[25] Y. K. Kato et al. "Observation of the Spin Hall Effect in Semiconductors". In: *Science* 306.5703 (2004), pp. 1910–1913. DOI: 10.1126/science.1105514. URL: http://www.sciencemag.org/content/306/5703/1910.abstract.

[26] V. Sih et al. "Spatial imaging of the spin Hall effect and current-induced polarization in two-dimensional electron gases". In: *Nat. Phys.* 1.1 (Oct. 2005), pp. 31–35. DOI: 10.1038/nphys009. URL: http://dx.doi.org/10.1038/nphys009.

[27] N. P. Stern et al. "Time-resolved dynamics of the spin Hall effect". In: *Nat. Phys.* 4.11 (Sept. 2008), pp. 843–846. DOI: 10.1038/nphys1076. URL: http://dx.doi.org/10.1038/nphys1076.

[28] S. A. Crooker et al. "Imaging Spin Transport in Lateral Ferromagnet/Semiconductor Structures". In: *Science* 309.5744 (2005), pp. 2191–2195. DOI: 10.1126/science.1116865. URL: http://www.sciencemag.org/content/309/5744/2191.abstract.

[29] D. Hagele et al. "Spin transport in GaAs". In: *Appl. Phys. Lett.* 73.11 (1998), pp. 1580–1582. DOI: 10.1063/1.122210. URL: http://link.aip.org/link/?APL/73/1580/1.

[30] H. Sanada et al. “Relaxation of photoinjected spins during drift transport in GaAs”. In: *Appl. Phys. Lett.* 81.15 (2002), pp. 2788–2790. DOI: 10.1063/1.1512818. URL: http://link.aip.org/link/?APL/81/2788/1.

[31] D. J. Hilton and C. L. Tang. “Optical Orientation and Femtosecond Relaxation of Spin-Polarized Holes in GaAs”. In: *Phys. Rev. Lett.* 89 (14 Sept. 2002), p. 146601. DOI: 10.1103/PhysRevLett.89.146601. URL: http://link.aps.org/doi/10.1103/PhysRevLett.89.146601.

[32] R. D. R. Bhat et al. “Two-photon spin injection in semiconductors”. In: *Phys. Rev. B* 71 (3 Jan. 2005), p. 035209. DOI: 10.1103/PhysRevB.71.035209. URL: http://link.aps.org/doi/10.1103/PhysRevB.71.035209.

[33] L. M. Smith et al. “Picosecond imaging of photoexcited carriers in quantum wells: Anomalous lateral confinement at high densities”. In: *Phys. Rev. B* 38 (8 Sept. 1988), pp. 5788–5791. DOI: 10.1103/PhysRevB.38.5788. URL: http://link.aps.org/doi/10.1103/PhysRevB.38.5788.

[34] Hui Zhao et al. “Spatiotemporal dynamics of quantum-well excitons”. In: *Phys. Rev. B* 67 (3 Jan. 2003), p. 035306. DOI: 10.1103/PhysRevB.67.035306. URL: http://link.aps.org/doi/10.1103/PhysRevB.67.035306.

[35] Hui Zhao. “Temperature dependence of ambipolar diffusion in silicon on insulator”. In: *Appl. Phys. Lett.* 92.11, 112104 (2008), p. 112104. DOI: 10.1063/1.2898711. URL: http://link.aip.org/link/?APL/92/112104/1.

[36] G. Vignale. “Many-body Effects in Spin-polarized Transport”. In: *Manipulating Quantum Coherence in Solid State Systems*. Ed. by Michael E. Flatté and I. Ţifrea. Vol. 244. NATO Science Series II: Mathematics, Physics and Chemistry. Springer Netherlands, 2007, pp. 53–96. ISBN: 978-1-4020-6135-6. DOI: 10.1007/978-1-4020-6137-0_2. URL: http://dx.doi.org/10.1007/978-1-4020-6137-0_2.

[37] Irene D’Amico and Giovanni Vignale. “Coulomb interaction effects in spin-polarized transport”. In: *Phys. Rev. B* 65 (8 Feb. 2002), p. 085109. DOI: 10.1103/PhysRevB.65.085109. URL: http://link.aps.org/doi/10.1103/PhysRevB.65.085109.

[38] C. P. Weber et al. “Observation of spin Coulomb drag in a two-dimensional electron gas”. In: *Nature* 437.7063 (Oct. 2005), pp. 1330–1333. DOI: 10.1038/nature04206. URL: http://dx.doi.org/10.1038/nature04206.

[39] M. M. Glazov and E. L. Ivchenko. “D’yakonov-Perel’ Spin Relaxation Controlled by Electron-Electron Scattering”. In: *J. Supercond.* 16 (4 2003), pp. 735–742. ISSN: 0896-1107. URL: http://dx.doi.org/10.1023/A:1025370024651.

[40] G. Giuliani and G. Vignale. *Quantum theory of the electron liquid*. New York; Cambridge: Cambridge University Press, 2005. ISBN: 9780521821124. DOI: 10.2277/0521821126.

[41] S. Oertel, J. Hubner, and M. Oestreich. "High temperature electron spin relaxation in bulk GaAs". In: *Appl. Phys. Lett.* 93.13, 132112 (2008), p. 132112. DOI: 10.1063/1.2993344. URL: http://link.aip.org/link/?APL/93/132112/1.

[42] J. H. Jiang and M. W. Wu. "Electron-spin relaxation in bulk III-V semiconductors from a fully microscopic kinetic spin Bloch equation approach". In: *Phys. Rev. B* 79 (12 Mar. 2009), p. 125206. DOI: 10.1103/PhysRevB.79.125206. URL: http://link.aps.org/doi/10.1103/PhysRevB.79.125206.

[43] Pil Hun Song and K. W. Kim. "Spin relaxation of conduction electrons in bulk III-V semiconductors". In: *Phys. Rev. B* 66 (3 July 2002), p. 035207. DOI: 10.1103/PhysRevB.66.035207. URL: http://link.aps.org/doi/10.1103/PhysRevB.66.035207.

[44] J H Jiang and M W Wu. "Comment on 'Density dependence of electron-spin polarization and relaxation in intrinsic GaAs at room temperature'". In: *J. Phys. D: Appl. Phys.* 42.23 (2009), p. 238001. DOI: 10.1088/0022-3727/42/23/238001. URL: http://stacks.iop.org/0022-3727/42/i=23/a=238001.

[45] J. M. Kikkawa and D. D. Awschalom. "Resonant Spin Amplification in n-Type GaAs". In: *Phys. Rev. Lett.* 80 (19 May 1998), pp. 4313–4316. DOI: 10.1103/PhysRevLett.80.4313. URL: http://link.aps.org/doi/10.1103/PhysRevLett.80.4313.

[46] M.W. Wu and C.Z. Ning. "A novel mechanism for spin dephasing due to spin-conserving scatterings". English. In: *Eur. Phys. J. B* 18.3 (2000), pp. 373–376. ISSN: 1434-6028. DOI: 10.1007/s100510070021. URL: http://dx.doi.org/10.1007/s100510070021.

[47] M. Q. Weng and M. W. Wu. "Spin dephasing in n-type GaAs quantum wells". In: *Phys. Rev. B* 68 (7 Aug. 2003), p. 075312. DOI: 10.1103/PhysRevB.68.075312. URL: http://link.aps.org/doi/10.1103/PhysRevB.68.075312.

[48] M.M. Glazov and E.L. Ivchenko. "Precession spin relaxation mechanism caused by frequent electron-electron collisions". English. In: *JETP Letters* 75.8 (2002), pp. 403–405. ISSN: 0021-3640. DOI: 10.1134/1.1490009. URL: http://dx.doi.org/10.1134/1.1490009.

[49] M.M. Glazov and E.L. Ivchenko. "Effect of electron-electron interaction on spin relaxation of charge carriers in semiconductors". English. In: *JETP* 99.6 (2004), pp. 1279–

1290. ISSN: 1063-7761. DOI: 10.1134/1.1854815. URL: http://dx.doi.org/10.1134/1.1854815.

[50] L. H. Teng et al. "Density dependence of spin relaxation in GaAs quantum well at room temperature". In: *EPL* 84.2 (2008), p. 27006. DOI: 10.1209/0295-5075/84/27006. URL: http://stacks.iop.org/0295-5075/84/i=2/a=27006.

[51] Shou Qian et al. "Carrier-Density-Dependent Electron Spin Relaxation in GaAs / AlGaAs Multi Quantum Wells". In: *Chin. Phys. Lett.* 22.9 (2005), p. 2320. DOI: 10.1088/0256-307X/22/9/050. URL: http://stacks.iop.org/0256-307X/22/i=9/a=050.

[52] Shen Ka. "A Peak in Density Dependence of Electron Spin Relaxation Time in n-Type Bulk GaAs in the Metallic Regime". In: *Chin. Phys. Lett.* 26.6 (2009), p. 067201. DOI: 10.1088/0256-307X/26/6/067201. URL: http://stacks.iop.org/0256-307X/26/i=6/a=067201.

[53] A A Abrikosov and I M Khalatnikov. "The theory of a fermi liquid (the properties of liquid 3 He at low temperatures)". In: *Rep. Prog. Phys.* 22.1 (1959), p. 329. DOI: 10.1088/0034-4885/22/1/310. URL: http://stacks.iop.org/0034-4885/22/i=1/a=310.

[54] J Sykes and G.A Brooker. "The transport coefficients of a fermi liquid". In: *Ann. Phys.* 56.1 (1970), pp. 1–39. ISSN: 0003-4916. DOI: 10.1016/0003-4916(70)90002-3. URL: http://www.sciencedirect.com/science/article/pii/0003491670900023.

[55] J.W. Jeon and W.J. Mullin. "Kinetic equation for dilute, spin-polarized quantum systems". In: *J. Phys. France* 49.10 (1988), pp. 1691–1706. DOI: 10.1051/jphys:0198800490100169100. URL: http://dx.doi.org/10.1051/jphys:0198800490100169100.

[56] V. P. Mineev. "Transverse spin dynamics in a spin-polarized Fermi liquid". In: *Phys. Rev. B* 69 (14 Apr. 2004), p. 144429. DOI: 10.1103/PhysRevB.69.144429. URL: http://link.aps.org/doi/10.1103/PhysRevB.69.144429.

[57] Hartmut Haug and Antti-Pekka Jauho. *Quantum Kinetics in Transport and Optics of Semiconductors*. Vol. 123. Springer Series in Solid-State Sciences. Berlin Heidelberg: Springer Berlin Heidelberg, 2008. ISBN: 978-3-540-73561-8. DOI: 10.1007/978-3-540-73564-9.

[58] P. Lipavský, V. Špička, and B. Velický. "Generalized Kadanoff-Baym ansatz for deriving quantum transport equations". In: *Phys. Rev. B* 34 (10 Nov. 1986), pp. 6933–6942. DOI: 10.1103/PhysRevB.34.6933. URL: http://link.aps.org/doi/10.1103/PhysRevB.34.6933.

[59] Gordon Baym and Christopher Pethick. "Landau Fermi-Liquid Theory and Low Temperature Properties of Normal Liquid 3He". In: *Landau Fermi-Liquid Theory*. Wiley-VCH Verlag GmbH, 2007, pp. 1–121. ISBN: 9783527617159. DOI: 10.1002/9783527617159.ch1. URL: http://dx.doi.org/10.1002/9783527617159.ch1.

[60] J. Zhou. "Effect of Singwi-Tosi-Land-Sjölander local field correction on spin relaxation in n-type GaAs quantum wells at low temperature". In: *Physica E* 41.1 (2008), pp. 50–53. ISSN: 1386-9477. DOI: 10.1016/j.physe.2008.06.004. URL: http://www.sciencedirect.com/science/article/pii/S1386947708002063.

[61] Carl A. Kukkonen and A. W. Overhauser. "Electron-electron interaction in simple metals". In: *Phys. Rev. B* 20 (2 July 1979), pp. 550–557. DOI: 10.1103/PhysRevB.20.550. URL: http://link.aps.org/doi/10.1103/PhysRevB.20.550.

[62] Saverio Moroni, David M. Ceperley, and Gaetano Senatore. "Static Response and Local Field Factor of the Electron Gas". In: *Phys. Rev. Lett.* 75 (4 July 1995), pp. 689–692. DOI: 10.1103/PhysRevLett.75.689. URL: http://link.aps.org/doi/10.1103/PhysRevLett.75.689.

[63] Massimiliano Corradini et al. "Analytical expressions for the local-field factor $G(q)$ and the exchange-correlation kernel $K_{\mathrm{xc}}(r)$ of the homogeneous electron gas". In: *Phys. Rev. B* 57 (23 June 1998), pp. 14569–14571. DOI: 10.1103/PhysRevB.57.14569. URL: http://link.aps.org/doi/10.1103/PhysRevB.57.14569.

[64] G. Vignale and K. S. Singwi. "Possibility of superconductivity in the electron-hole liquid". In: *Phys. Rev. B* 31 (5 Mar. 1985), pp. 2729–2749. DOI: 10.1103/PhysRevB.31.2729. URL: http://link.aps.org/doi/10.1103/PhysRevB.31.2729.

[65] D.D Awschalom. "Manipulating and storing spin coherence in semiconductors". In: *Physica E* 10.1-3 (2001), pp. 1–6. ISSN: 1386-9477. DOI: 10.1016/S1386-9477(01)00042-X. URL: http://www.sciencedirect.com/science/article/pii/S138694770100042X.

[66] R. I. Dzhioev et al. "Low-temperature spin relaxation in n-type GaAs". In: *Phys. Rev. B* 66 (24 Dec. 2002), p. 245204. DOI: 10.1103/PhysRevB.66.245204. URL: http://link.aps.org/doi/10.1103/PhysRevB.66.245204.

[67] T. Jungwirth et al. "Theory of ferromagnetic (III,Mn)V semiconductors". In: *Rev. Mod. Phys.* 78 (3 Aug. 2006), pp. 809–864. DOI: 10.1103/RevModPhys.78.809. URL: http://link.aps.org/doi/10.1103/RevModPhys.78.809.

[68] A. H. MacDonald, P. Schiffer, and N. Samarth. "Ferromagnetic semiconductors: moving beyond (Ga,Mn)As". In: *Nat. Mater.* 4.3 (Mar. 2005), pp. 195–202. DOI: 10.1038/nmat1325. URL: http://dx.doi.org/10.1038/nmat1325.

[69] H. Ohno et al. "Magnetotransport properties of p-type (In,Mn)As diluted magnetic III-V semiconductors". In: *Phys. Rev. Lett.* 68 (17 Apr. 1992), pp. 2664–2667. DOI: 10.1103/PhysRevLett.68.2664. URL: http://link.aps.org/doi/10.1103/PhysRevLett.68.2664.

[70] H. Munekata et al. "Diluted magnetic III-V semiconductors". In: *Phys. Rev. Lett.* 63 (17 Oct. 1989), pp. 1849–1852. DOI: 10.1103/PhysRevLett.63.1849. URL: http://link.aps.org/doi/10.1103/PhysRevLett.63.1849.

[71] H. Ohno et al. "(Ga,Mn)As: A new diluted magnetic semiconductor based on GaAs". In: *Appl. Phys. Lett.* 69.3 (1996), pp. 363–365. DOI: 10.1063/1.118061. URL: http://link.aip.org/link/?APL/69/363/1.

[72] Hideo Ohno. "A window on the future of spintronics". In: *Nat. Mater.* 9 (12 Dec. 2010), p. 952. DOI: 10.1038/nmat2913. URL: http://dx.doi.org/10.1038/nmat2913.

[73] Tomasz Dietl. "A ten-year perspective on dilute magnetic semiconductors and oxides". In: *Nat. Mater.* 9 (12 Dec. 2010), p. 965. DOI: 10.1038/nmat2898. URL: http://dx.doi.org/10.1038/nmat2898.

[74] T. Jungwirth et al. "Spin-dependent phenomena and device concepts explored in (Ga,Mn)As". arXiv:1310.1944. 2013.

[75] Hilbert v. Löhneysen et al. "Fermi-liquid instabilities at magnetic quantum phase transitions". In: *Rev. Mod. Phys.* 79 (3 Aug. 2007), pp. 1015–1075. DOI: 10.1103/RevModPhys.79.1015. URL: http://link.aps.org/doi/10.1103/RevModPhys.79.1015.

[76] M. Dobrowolska et al. "Controlling the Curie temperature in (Ga,Mn)As through location of the Fermi level within the impurity band". In: *Nat. Mater.* 5 (12 May 2012), p. 444. DOI: 10.1038/nmat3250. URL: http://dx.doi.org/10.1038/nmat3250.

[77] J. Mašek et al. "Microscopic Analysis of the Valence Band and Impurity Band Theories of (Ga,Mn)As". In: *Phys. Rev. Lett.* 105 (22 Nov. 2010), p. 227202. DOI: 10.1103/PhysRevLett.105.227202. URL: http://link.aps.org/doi/10.1103/PhysRevLett.105.227202.

[78] Gustavo M. Dalpian and Su-Huai Wei. "Electron-induced stabilization of ferromagnetism in $Ga_{1-x}Gd_xN$". In: *Phys. Rev. B* 72 (11 Sept. 2005), p. 115201. DOI: 10.1103/PhysRevB.72.115201. URL: http://link.aps.org/doi/10.1103/PhysRevB.72.115201.

[79] M. Roever et al. "Electron stabilized ferromagnetism in GaGdN". In: *physica status solidi (c)* 5.6 (2008), pp. 2352–2354. ISSN: 1610-1642. DOI: 10.1002/pssc.200778560. URL: http://dx.doi.org/10.1002/pssc.200778560.

[80] V. Novák et al. “Curie Point Singularity in the Temperature Derivative of Resistivity in (Ga,Mn)As”. In: *Phys. Rev. Lett.* 101 (7 Aug. 2008), p. 077201. DOI: 10.1103/PhysRevLett.101.077201. URL: http://link.aps.org/doi/10.1103/PhysRevLett.101.077201.

[81] E. H. Hwang and S. Das Sarma. “Transport properties of diluted magnetic semiconductors: Dynamical mean-field theory and Boltzmann theory”. In: *Phys. Rev. B* 72 (3 July 2005), p. 035210. DOI: 10.1103/PhysRevB.72.035210. URL: http://link.aps.org/doi/10.1103/PhysRevB.72.035210.

[82] F. V. Kyrychenko and C. A. Ullrich. “Temperature-dependent resistivity of ferromagnetic $Ga_{1-x}Mn_xAs$: Interplay between impurity scattering and many-body effects”. In: *Phys. Rev. B* 80 (20 Nov. 2009), p. 205202. DOI: 10.1103/PhysRevB.80.205202. URL: http://link.aps.org/doi/10.1103/PhysRevB.80.205202.

[83] F. V. Kyrychenko and C. A. Ullrich. “Response properties of III-V dilute magnetic semiconductors including disorder, dynamical electron-electron interactions, and band structure effects”. In: *Phys. Rev. B* 83 (20 May 2011), p. 205206. DOI: 10.1103/PhysRevB.83.205206. URL: http://link.aps.org/doi/10.1103/PhysRevB.83.205206.

[84] T. Dietl et al. “Zener Model Description of Ferromagnetism in Zinc-Blende Magnetic Semiconductors”. In: *Science* 287.5455 (2000), pp. 1019–1022. DOI: 10.1126/science.287.5455.1019. URL: http://www.sciencemag.org/content/287/5455/1019.abstract.

[85] J. H. Jiang et al. “Electron spin relaxation in paramagnetic Ga(Mn)As quantum wells”. In: *Phys. Rev. B* 79 (15 Apr. 2009), p. 155201. DOI: 10.1103/PhysRevB.79.155201. URL: http://link.aps.org/doi/10.1103/PhysRevB.79.155201.

[86] K. Shen and M. W. Wu. “Hole spin relaxation and coefficients in Landau-Lifshitz-Gilbert equation in ferromagnetic (Ga,Mn)As”. In: *Phys. Rev. B* 85 (7 Feb. 2012), p. 075206. DOI: 10.1103/PhysRevB.85.075206. URL: http://link.aps.org/doi/10.1103/PhysRevB.85.075206.

[87] C. Zener. “Interaction Between the d Shells in the Transition Metals”. In: *Phys. Rev.* 81 (3 Feb. 1951), pp. 440–444. DOI: 10.1103/PhysRev.81.440. URL: http://link.aps.org/doi/10.1103/PhysRev.81.440.

[88] A. S. Arrott. “Approximations to Brillouin functions for analytic descriptions of ferromagnetism”. In: *J. Appl. Phys.* 103.7, 07C715 (2008), p. 07C715. DOI: 10.1063/1.2836337. URL: http://link.aip.org/link/?JAP/103/07C715/1.

[89] F Aryasetiawan and O Gunnarsson. “The GW method”. In: *Rep. Prog. Phys.* 61.3 (1998), p. 237. DOI: 10.1088/0034-4885/61/3/002. URL: http://stacks.iop.org/0034-4885/61/i=3/a=002.

[90] Václav Špička and Pavel Lipavský. “Quasiparticle Boltzmann Equation in Semiconductors”. In: *Phys. Rev. Lett.* 73 (25 Dec. 1994), pp. 3439–3442. DOI: 10.1103/PhysRevLett.73.3439. URL: http://link.aps.org/doi/10.1103/PhysRevLett.73.3439.

[91] O. Morandi, P.-A. Hervieux, and G. Manfredi. “Time-dependent model for diluted magnetic semiconductors including band structure and confinement effects”. In: *Phys. Rev. B* 81 (15 Apr. 2010), p. 155309. DOI: 10.1103/PhysRevB.81.155309. URL: http://link.aps.org/doi/10.1103/PhysRevB.81.155309.

VITA

Matthew D. Mower was born on July 14, 1983 in Seaside, Oregon. He received a B.S. in Physics from Western Washington University in 2006. He has worked as a Ph.D. seeking research assistant for Dr. Giovanni Vignale at the University of Missouri in Columbia, Missouri since 2007. After graduation in 2013, he will begin a post-doctoral research position with Dr. Michael Flatté at the University of Iowa in Iowa City, Iowa.